EFFECT OF DUALLY COMBINED UNDER-INHIBITION AND ANTI-AGGLOMERANT TREATMENT ON HYDRATE SLURRIES

by

Martin J. Braniff

A thesis submitted to the Faculty and the Board of Trustees of the Colorado School of Mines in partial fulfillment of the requirements for the degree of Master of Science (Chemical Engineering).

Golden, Colorado

Date ____________________

Signed: ____________________
Martin J. Braniff

Signed: ____________________
Dr. Amadeu K. Sum
Thesis Advisor

Signed: ____________________
Dr. Carolyn A. Koh
Thesis Advisor

Golden, Colorado

Date ____________________

Signed: ____________________
Dr. David Marr
Professor and Head
Department of Chemical and Biological Engineering

ABSTRACT

Gas hydrates in deepsea pipelines can cause problems to flow assurance and also be a safety hazard. It can be expensive to prevent hydrate formation as this requires methanol injection in proportion to the water content of the system. As deepsea production facilities go to deeper depths of seawater and as the fields mature, the water content will increase, thereby reducing the economic viability of the production facility. This thesis explores the possibility of using an under-inhibited system to control hydrate formation along with an anti-agglomerant to prevent the hydrates from agglomerating together and plugging the pipeline. A high pressure autoclave cell was used as the primary apparatus for this work. The volume of hydrates formed and their morphology within the cell could be discerned by monitoring the motor current and pressure, temperature conditions within the cell. Different inhibition and anti-agglomerant conditions were used to explore the effects on the resulting hydrate morphology and the volume of hydrates formed. Experiments were also performed that investigated the effect of combining the inhibition and anti-agglomerant chemicals into the same system. Two experimental fluids were tested, mineral oil and a crude oil. The mineral oil was used in order to eliminate the uncertainty of using a fluid which has a lot of unknown chemistry present and to highlight the effects of the added chemicals. Results showed that there was no clear advantage to using a combined system of under-inhibition and anti-agglomerants. When the two chemicals were used, results did not show a significant improvement between cases that had just one chemical present and cases that had both chemicals present. Crude oil experiments showed that the usage of anti-agglomerants and salt at high water cuts would cause a highly viscous foam to form which would likely be unflowable in a pipeline. Hydrates that formed from this foam system, however, appeared to be very flowable.

The foam did not form in the mineral oil experiments under the same conditions, showing that the natural chemistry within the crude oil causes the foam to appear.

Results showed that both the mineral oil and crude oil system could be under-inhibited with 5 wt.% methanol and remain non-plugging. A slurry of hydrates would be formed from these experiments.

TABLE OF CONTENTS

LIST OF FIGURES

LIST OF TABLES

ACKNOWLEDGMENTS

The author would like to thank the directors and my advisors of the Center for Hydrate Research, Dr. Carolyn Koh, Dr. Amadeu Sum and Dr. Dendy Sloan. Their help, advice and guidance have been instrumental in the shaping of this work.

Thanks also to Dr. Sergey Skiba, Dr. Zach Aman and Dr. Jose Delgado for their help in the lab and in the office. Their in-depth discussions have helped me to analyze and interpret the results discussed throughout this thesis. Thanks to the other hydrate busters who have showed their support throughout the years via helpful comments, help in the lab and also for their genuine friendship.

Many thanks to the Deepstar group for their financial support (CTR 10205) and for their support and feedback throughout this work. Thanks also to Dr. Jeff Creek for his advice and comments.

Last but not least, a special thanks to all of my friends and family who have encouraged me and supported me throughout this thesis. Especially to my parents who have always steadily guided and supported me throughout my life and also to my dear and loving wife, Amanda. Thank you for your love and words of encouragement, they have always kept me going, even during the hard times.

CHAPTER 1

INTRODUCTION

This thesis explores the possibility of using a combined system of anti-agglomerants and methanol as a means of converting a buildup of problematic hydrates into a flowable hydrate slurry for a high water cut system. As the production time of oil from deep sea wells increases, the associated water content, also called water cut (WC), from that well will also tend to increase, simultaneously making the production of oil less profitable and the risk of a hydrate plug more likely (Azarinezhad *et al.*, n.d.). The current hydrate strategy is one of hydrate avoidance, i.e., not allowing any hydrates to form at all. To achieve this result methanol or monoethylene glycol, which are hydrate inhibitors, can be injected into the pipeline. The volume of inhibitor required for hydrate avoidance increases proportionally with the amount of water in the system, as time goes on, the operating expense can rise dramatically as the water cut increases. For example the water cut of one field went from around relative 0 vol% when it first opened to around 60 vol% after 8 years of operation (Gluyas & Hichens, 2003). This type of increase in water cut would result in a substantial increase in MeOH usage, simultaneously driving up the operating costs and decreasing the profitability of the field. By using a combination of anti-agglomerants and methanol, it could be possible to reduce the volume of chemicals required to keep the system from plugging by utilizing a hydrate management strategy rather than one of avoidance. Reducing the chemical volume will reduce the associated costs of keeping the pipeline operating, effectively increasing the profitable time of each well.

1.1 Clathrate Hydrates

Clathrate hydrates are crystalline inclusion compounds that are composed of water and light hydrocarbon compounds such as methane, ethane and propane. They tend to form in high pressure and low temperature conditions, although some clathrates have been known to form at atmospheric conditions (Sloan & Koh, 2008). Hydrates were first discovered by Sir Humphrey Davy in 1810 while carrying out experiments with chlorine gas and water (Davy, 1811). Since the discovery of hydrates, over 20,000 thousand articles have been published on the subject. From 1811 to the 1920s hydrates were studied as a scientific curiosity in the lab (Faraday & Davy, 1823), (Wroblewski, 1882). In 1934 it was discovered, however, that hydrates were forming in oil and gas pipelines and were causing flow assurance problems (Hammerschmidt, 1934). More recently, research investigating naturally occurring hydrates and their potential as an energy source has been initiated (Makogen, 1965).

There are three common crystal structures that hydrates can form, structure I, II and H (Figure 1.1). The type of hydrate structure formed depends largely on the guest molecule size, e.g. Methane will form sI, propane will form sII and an even larger guest molecule such as methylcyclohexane will form sH (Sloan & Koh, 2008). Each unit cell within the hydrate structure is made up of a number of cages which are formed from water molecules. Inside the water cage is located the non-polar guest molecule. The nomenclature of the cages follows an accepted format, where the number of sides to the polygon is stated and a superscript describes how many of that polygon makes up the unit cell. For example, the unit cell of structure I is comprised of two 5^{12} cages and six $5^{12}6^{2}$ cages. These cages are made up of water molecules and structure I would be made up of 46 water molecules.

1.2 Hydrates as a Flow Assurance Challenge

Hydrates are one of many factors that can cause flow assurance issues in deep sea pipelines (Gao, 2008), since water and gases such as methane, ethane, propane, etc. are produced along with oil. Coupled with the high pressure and low temperature conditions, an untreated pipeline has the potential to lead to hydrate growth (Sloan, 2003). This growth can lead to a plugging of the pipeline, a situation that leads

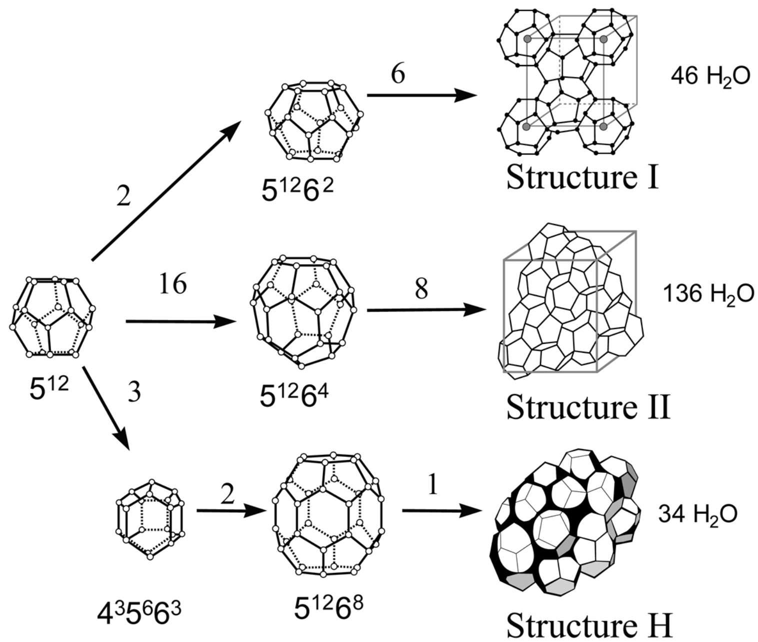

Figure 1.1: Clathrate hydrate structures and associated cages (Sloan & Koh, 2008).

to a decrease in the flow of oil. Once a hydrate plug occurs, a number of different techniques can be employed to remedy a plugging scenario, such as depressurization, heating or chemical injection. During this remediation process, however, the pipeline can be shut down for days leading to a significant economic loss and potential safety risks to personnel and equipment (Sloan, 1991).

1.2.1 Hydrate Avoidance Strategies

Removing water from a pipeline by using a deep sea separator unit, the main component of hydrates can be effectively removed, which can help prevent hydrate formation (Ilahi, 2005). Such a system can be expensive to install and maintain and furthermore several such units may be required in sequence in order to increase the water removal efficiency to the point where hydrates will not form. When such a system is not used or when the separator efficiency is not high enough, the most common form of hydrate inhibition is thermodynamic hydrate inhibitor injection (THI) (such as methanol or monoethylene glycol). The major function of the THI is to displace the hydrate formation curve to harsher conditions, i.e. by increasing the pressure and decreasing the temperature required for hydrate formation (Figure 1.2).

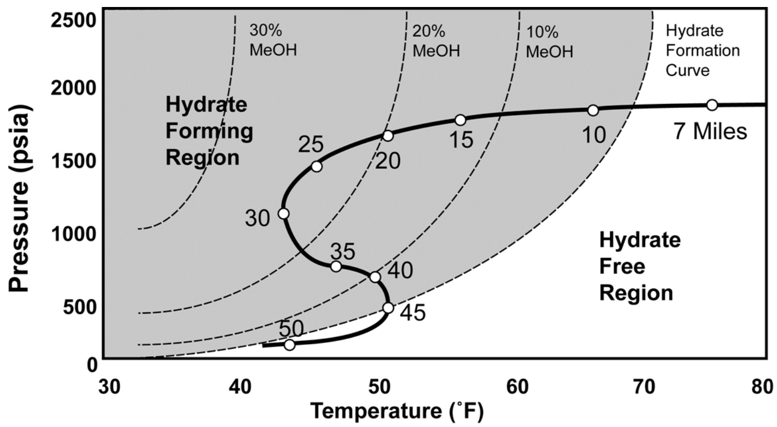

Figure 1.2: Hydrate formation curve can be moved to harsher conditions by the addition of a hydrate inhibitor such as methanol(Sloan & Koh, 2008).

Specifically on a molecular level hydrate inhibition via methanol is achieved by methanol molecules hydrogen bonding with the water molecules (Yousif, 1998). In order for hydrate growth to occur, the hydrogen bonds between the methanol and the water have to be broken which is achieved via lower temperature and higher pressures. Methanol injection can be expensive, (2$/gallon, Creek *et al.* (n.d.)) however, as the volume of methanol required for complete hydrate inhibition is dictated by both thermodynamic conditions, as can be seen in Figure 1.2, and also by the volume of water present in the system (Figure 1.3). In addition to this, since methanol is miscible in water, the two components have to be separated once they have been recovered. This is therefore an additional expense that has to be considered (Esteban *et al.*, 2000). It has been suggested that it could be possible to operate a system by using a volume of methanol less than the full amount needed to have full inhibition, this is called under-inhibition. Early work on this, however, has suggested that under-inhibiting a system can lead to a greater potential in a hydrate plug than if there was no methanol present at all (Hemmingsen *et al.*, n.d.).

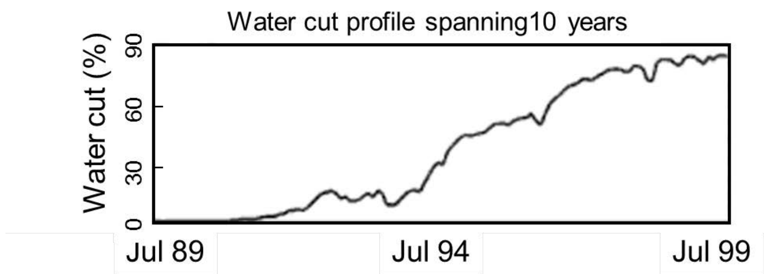

Figure 1.3: Plot showing how the water cut of a typical oil field can increase over time (Gluyas & Hichens, 2003).

In light of these issues, the industry is shifting to risk management strategies such as using low-dosage hydrate inhibitors such as kinetic inhibitors and anti-agglomerants (Kelland, 2006). Kinetic inhibitors operate by delaying hydrate growth for a period of time beyond the residence time of the fluid in the hydrate-prone zone (Lederhos *et al.*, 1996). The main advantage to this method is that the chemical dosage can remain low (0.5-1 wt %) while remaining effective, cutting down on chemical and end point separation costs. Anti-agglomerants (AA) are also useful due to their low dosage requirement. The mechanism of AA operation, however, is very different from kinetic inhibitors. Anti-agglomerants are typically surfactant type compounds that allow small hydrate particles to form but not agglomerate with other hydrate particles (Kelland *et al.*, n.d.), (Zanota *et al.*, 2005) by keeping the water droplets dispersed throughout the oil as well as reducing the particle-particle interaction that can lead to large hydrate particles (Aman, 2012). By keeping the water dispersed, this effectively keeps the hydrate particle size to a minimum and can prevent a large mass of hydrates from forming that could plug the pipeline. The resulting hydrate slurry can then flow through the pipeline. The main limitation of anti-agglomerants are that they typically cannot be used at water cuts greater than 50 vol% (Alapati *et al.*, n.d.), (Gao, 2009). The study of anti-agglomerants used in conjunction with methanol (MeOH) will be the main topic of this thesis. The main idea behind this work is to cut down on the volume of hydrates that can form by using MeOH and keep the hydrates that do form well dispersed by using AA.

1.3 Thesis Outline

This thesis has been divided into five chapters. Chapter 2 is an overview of the equipment used throughout this work and the procedures used for each piece of equipment. Chapter 2 also discusses experimental repeats, as well as the potential sources of error that are associated with the measurements and calculations performed throughout this work.

Chapter 3 details the results obtained using mineral oil and discusses the different effects for additions of inhibitors and anti-agglomerants. This chapter also discusses the different possible mechanisms that may lead to a hydrate plug or a non-plugging situation.

Chapter 4 covers the work performed with a crude oil and, similar to chapter 3, discusses the different results obtained when different chemicals are added to the system as well as some of the possible mechanisms behind the different phenomena observed throughout this work.

Chapters 5 and 6 present the Conclusions and Recommended Way Forward respectively.

In Appendix A, a summary of all the experiments performed and the results are listed. Appendix B and C detail the fluid physical properties and the experimental procedures respectively. Appendix D provides a sample calculation for the hydrate volume fraction that forms with each experiment.

CHAPTER 2

EXPERIMENTAL APPARATUS

This chapter details the different experimental apparatuses as well as the procedures that were used in this work.

2.1 Autoclave Cell Setup

The primary apparatus that was used in this project was a high pressure, stirred autoclave cell designed by David Greaves and John Boxall and built by Challenger Manufacturing (Greaves, 2007) (Boxall, 2009). The cell design was modeled after a similar cell used by Douglas Turner (Turner, 2006). The cell has a removable false bottom that, when in place, gives the cell a total volume of 1.89 L. The cell is pressure rated to 1500 psig and has two available ports into which can be inserted a Particle Video Microscope (PVM) probe (from Mettler-Toledo®, model 800) and a Focused Beam Reflectance Measurement (FBRM) probe (from Mettler-Toedo®, model D600X). Figure 2.1 shows the autoclave cell schematic. The entire cell was placed into a glycol cooling bath, for a temperature range between 50 and -15°C.

The cell has a 1/8 inch stainless steel gas injection line that extends to near the bottom of the cell. This allows the gas to be injected directly in contact with the liquid to help with saturation. The gas line is connected to a gas reservoir which allows the cell to be maintained at a constant pressure during experiments via a solenoid pressure valve controlled by Labview®. A vane blade impeller that is stirred via an impeller shaft coupled to a magnetic motor is used to mix the system. A tachometer measures the RPM speed which the motor drive attempts to keep constant by adjusting the motor current when an increase or decrease in the RPM is detected. Changes to the RPM will usually occur due to a change in the fluid viscosity or an appearance of solids as hydrates are formed in the system. To help with mixing within the cell, four

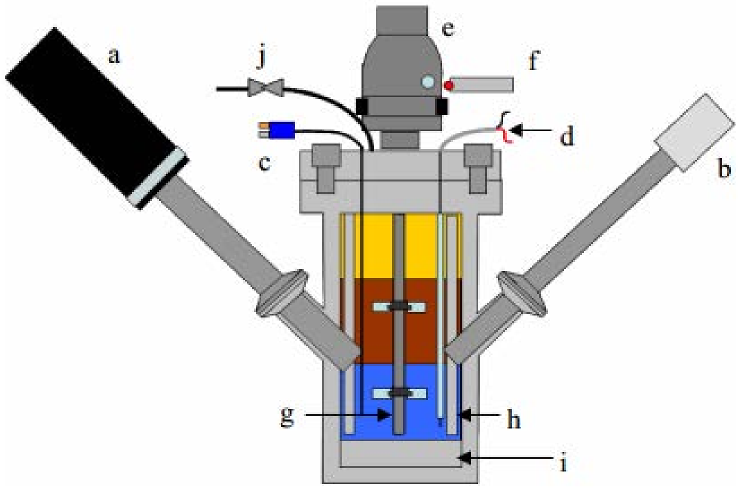

Figure 2.1: Schematic of the high pressure autoclave cell used throughout this project. (a) PVM probe, (b) FBRM probe, (c) Thermocouple, (d) Conductivity probes, (e) Magnedrive, (f) Mixer belt, (g) Impeller, (h) Baffles, (i) False bottom, (j) Gas inlet line, (k) Vent, (l) Safety release valve.

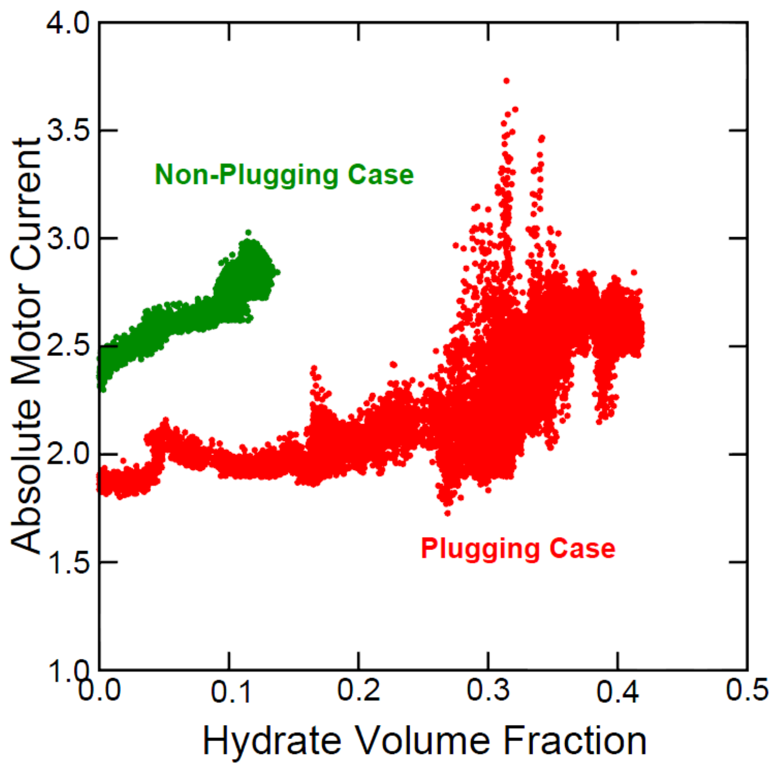

Figure 2.2: Example of the motor current trace against the hydrate volume fraction. Red trace: Typical plugging case characterized by spikes in motor current data as hydrate chunks are formed in the system. Blue trace: Typical non-plugging case, Minimum spikes indicate flowable hydrate slurry.

baffles surround the vane blade impeller, each located at 90° intervals. Each blade in the impeller has a height of 5.5 inches and a width of 0.9 inches (Figure 2.3).

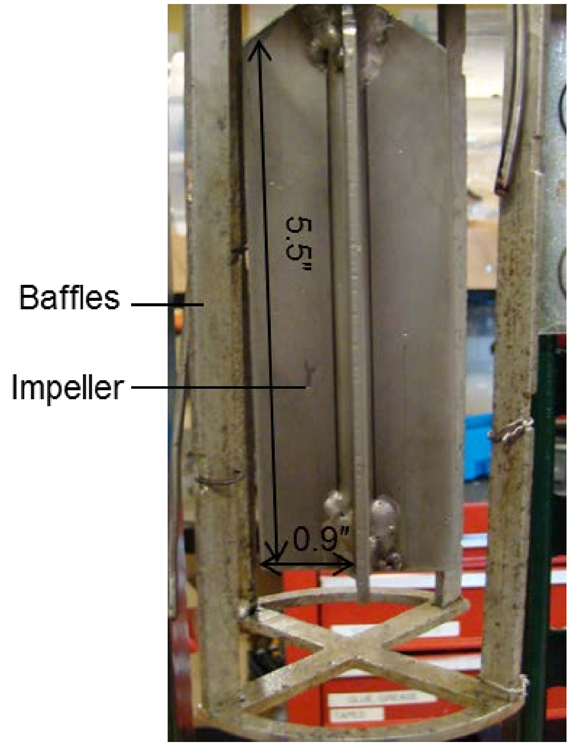

Figure 2.3: Figure showing the impeller and baffle system that was used in the autoclave cell for this work.

The motor current is monitored since the change in motor current is one of the main techniques of discerning what is happening inside of the autoclave cell, as a measure of the relative viscosity of the fluid/solids. The motor current can also give an indication of the morphology of any hydrates that form in the cell. For example, spikes in the motor current can be indicative of hydrate chunks, while a smooth increase can be indicative of a hydrate slurry. For all experiments discussed in this thesis, the motor current is plotted against the volume of hydrates formed in the cell. An example of a motor current vs hydrate volume fraction plot for a typical plugging case compared to a non-plugging case is shown in Figure 2.2.

The cell is also equipped with thermocouples and a pressure transducer. There are two thermocouples in the cell, one at the bottom of the cell and one at the top. The pressure transducer is located outside of the cell and is attached to the gas inlet line. The temperature and pressure data are recorded using a data acquisition program controlled by a Labview® program. As mentioned previously both an FBRM and PVM probe can be inserted into the cell at a 45°angle and are secured using a tri-clamp flange fitting. Only the PVM probe was used in this work and it can be used to gain visual images of the fluid and solids within the cell.

2.1.1 Autoclave Cell Experimental Procedure

The experimental procedure for the autoclave cell consisted of loading the cell with 1 L of fluid. The liter of fluid was typically made up of a mixture of water and oil on a volume percent basis. The typical water cut was from 50-75 vol.% in order to mimic a high water cut system. Using a liter of fluid leaves the internal volume available for gas to be around 890 ml. Deionized water was used for every experiment in order to eliminate any anomalies that could be present in regular tap water. The remainder of the fluid was made up of crude oil or mineral oil. Before being added, the crude oil was heated at 60 °C for 4 hours in order to allow the viscosity of the oil to be lowered and to allow all of the components to be fully dissolved within the oil (Thompson *et al.*, 1985). When mineral oil was used, it did not need to be heat up in this manner as the mineral oil was assumed to already be homogenized. Any additional chemicals that were being investigated, such as AA, methanol or salt, were added as a weight percent based on the water cut for that experiment.

Once the cell was loaded, it was sealed and placed into the cooling bath, kept at 20 °C. The mixing motor was turned on and the RPM set to 300. These experiments were performed at 300 RPM for two reasons. The first was that there were a large number of potential variables that could be changed throughout this work. Since the main aim of this work was to investigate the chemical impact on the hydrate slurry, changing the RPM would not help gain significant insights into the chemical impact. The second reason was that John Boxall has shown that this shear rate is high enough to induce a good amount of fluid mixing within this particular autoclave system (Boxall, 2009).

At this point 99.9% methane gas (ultra-high purity from General Air) would be injected into the system until a pressure of 950 psig was reached. As mentioned previously, this pressure was maintained at 950 psig throughout the entire experiment. The system was then saturated at 20 °C and 950 psig at 300 RPM for 6-12 hours (Joshi, 2012). Once the system was fully saturated, which would take around four hours for crude oil and seven hours for mineral oil, the bath temperature set point was lowered to 1 °C. Since the hydrate equilibrium temperature at this pressure is 9.2 °C, this provides a driving force of around 8.2 °C for hydrate formation (CSMGem) (Sloan & Koh, 2008). For some experiments, methanol or salt were present which would change the hydrate formation driving force. A note on the driving force for these experiments will be made when appropriate. Hydrates would then be allowed to form in the autoclave cell for around 24 hours. If the cell had not plugged at this point the cell would be put into shut-in conditions for around 16 hours, with no agitation, and then restarted. At this point, regardless of whether the cell had plugged or not the experiment would be at an end. The hydrate morphology was examined by rapidly venting the cell and then opening it before hydrates could dissociate. Although some of the hydrate would of course have dissociated during the venting process, the overall hydrate morphology would be maintained and it would be possible to identify whether a hydrate slurry or hydrate chunks had formed throughout the experiment. The autoclave procedure is explained in more detail in the appendix.

2.1.2 Hydrate Volume Fraction Calculation

For every experiment, the associated volume of hydrates that formed in that experiment has been calculated using the recorded pressure and temperature data; an example of such a trace can be seen in Figure 2.4. A plot such as this one is recorded for every experiment performed in the autoclave cell and can be used to locate the formation point of hydrates, that is, the point where hydrates were first observed to form. Since hydrate formation is an exothermic reaction, a spike in the temperature plot is usually indicative of hydrate nucleation. This along with a drop in the reservoir pressure, as hydrate formation depletes the gas in the cell, can be used to determine the formation point of each experiment.

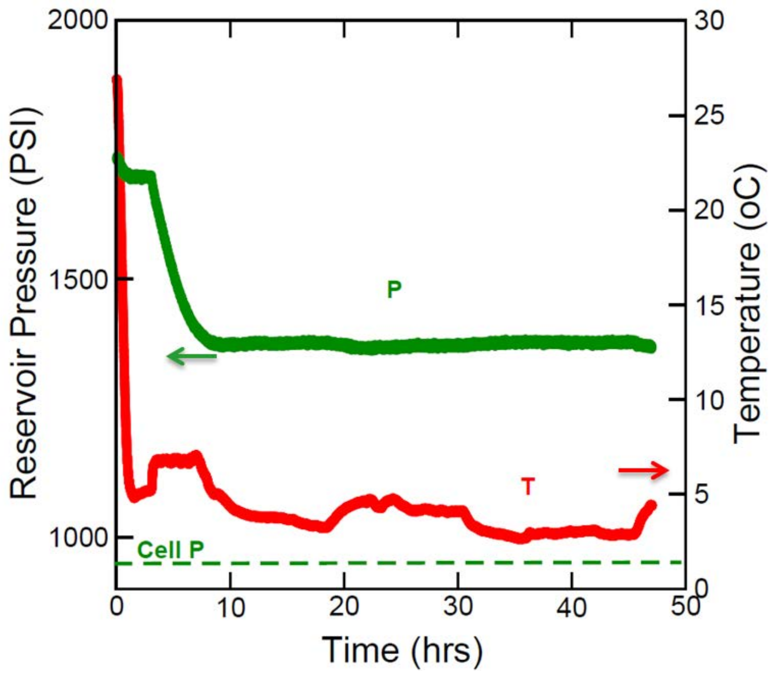

Figure 2.4: Example plot of recorded temperature and pressure data. Red trace: Temperature curve. Green trace: Reservoir pressure curve.

The calculation method used is an iterative calculation using the Peng-Robinson equation of state. The following section details the equations used to calculate the hydrate volume fraction. Starting with the Peng-Robinsion EOS (2.1):

$$P = \frac{RT}{V_m - b} - \frac{a\alpha}{V_m^2 + 2bV_m - b^2} \tag{2.1}$$

Where$P$ is the recorded cell or reservoir pressure, R is the universal gas constant, T is the cell or reservoir temperature. V_m is the molar volume, a is a constant which is based on the critical temperature (T_c) and pressure (P_c) of methane and is calculated using (2.2). b is another constant and is calculated using (2.3), α is calculated using (2.4). In (2.4), T_r is the reduced temperature and is calculated using (2.5), κ is calculated using 2.6. From (2.1) the molar volume can be calculated at every time step which can then be used to calculate the number of moles of gas, since the total volume available for gas is known, using (2.7).

$$a = \frac{0.457235R^2T_c^2}{P_c} \tag{2.2}$$

$$b = \frac{0.077796RT_c}{P_c} \tag{2.3}$$

$$\alpha = (1 + \kappa(1 - T_r^{0.5}))^2 \tag{2.4}$$

$$T_r = \frac{T}{T_c} \tag{2.5}$$

$$\kappa = 0.37464 + 1.54226\omega 0.26992\omega^2 \tag{2.6}$$

$$n_g = \frac{V}{V_m} \tag{2.7}$$

The molar volume is calculated separately for both the gas reservoir and for the autoclave cell since they are at different thermodynamic conditions. Adding the number of gas moles from both vessels together gives the total number of moles of gas in the system. Calculating this value for every time step throughout the experiment allows the gas consumption to be tracked. sI hydrates formed since only methane is present (Sloan & Koh, 2008). The methane cage occupancy is calculated at this point, so as to find out the number of methane molecules that occupy each cage in the hydrate structure. This can be calculated using CSMGem. The gas occupancy of the small cage is labeled s_o and the gas occupancy of the large cage is labeled l_o. Since it is known that there are 2 small cages and 6 large cages in the unit cell of sI, the number of mols of gas per unit cell (n_{guc}) can be calculated using (2.8) and (2.9). Since the total number of gas moles is known, the total number of unit cells ($N_{UnitCell}$) that this gas would occupy can be calculated using (2.10). Since the volume of a unit cell ($V_{UnitCell}$) is known (McMullan & Jeffrey, 1965) the total hydrate volume ($V_{Hydrate}$)

can be calculated using (2.11).

$$n_{gc} = s_o \times 2 + l_o \times 6 \tag{2.8}$$

$$n_{guc} = \frac{n_{gc}}{6.02E23} \tag{2.9}$$

$$N_{UnitCell} = \frac{n_g}{n_{guc}} \tag{2.10}$$

$$V_{Hydrate} = V_{UnitCell} \times N_{UnitCell} \tag{2.11}$$

$$n_w = n_g \times 6 \tag{2.12}$$

The value that is plotted when the hydrate volume fraction is reported is the fraction of solids (ϕ_H) in the system as a function of the total volume of fluids in the system and is calculated using (2.13)

$$\phi_H = \frac{V_{Hydrate}}{V_{Hydrate} + V_{remainingwater} + V_{oil}} \tag{2.13}$$

A full example calculation can found in the appendix.

2.1.3 Fluid and Chemical Characteristics

There were two types of experimental fluids used throughout this work. The first was a crude oil which was provided by Total. The oil was a high viscosity oil with a viscosity value of 100 ±1.5 cP at 20 °C and 100 s^{-1} and had a density of 0.908 ±0.003 g/cm^3. The interfacial tension value for the oil was measured to be 28.9 ±0.4 mN/m at atmospheric conditions.

The second type of fluid was a mineral oil, of which there were two varieties, 200T and 500T mineral oil. Both were supplied by STE Oil Company Inc. and were chosen to be studied in order to eliminate any effects observed in the crude oil experiments that could arise from the presence of natural chemistry associated with crude oil. The main difference between the 500T and 200T mineral oil was in their physical properties. The 200T mineral oil was lighter and less viscous, with a density of 0.856 g/cm^3 and a viscosity of 40 cP at 37.8 °C . The 500T mineral oil had physical properties slightly more similar to the crude oil with a density of 0.864 g/cm^3 and a viscosity of 88 cP at 37.8 °C. Mineral oil physical properties were stated by STE Oil and no error values were reported.

Sodium chloride was added to deionized water for most experiments in order to mimic the sea water that would be present in a deepsea pipeline. 3.5 wt.% of salt was dissolved in the water before it was added to the cell

The anti-agglomerant that was studied throughout this work was Arquad 2HT-75 (75% dehydrogenated tallow dimethylammonium chloride in water/isopropyl alcohol) which was a cationic surfactant, the structure of which can be seen in Figure 2.5. This chemical was supplied by Sigma-Aldrich textsuperscript® (88 92% purity) and was chosen for two reasons. The first reason was that the surfactant structure is known and from the structure, any chemistry effects can be more easily traced back to the inherent structure. Often, when an industrial anti-agglomerant is used, the structure or chemistry is proprietary and not available in the public domain, making it harder to determine why exactly certain phenomena are observed. The second reason is that previous work on this surfactant have been performed by Dr. Mark Anklam et al. who demonstrated, using glass beads in water/oil systems, that this surfactant could be successfully used as a model anti-agglomerant (Mcculfor *et al.*, 2011).

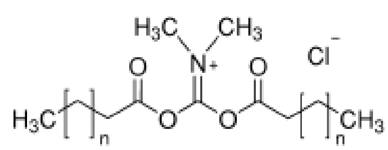

Figure 2.5: Molecular structure of Arquad 2HT-75, the model anti-agglomerant used throughout this work.

Methanol was chosen as the thermodynamic inhibitor to be studied, as it is a standard inhibitor commonly used by industry in the Gulf of Mexico.

2.2 Interfacial Tensiometer

The pendant drop technique was used to find the interfacial tension value between different fluids, such as between oil and water. The change to the interfacial tension via the addition of surfactant was then investigated. To investigate this, the pendant drop method using an interfacial tensiometer apparatus (CAM200, manufactured by KSV Instruments, Ltd.) was used (Figure 2.6). The main workings of this instrumentation are a needle which contains one of the test fluids which is injected into a quartz cuvette which is filled with the other test fluid. A camera, with the help of a high intensity light source, is set up to take pictures of the injected droplet every 30 seconds in order to track the droplet curvature over time. Software is then used to analyze the droplet picture and calculate the interfacial tension value of the droplet using (2.14) (Neumann *et al.*, 2010).

$$\gamma = \frac{\delta\rho.g_c.R_o^2}{\beta} \tag{2.14}$$

Where γ is the calculated interfacial tension value, $\delta\rho$ is the density difference between the two fluids, which is a value entered into the software by the user, R_o is the radius of drop curvature and β is a shape (curvature) factor that is calculated using the software, an example of this can be seen in Figure 2.7.

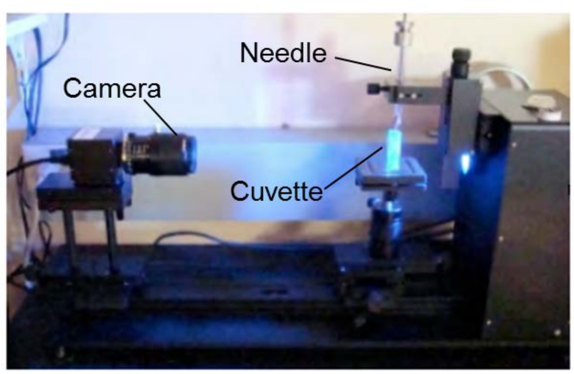

Figure 2.6: Interfacial tensiometer apparatus supplied by KSV Instruments, Ltd.

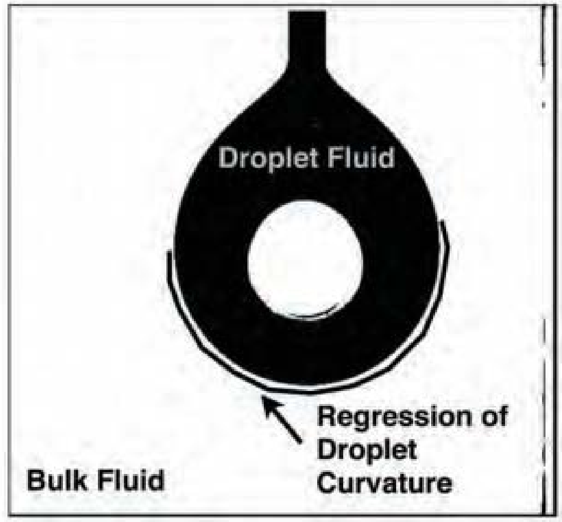

Figure 2.7: Image of a droplet in a typical pendant drop interfacial tension experiment (Aman, 2012).

The impact on interfacial tension when the model surfactant is added to the system can be studied using this apparatus. This is considered an important variable as the interfacial tension can dictate the droplet size in the system (Zerpa *et al.*, 2011). For a hydrate slurry, a small water droplet size is preferred as this will mean that when water is converted to hydrates, the hydrate particle will also remain small (Frostman *et al.*, n.d.). If the particles are small and do not agglomerate, which is the primary function of the anti-agglomerant, then it can be possible to achieve a low viscosity hydrate slurry (Clark *et al.*, n.d.).

2.2.1 Interfacial Tensiometer Procedure

The procedure for the IFT was as follows. First of all the oil component was prepared by measuring out around 12-25 ml of oil in a beaker. If anti-agglomerant (AA) was being used in the experiment then it was added to the oil phase (typically 0.5 2 wt.%) and dissolved for two minutes using a magnetic stirrer. The water component was prepared by adding 25-37.5 ml of water to a beaker, and if salt was used (3.5 wt.%) it was measured out and added to the water. All components were measured gravimetrically at atmospheric temperature and pressure. The water and salt mixture was then mixed by swirling the beaker by hand to ensure that the salt was fully dissolved. The water is then placed into a cuvette and a needle is loaded with the oil phase. The cuvette is then positioned on a platform in front of the camera and the needle was slowly lowered until it was around half way down the cuvette and was fully immersed into the water phase. An oil droplet was then slowly injected into the water phase, until there was a stable droplet, around 2 $\pm$0.5 mm, suspended at the tip of the needle. The computer program (CAM2008) was then run in order to capture the droplet suspended in the water over a period of 15 minutes with a picture taken every 30 seconds. Once this was completed, the program cycled through every picture and regressed the droplet curvature and from (2.14), calculated the interfacial tension. Around 3-5 experiments were run with each system and the reported value was the average of these runs.

2.3 Emulsions

As will be discussed throughout this thesis many bottle tests were performed in order to get an idea on the type of emulsions that each system formed. This information was desired since knowing the type of emulsion that a system would form can give a lot of insight into how hydrates will form in that system, as well as giving an idea on how readily a system might plug (in some cases). This section details how emulsions were prepared and the equipment used to form those emulsions (Sjöblom *et al.*, 2010).

The homogenizer equipment can be seen in Figure 2.8 (supplied by Virtis, model Cyclone IQ2). It consists of a control box and a high RPM mixing unit that ranges from 5000 to 30,000 RPM. The procedure used to prepare emulsions was as follows. Around 12 25 ml of oil was measured out in a glass beaker. If AA was being used in the emulsion, then the AA (typically 0.5 2 wt.%) was measured at this point and added to the oil, at which point the AA was dissolved in the oil using a magnetic stirrer. The appropriate amount of salt was then measured and placed into another

Figure 2.8: Homogenizer equipment used to prepare emulsions.

glass beaker and then the required water was measured out and added to this beaker. The water and salt were mixed together in a beaker by swirling the beaker by hand, in order to allow full salt dissolution. The beaker with the oil was then placed under the homogenizer and the control box was set to mix at 8000 RPM for 7 minutes. During the first 5 minutes of this mixing, the salt/water mixture was added drop by drop using a plastic syringe. The last two minutes were focused on ensuring that the components were well mixed. At the end of this time period, the emulsion would be ready and the type of emulsion formed was tested by taking a drop of the resulting mixture and mixing it into a beaker full of water (Ese & Kilpatrick, 2004). If the droplet could dissolve into the water then the emulsion was determined to be water continuous. If the droplet could not dissolve then it was determined to be oil continuous. The emulsion mixture would then be observed for 24 hours to determine the emulsion stability. The emulsion was stable if no phase separation after 24 hours was observed. If phase separation had occurred then the emulsion was unstable.

In order to determine whether the emulsions formed in the homogenizer could be compared to the emulsion formed in the autoclave cell (since different geometries and shear rates would be applied in both systems) autoclave emulsion experiments were also performed on a few of the systems that were tested with bottle tests. These experiments were prepared in a similar fashion to the procedure outlined for a typical autoclave experiment. The autoclave cell emulsion tests would not be put into hydrate formation conditions, they only looked at the emulsion types that would be formed before hydrate formation. These tests were found to give similar emulsion types between the homogenizer and the autoclave cell emulsions. A summary of the emulsion experiments can be found in the appendix.

2.4 Repeats and Errors

This section will discuss the repeatable nature of the experiments in the autoclave and will also detail the criteria used to determine whether an experiment should be repeated or not. Due to the time constraints of this project and the amount of time required to run an experiment (4 days/experiment), not to mention unforeseen delays and downtime necessary for equipment maintenance, it was not possible to repeat every experiment that was performed in the autoclave. Efforts were made to have repeats on key experiments. Key experiments are defined here as experiments that showcase the key phenomena that is of great interest in this thesis. For example, repeats were made on the AA + salt system, as they showed very interesting behavior, but repeats were not always made on experiments that followed the behavior that was expected. In order to justify the experiments that were or were not repeated, all available information from emulsion tests, motor current data and hydrate morphology was used to determine whether the result made sense with the overall picture and understanding of the tested system. If the result was in line with this understanding then the experiment was usually not repeated. If the result was unusual then the experiment would be repeated to ensure that the unusual result was real and repeatable. Just about all of the experiments that were repeated gave the same result from one experiment to the next. Evidence will be shown to demonstrate that the autoclave cell experiments are fairly repeatable. In addition to this, this section will also detail the different sources of error that could be found throughout the results of this thesis. This will include associated errors for calculations as well as errors on the various measurements that were taken for each experiment.

2.4.1 Repeats

As mentioned above due to time constraints and the fact that it takes around 4 days for an experiment to complete, not every experiment performed in this project could be repeated. Unusual results would prompt a repeat to be performed and were found to give similar results from experiment to experiment. An example of such a repeat can be seen in Figure 2.9.

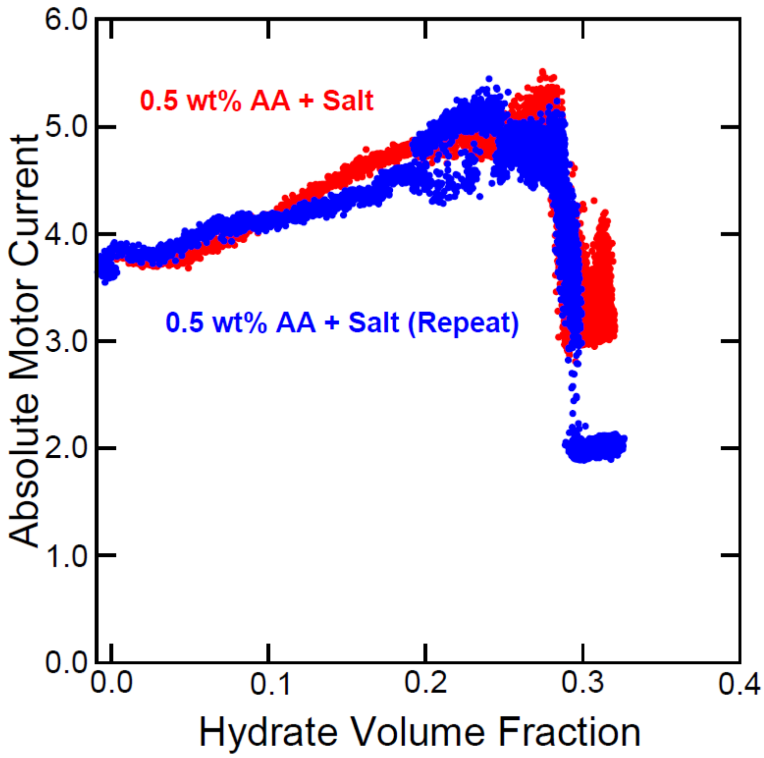

Figure 2.9: Example of a repeat experiment of 75 vol.% WC + 0.5 wt.% AA + 3.5 wt.% salt. Red trace: Original experiment. Blue trace: Repeat experiment showing consistent behavior.

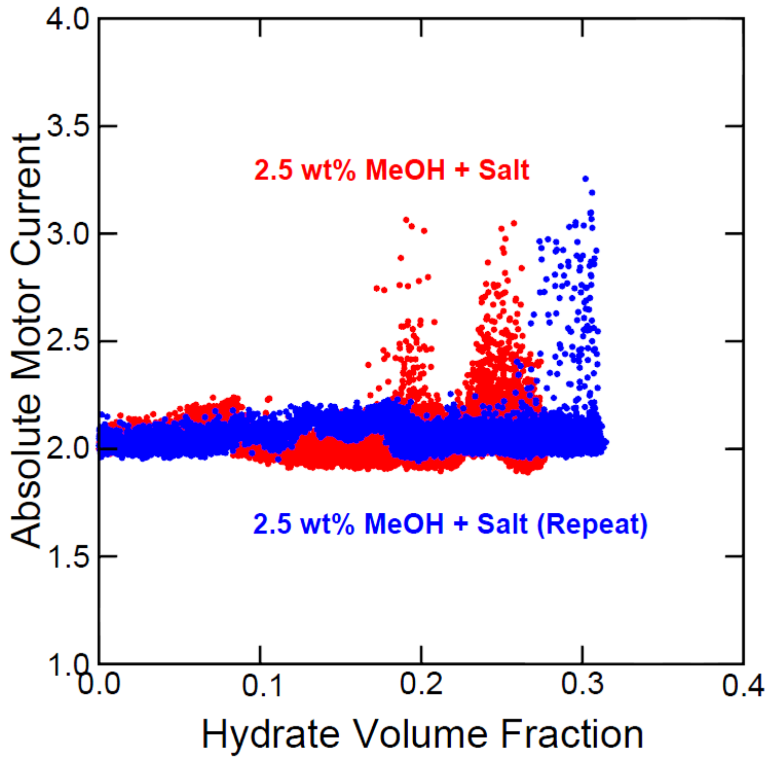

Figure 2.10: Example of a repeat experiment of 75 vol.% WC + 2.5 wt.% MeOH + 3.5 wt.% salt. Red trace: Original experiment. Blue trace: Repeat experiment showing consistent behavior.

As can be seen from Figure 2.9 results are fairly consistent from experiment to experiment. Another example of the repeatable nature of autoclave experiments can be seen in Figure 2.10. This repeat was for 2.5 wt.% MeOH at 75 vol.% WC and mineral oil, and was performed to ensure that this system was actually a plugging case and not a borderline case.

Again, this experiment shows fairly consistent behavior. There are some differences in the motor current, however, the overall trend of spikes in the motor current, a hydrate plug after shut-in conditions and similar hydrate morphology observed at the end of the experiment is convincing of repeatable behavior.

2.4.2 Errors

One of the main calculations done in this work is the calculation of the hydrate volume fraction, the details of which have been described above. Due to the fact

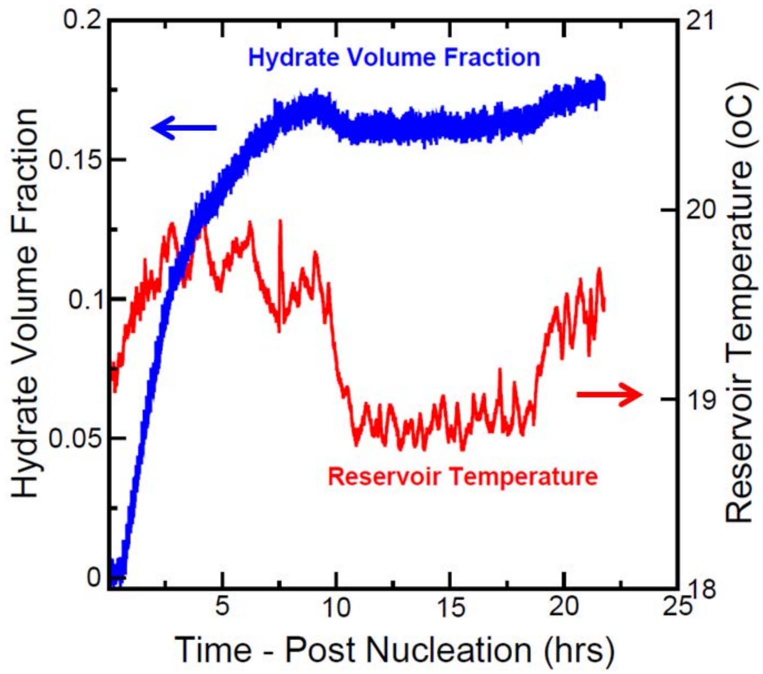

Figure 2.11: Example of how hydrate volume fraction calculation can be influenced by atmospheric temperature.

that the data for this calculation comes from a number of different sensors, such as temperature and pressure sensors, there are a number of potential sources for error that can creep into the calculations. In addition to this, since the hydrate volume fraction is calculated directly from both reservoir and cell temperatures, a change in the atmospheric temperature, due to the building heating cycle, will have a direct effect on the hydrate volume fraction. This can be well observed in Figure 2.11.

As can be observed in Figure 2.11, at around hour 10 there is a drop in the reservoir temperature, which is to say that there is a drop in the atmospheric temperature as night falls. This results in a slight drop in the hydrate volume fraction which then starts to rise again 10 hours later when the atmospheric temperature increases. This fluctuation in temperature corresponds to around 0.1 vol.% change in the hydrate volume fraction, while not a large change, corresponds to a 6% error in the calculated hydrate volume fraction. In addition to this, there will be an error associated with the temperature probes by about ± 0.5 °C. This can correspond to an additional error of $\pm$ 5 vol.% in the volume of hydrates calculated.

Although the error for the calculated volume of hydrates in the system appears to be high, it is still a good way of calculating the amount of hydrates present in the system, which is an important variable to know when to comparing the effectiveness of inhibitors, or knowing what volume of hydrates can be flowed in a hydrate slurry.

CHAPTER 3

MINERAL OIL

This chapter details the work performed with 500T and 200T mineral oil (supplied by STE Oil ®). Work was performed using mineral oil in order to more effectively decouple the effects of the natural chemistry in crude oil from the oil physical properties and inhibitor addition as the natural crude oil chemistry has been shown to have a significant effect on the plugability of an oil (Erstad *et al.*, 2009), (Borgund, 2007). By using mineral oil all of the natural chemistry components in crude oil are effectively removed. Therefore, when work was done on the crude oil, it was easier to determine which effects were due to the added surfactant and thermodynamic hydrate inhibitor (THI), and which effects were facilitated by the presence of natural chemistry such as asphaltenes, resins, etc. The majority of the mineral oil work was performed with 200T mineral oil, with work moving to 500T mineral oil following a suggestion that physical properties may be a more important factor than chemical properties.

3.1 200T Mineral Oil Results

Experiments with the 200T mineral oil were performed at a water cut of 75 vol.% with various additions of surfactant and THI. As well as autoclave experiments, bottle tests were conducted in order to gain insight into the emulsions that were being formed in the autoclave such as their type: oil-in-water (O/W) or water-in-oil (W/O) and their typical stability time.

When analyzing autoclave results it is important to keep in mind the two basic mechanisms that can lead to a hydrate plug in high water cut systems. The dominant plugging mechanism tends to be dictated by the type of emulsion formed within the cell, which can be influenced by the presence of chemicals, natural or otherwise.

The first mechanism tends to arise when water is the continuous phase (Figure 3.1). Hydrate nucleation will take place at the gas-water or oil-water interface. After nucleation, hydrate growth will proceed consuming more water and lead to hydrate particles agglomerating together. A hydrate plug formed from this mechanism tends to form a dense plug and leads to large hydrate chunks that are not easily broken. Complete hydrate conversion might take longer due to initial hydrate shells forming followed by the interior water being converted to hydrate. When water is the continuous phase, the chances of a hydrate plug occurring are high, mainly because there is a high degree of agglomeration between hydrate particles leading to hard hydrate chunks that are not easily broken apart from shear and large hydrate chunks tend to lead to a plugging scenario due to chunks being caught between the impeller and baffle system.

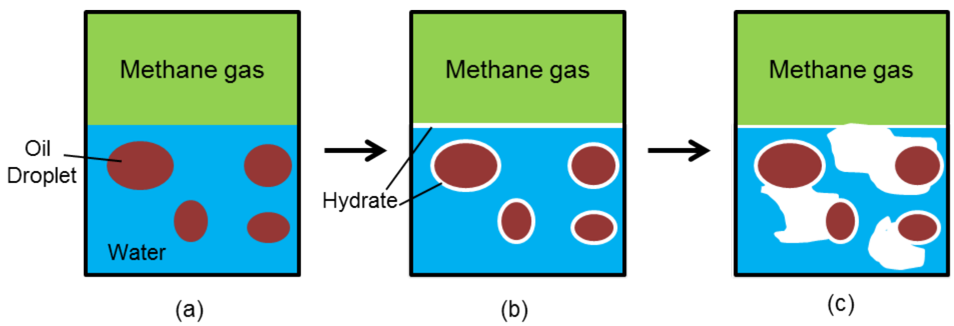

Figure 3.1: Hydrate formation from an O/W emulsion: (a) initial O/W emulsion; (b) initial hydrate nucleation occurring at oil-water and gas-water interface; (c) hydrate networks forming leading to hard hydrate chunks.

The second type of mechanism occurs when oil is the continuous phase (Figure 3.2). In this scenario, hydrate formation tends to be rapid due to the large interfacial area between water and oil. However, despite the rapid hydrate growth, a water-in-oil system is capable of leading to a non-plugging situation, particularly if there is an anti-agglomerant present that can prevent the hydrate particles from adhering together to form larger hydrate chunks. The basic mechanism starts with hydrate formation occurring at the water-oil and water-gas interface as before. Assuming that there are no anti-agglomerants present, hydrate particles that come into contact with each other can adhere together, leading to large hydrate chunks and possibly a hydrate plug similar to the oil-in-water situation (Colombel *et al.*, 2009). Similarly if the hydrate particles are coated with a thin layer of water, liquid bridges can form between the hydrate particles. These liquid bridges can, over time, convert to a hydrate bridge which again leads to hydrate chunks (Aman *et al.*, 2011).

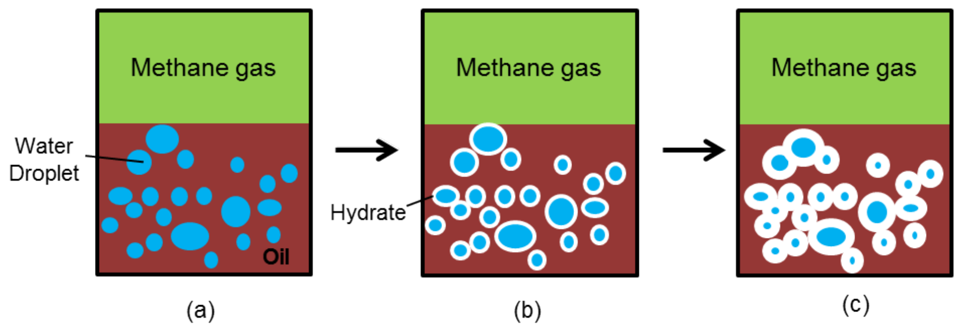

Figure 3.2: Hydrate formation from a W/O emulsion: (a) initial W/O emulsion; (b) initial hydrate nucleation occurring at oil-water interface; (c) hydrate particles adhering together leading to hydrate chunks.

3.1.1 Untreated 200T Mineral Oil

In order to be able to analyze the effect that adding a model surfactant or THI would have on the system, it was important to run a blank experiment, i.e. an experiment using only mineral oil and water with no other chemicals present. It was expected that such an experiment would plug immediately due to the high volume of water available for hydrate formation. In addition bottle tests showed that the untreated mixture would form an unstable oil-in-water emulsion, therefore it was expected that large hydrate chunks would form from the water continuous phase resulting in a hard hydrate plug. An additional blank experiment was also performed using 3.5 wt.% saline (NaCl) water. Bottle tests for this system indicated that an unstable oil-in-water emulsion also formed, suggesting that the behavior of the two blank systems should be similar. The results for these two experiments can be seen in Figure 3.3.

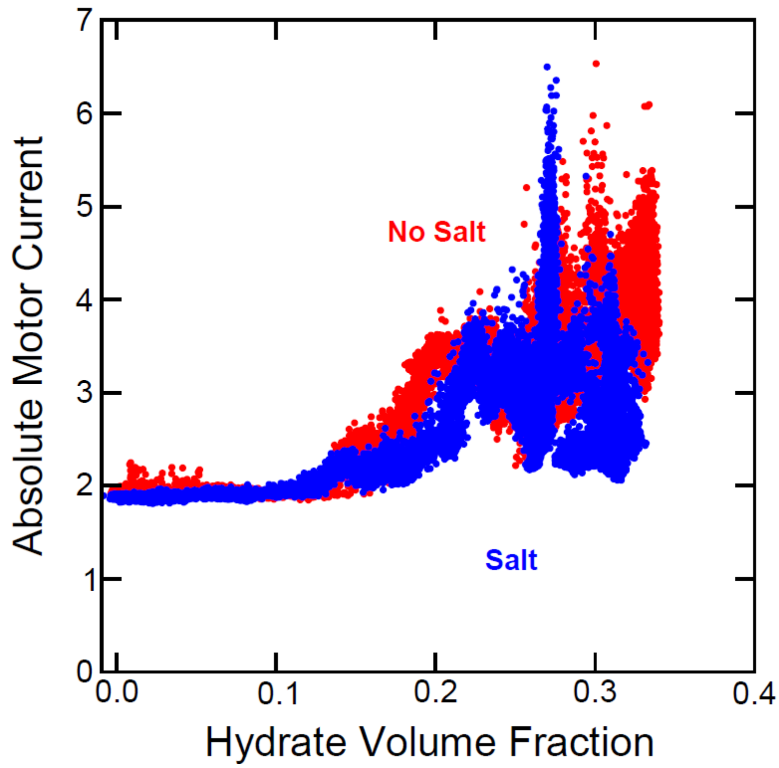

Figure 3.3: Motor current trace for the two base line experiments performed. Red trace: 75 vol.% WC, 200T mineral oil with no salt. Blue trace: 75 vol.% WC, 200T mineral oil with salt. Both experiments show rapid fluctuations in motor current suggesting plugging occurs. Experiments did plug after shut-in conditions.

Figure 3.3 plots the motor current that the impeller is drawing, as a function of the hydrate volume fraction. Looking at the two traces, it is clear that the trends between the two experiments underwent very similar behavior, as expected from the emulsion tests that were performed. After around 16 vol.% hydrate conversion, both experiments exhibited an increase in the motor current which is indicative of an increase in the fluid viscosity. The fluid viscosity is increasing due to an increase in the volume of solid particles in the system. Once the experiment reached around 20 vol.% hydrates, sharp fluctuations in the motor current can be observed. These fluctuations were most likely caused when the impeller struck a large hydrate chunk. The impeller would suddenly need more power to keep the impeller rotating; however, once the hydrate chunk is out of the impellers path, the power draw is lowered as the flow is no longer impeded. This results in the motor controller fluctuating the power demand as hydrate chunks are encountered in the system. The extremely large spike in the blue trace was probably an incident where the impeller became stuck temporarily, due to a buildup of hydrates, before clearing the jam and coming back down to a lower motor current level.

After a 24 hour period, if an experiment had not plugged it was not likely to plug during normal operating conditions. It can be hard to determine, however, due to the stochastic nature of plugging within the autoclave. Therefore a few criteria have to be met before an experiment can be declared a plugging or a non-plugging case. As mentioned in the autoclave operating procedure (section 2.1.1), if an experiment had not plugged after a 24 hour period, then the experiment was put into shut-in conditions. A Shut-in is defined as when the impeller is stopped so that there is no mixing within the cell, but the thermodynamic conditions are kept stable. Shut-in conditions would be maintained for 12-16 hours at which point the impeller was restarted. If the impeller could no longer freely rotate in the cell, then the experiment was declared to be a plugging case. If the impeller could restart then the experiment could be declared either a non-plugging case or a borderline case. A borderline case would exist if the motor current profile during operating conditions was similar to a plugging case, i.e., regular fluctuations in the motor current indicating hydrate chunks are present in the system. This case would be declared borderline because even though the experiment did not plug after shut-in conditions, the presence of hydrate chunks suggests that the system could, in repeat cases, plug. A non-plugging case, therefore, is one which is able to restart successfully and also exhibits a smooth motor current profile, indicating a flowable hydrate slurry.

After shut-in conditions, the two blank experiments plugged upon restarting. When the cell was rapidly depressurized and opened, hard hydrate chunks were observed (Figure 3.4). The cell was put into shut-in conditions because in a real pipeline scenario, often time a flowing system will have a low risk of plugging, even if hydrate formation has occurred within the pipeline. Often, the real danger will occur if hydrates are present in a pipeline during shut-in conditions, i.e., flow is stopped (Sloan *et al.*, 2010). A pipeline may be shutdown for a number of different reasons such as; for maintenance, pigging, or because of an impending natural hazard. During this shut-in period, hydrate particles will have the opportunity to be in contact with each other for extended periods of time. This will usually lead to the hydrate particles agglomerating, and forming one large hydrate plug which can be difficult, and sometimes impossible, to move when the pipeline is restarted. Therefore, if a hydrate slurry system is to be suggested to the oil and gas industry, there must be evidence showing that the system will have a low risk of plugging by demonstrating flowability during operating conditions and after shut-in conditions.

(a) (b)

Figure 3.4: Hydrate chunks, obtained after depressurizing cell after shut-in conditions: (a) 75 vol.% WC; (b) 75 vol.% WC + 3.5 wt.% salt.

3.1.2 200T Mineral Oil with AA

Once the untreated mineral oil experiments had been established and found to plug as expected, experiments at the same water cut, 75 vol.%, were performed with various concentrations of anti-agglomerant (AA). The initial investigation examined the behavior of the model anti-agglomerant with and without salt. As an additional detail, according to CSMGem, which is a hydrate phase equilibrium prediction program developed by the Center for Hydrate Research (Sloan & Koh, 2008), the driving force (or subcooling, i.e., T_{eqm} - T_{op}) for hydrate formation when salt is present in the system is 6.7 °C compared to 8 °C when salt is not present. 2 wt.% of AA was chosen as it is within the concentration typically used in industry (Huo *et al.*, 2001), albeit the upper end of that concentration. The results from these two experiments can be observed in Figure 3.5.

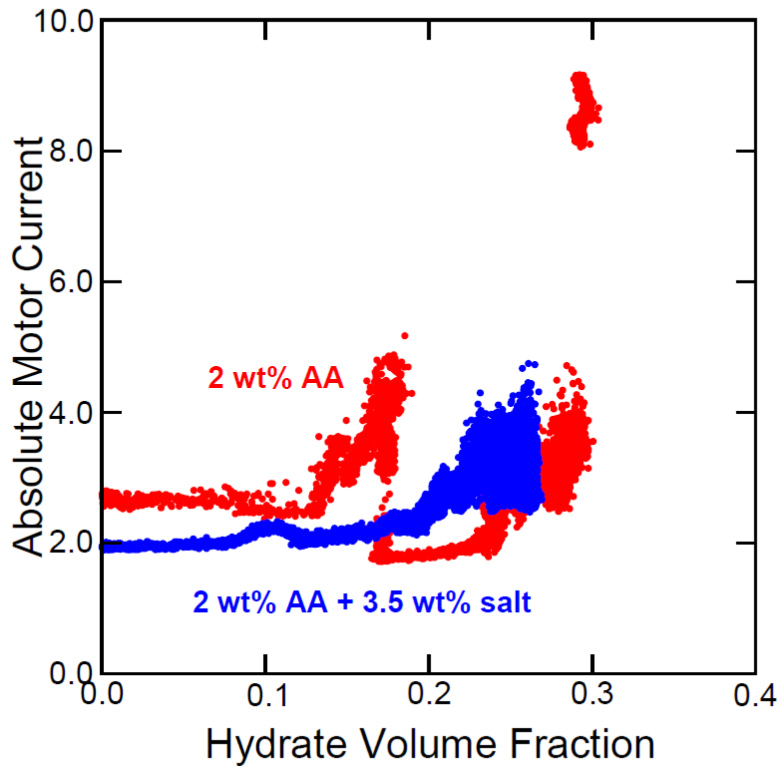

Figure 3.5: Motor current trace for the two AA experiments performed. Red trace: 75 vol.% WC, 200T mineral oil with 2 wt.% AA, no salt. Blue trace: 75 vol.% WC, 200T mineral oil with AA and salt. Experiment with no salt spiked at 30 vol.% hydates indicating a plug. With salt, experiment experienced motor current fluctuations and plugged after shut-in.

Following the red trace in Figure 3.5 (no salt) it can be seen that in this experiment a sharp increase in the motor current appeared at around 15 vol.% hydrates, which was then followed by a sharp decrease at around 18 vol.% hydrates. It is likely that at this point within the cell, large hydrate chunks were formed which were then broken up by the impeller, or displaced somewhere in the cell where the impeller was no longer encountering the hydrate chunks. Regardless of the event, it is clear from the motor current profile that hydrate chunks started to appear once again at around 30 vol.% hydrates and a plugging incident took place. This event was evident due to the large spike in the motor current, indicating that the impeller is straining against an immovable object, as well as a visual observance of the impeller being unable to move. The blue trace (with salt) did not plug during operating conditions, however, as can be observed, the motor current exhibited plugging tendency behavior (motor current fluctuations) and had plugged after shut-in conditions. The hydrate morphology was very similar to the base line plugging experiments as can be seen in Figure 3.6. Additionally, bottle tests indicated that the AA systems with and without salt would both form an oil-in-water emulsion, which, as has been discussed previously, can lead to a more likely plugging scenario. An additional experiment at 5 wt.% AA was performed in order to investigate whether an overdosing of anti-agglomerant could lead to a change in the plugging behavior of the system. The results obtained from this experiment showed no change in the behavior between 2 wt.% AA and 5 wt.% AA. The motor trace still indicated that hydrate chunks were present in the system and after shut-in conditions, the experiment had plugged.

To gain further understanding of what is happening in the mineral oil system, the bottles tests can be examined. Although bottle tests indicate that both systems will form an oil-in-water emulsion, the AA + salt emulsion system will phase separate much quicker than the AA only system. This suggests that there is an interaction between the salt and the AA that is accelerating the phase separation within the system. To understand this phenomenon, it is important to remember that the salt will dissolve into the water phase and the AA will dissolve into the oil phase. Taking the AA case only, it is known that in this system oil droplets will be suspended

(a) (b)

Figure 3.6: Hydrate chunks, obtained after depressurizing cell after shut-in conditions: (a) 75 vol.% WC +2 wt.% AA ; (b) 75 vol.% WC + 2 wt.% AA + 3.5 wt.% salt.

in water. Assuming that the surfactant is located at the oil/water interface, the hydrophobic tail will be in the oil phase and the hydrophilic head will be in the water phase. In this arrangement, the emulsion will be stable as the surfactant will help to stabilize the suspended oil droplets. The surfactant keeps the oil droplets suspended due to the repulsion interaction between the cationic head groups. This repulsion effect keeps the droplets from agglomerating together and so maintains the emulsion. When salt is added to this system there will be a new attractive interaction between the negative Cl^- ions and the cationic head group. This positive interaction will have the overall effect of reducing the repulsion interaction between the surfactant molecules, which means, when two oil droplets approach each other, they will likely agglomerate together causing the emulsion to become destabilized and two separate, water and oil phases to appear (Figure 3.7). The conclusion from this observation is that the mineral oil system will tend to form an oil-in-water emulsion, which increases the likelihood that this type of system will plug.

3.1.3 200T Mineral Oil with MeOH

Experiments with various concentrations of methanol (MeOH) were performed at 75 vol.% WC with 200T mineral oil. The purpose of this series of experiments was to find the MeOH concentration where the system would no longer plug. Once this

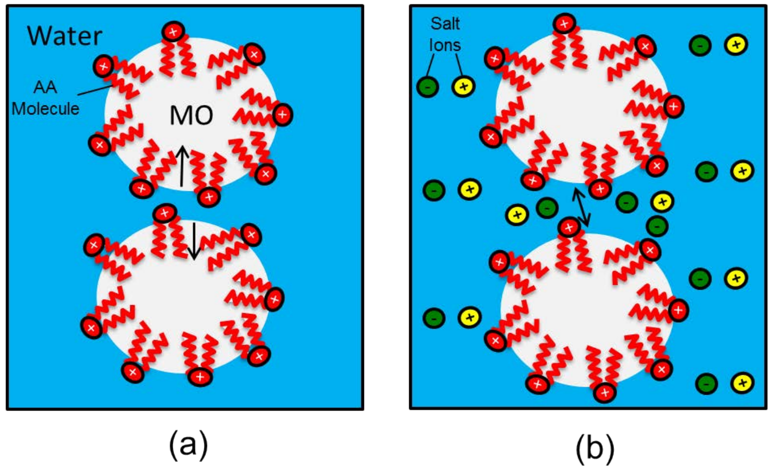

Figure 3.7: Conceptual picture depicting surfactant and salt effect on emulsion: (a) Surfactant only; cationic charge on surfactant repulses other droplets. (b) Surfactant in the presence of salt; salt reduces repulsive charges between molecules allowing droplets to agglomerate together.

concentration had been identified, the idea was to use a concentration of MeOH that would plug, and then attempt to alleviate this plug by adding anti-agglomerant. It is known that the mineral oil system at 75 vol.% WC with up to 5 wt.% AA leads to a plug, if the combination of AA and MeOH helped the system to not plug, then it could be concluded that there was a synergistic effect between the two chemicals. Two MeOH systems were tested, 2.5 wt.% and 5 wt.%, and both systems formed a water-in-oil emulsion.

Figure 3.8 shows the two experiments that were run at 2.5 and 5 wt.% MeOH. Both experiments were run at 75 vol.% WC and 3.5 wt.% salt water. According to CSMGem calculations, the driving force (subcooling) for hydrate formation was 5.6 and 4.4 °C, respectively. The red trace in Figure 3.8 shows the 2.5 wt.% MeOH which plugged after shut-in conditions. At around 24 vol.% hydrates, this experiment exhibited some smaller chunks of hydrate as indicated by the relatively small, yet frequent spikes in the motor current trace. This experiment plugged after shut-in conditions. The blue trace shows the 5 wt.% MeOH experiment. The motor current trace indicates that no significant hydrate chunks were present in the system and that the hydrates that were formed remained in a flowable hydrate slurry. Even after shut-in conditions, this experiment had not plugged indicating that at 5 wt.% MeOH, a non-plugging situation can be achieved. At the thermodynamic operating conditions for this experiment, 14 wt.% of MeOH as well as 3.5 wt.% of salt have to be present in the system for total inhibition. That is, hydrate formation conditions are displaced to harsher conditions than the operating conditions. This means that when only 40% of the full inhibition amount is used, a flowable hydrate slurry can be achieved. To clarify this point, taking 5 wt.% and dividing it by the 14 wt.% it would take to fully inhibit a system at these thermodynamic conditions, it can be seen that 5 wt.% is around 40% of the total inhibition amount.

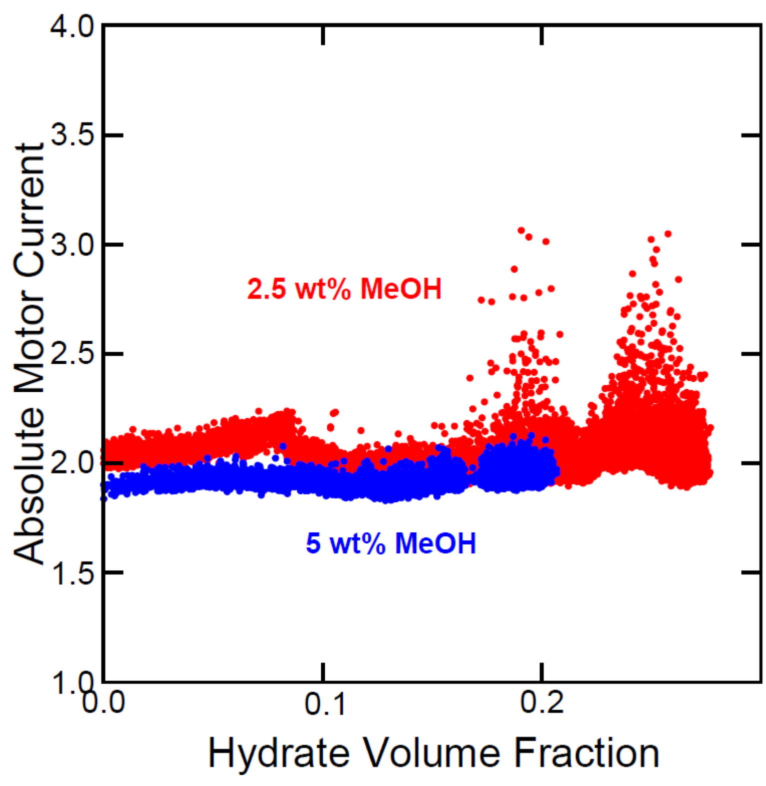

Figure 3.8: Motor current traces for 200T mineral oil under-inhibited with MeOH. Red trace shows 200T mineral oil, 75 vol.% WC, 3.5 wt.% salt + 2.5 wt.% MeOH. Experiment did plug after shut-in conditions. Blue traces shows 200T mineral oil, 75 vol.% WC, 3.5 wt.% salt + 5 wt.% MeOH. Experiment did not plug after shut-in conditions.

Looking at Figure 3.9, it appears that the morphology of the 2.5 wt.% MeOH experiment is much different than the hydrate morphology for the AA or even the blank experiments. The hydrates from this experiment appear to be coated with a layer of water, making them appear to be very wet. This is not an unknown effect, as previous authors have suggested and reported that under-inhibiting a system with MeOH can lead to a worse plugging scenario than if there was no MeOH present in the system whatsoever (Hemmingsen *et al.*, n.d.).

(a) (b)

Figure 3.9: Hydrate morphology for experiments under-inhibited with MeOH: (a) 75 vol.% WC, 3.5 wt.% salt + 2.5 wt.% AA. Very wet, agglomeration of hydrates.; (b) 75 vol.% WC, 3.5 wt.% salt + 5 wt.% MeOH. Hydrate slurry.

Examining why the hydrate morphology appears to be different when under-inhibiting with MeOH, it is important to think about the main reason MeOH is used in a system. MeOH inhibition is used in order to stop hydrates from forming by tying up the water, so that it is not free to take part in hydrate formation. If only a small amount of MeOH is injected, then it can be assumed that only a small amount of water will be tied up in this way. Therefore, although a reduction in the amount of hydrates formed will be observed, it will tend to only be a slight reduction. Indeed, the reduction between the experiment with salt and no MeOH and with 2.5 wt.% MeOH and salt is around 7 vol.% hydrates. Although a relatively small amount, this equates to an extra 53 ml that will remain in the water phase. This extra water is now free to coat the hydrate particles that form, which, as discussed earlier, can allow liquid bridges to form between the hydrate particles which in turn can lead to strongly agglomerated hydrate chunks, such as the ones observed in Figure 3.9.

As the MeOH concentration is increased, even more water will be tied up and will remain in the liquid phase. In the 5 wt.% MeOH experiment, the reduction in the hydrate volume fraction is now around 14 vol.%, equating to 137 ml extra water in the system. As observed in Figure 3.9 this causes a hydrate slurry to appear where only smaller hydrate particles exist, rather than large, strongly agglomerated hydrate chunks. The appearance of a hydrate slurry occurs because now there is an abundance of water system, and liquid bridges will not be able to form between particles. Effectively this abundance of water actually prevents the hydrate particles from agglomerating together because there is a smaller chance of the particles encountering each other. If the hydrates cannot encounter other hydrate particles, then they cannot agglomerate together and form larger particles. This reduction in the hydrate volume also effectively helps to maintain a flowable hydrate slurry. A conceptualized picture of this effect is shown in Figure 3.10.

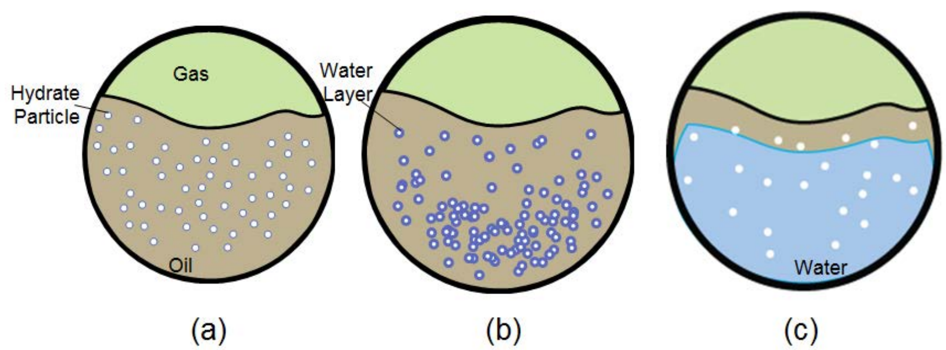

Figure 3.10: Conceptual picture of MeOH under-inhibition: (a) No MeOH present, all water available for hydrate formation; (b) 2.5 wt.% MeOH, water coats hydrate particles leading to strongly agglomerated hydrate chunks; (c) 5 wt.% MeOH, liquid bridges break down and reduced number of hydrate particles.

3.1.4 200T Mineral Oil with MeOH and AA

Now that it was known that the mineral oil system would plug at 2.5 wt.% MeOH and with any concentration of AA, a series of experiments were performed to investigate whether combining MeOH and AA in the same system would have any beneficial effect, i.e. prevent the system from plugging.

Two sets of experiments were performed using a combination of AA and MeOH. 2 wt.% AA + 2.5 wt.% MeOH and 2 wt.% AA + 5 wt.% MeOH. The first experiment was performed to investigate whether this combination could help convert a plugging case to a non-plugging case by utilizing a synergistic effect between the two chemicals. The second experiment was performed to understand whether any additional benefit could be gained in the hydrate slurry when AA was added. These experimental traces can be observed in Figure 3.11.

Before going deeper into the data presented here, it is important to note that there are two perspectives when looking at these data. It can be looked at either by examining it in comparison to the experiments run with AA and salt or, the experiments run with MeOH and salt. For completeness, the following discussion will look at both standpoints, starting with the MeOH only point of view.

Looking at the red trace which depicts the 2 wt.% AA + 2.5 wt.% MeOH experiment and comparing it to the 2.5 wt.% MeOH from Figure 3.8, it appears that the addition of AA has done a number of things to change the system. The first change is that the motor current appears to be much smoother than the 2.5 wt.% experiment. This suggests that there is a lack of hydrate chunks present in the system, as hydrate chunks would cause spikes to appear in the motor current trace. In the 2.5 wt.% MeOH experiment, some small spikes were appearing in the motor current trace, suggesting small hydrate chunks, but the absence of spikes from the AA and MeOH experiment would suggest that the addition of AA is able to keep the hydrates from agglomerating together. The second apparent effect that the addition

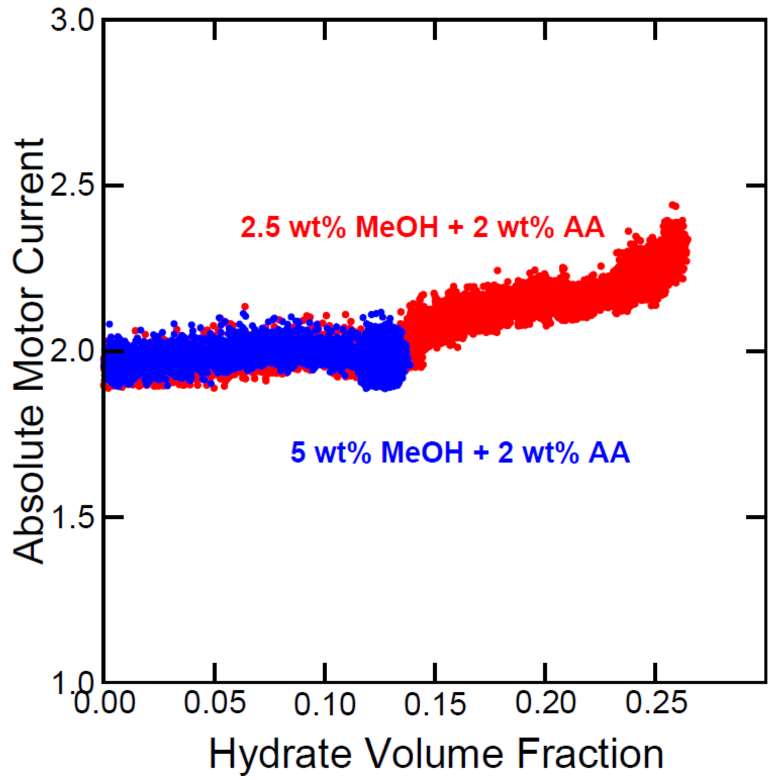

Figure 3.11: Motor current traces for 200T mineral oil under-inhibited with MeOH and AA. Red trace shows 200T mineral oil, 75 vol.% WC, 3.5 wt.% salt, 2.5 wt.% MeOH + 2 wt.% AA. Experiment did plug after shut-in conditions. Blue traces shows 200T mineral oil, 75 vol.% WC, 3.5 wt.% salt, 5 wt.% MeOH + 2wt.% AA. Experiment did not plug after shut-in conditions.

of AA has is to increase the fluid viscosity. This is indicated by the large increase in the motor current. It is likely then that the overall picture here is that a significant amount of hydrate formation is taking place, causing the fluid viscosity to increase, however, the particle size is remaining small, as indicated by the lack of spikes in the motor current. After shut-in conditions, however, this experiment had plugged and soft hydrate chunks were observed after depressurizing the system (Figure 3.12). This suggests that during shut-in conditions the small hydrate particles agglomerated together despite the presence of the anti-agglomerant. These results indicate that the model anti-agglomerant is most effective when the system is under flow but that no advantage is gained during shut-in conditions.

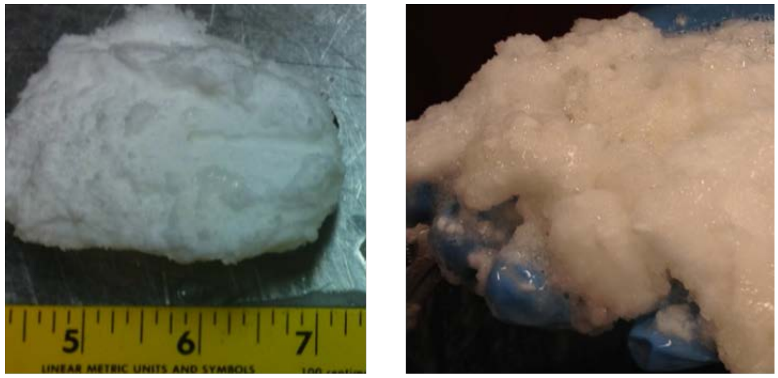

(a) (b)

Figure 3.12: Hydrate morphology from mineral oil MeOH and AA experiments. (a) 75 vol.% WC + 2.5 wt.% MeOH + 2 wt.% AA + 3.5 wt.% salt. Soft hydrate chunks. (b) 75 vol.% WC + 5 wt.% MeOH + 2 wt.% AA + 3.5 wt.% salt. Hydrate slurry with small chunks of hydrate.

The 5 wt.% MeOH + 2 wt.% AA experiment does not exhibit significantly different behavior when compared to the 5 wt.% MeOH experiment. Both experiments show smooth motor currents indicating that large hydrate chunks did not form. The motor current also did not change much from its original base line value, indicating that the fluid viscosity also did not increase significantly. The only real difference between the two experiments is that the 5 wt.% MeOH + 2 wt.% AA appeared to form about 8 vol.% less hydrates. This suggests that the presence of the AA is helping with hydrate inhibition via an unknown mechanism. When the 5 wt.% MeOH + 2 wt.% AA is compared to the 2 wt.% AA case it is clear that the severe reduction in the hydrate volume has helped to eliminate the hydrate chunks and subsequent hydrate plug that formed in the 2 wt.% AA experiment.

Examining Figure 3.11 and Figure 3.5 the 2.5 wt.% MeOH + 2 wt.% AA + 3.5 wt.% salt experiment can be compared to the 2 wt.% AA + 3.5 wt.% salt experiment. The behavior between these two experiments appears to be similar, where a relative increase in the motor current can be observed once the hydrate volume fraction reaches around 15 vol.%. However, once the volume fraction reaches around

22 vol.% in the 2 wt.% AA + 3.5 wt.% salt experiment the motor current starts to experience fluctuations in the motor current. These fluctuations appear to be mostly absent from the 2.5 wt.% MeOH + 2 wt.% AA + 3.5 wt.% salt experiment suggesting that the presence of large hydrate chunks is low during operating conditions. This would suggest that the presence of MeOH is assisting in keeping the hydrate particle size low. In this case, the MeOH could be acting as a co-surfactant with the AA (York & Firoozabadi, 2008). In this case the mechanism allowing MeOH to act as a co-surfactant is similar to the mechanism that exists between the salt and the anti-agglomerant that has been discussed previously, namely there will exist an interaction between the negative OH ions from the MeOH and the cationic head group from the surfactant molecule. As in the case with the salt and surfactant, the repulsive interaction between the anti-agglomerant will be reduced which will allow the surfactant packing factor at the oil/water interface to be increased. This increase in the packing factor will essentially increase the anti-agglomerants effectiveness making it more useful at keeping the hydrate particles away from each other, possibly via an alternative mechanism such as steric repulsion. This line of thought would also help to explain why after shut-in conditions hydrate chunks are observed (Figure 3.12) despite not being detected by fluctuations in the motor current. Once shut-in conditions are reached, the mechanisms mentioned before, lead to a rapid phase separation which allows the hydrate particles to come into physical contact with each other, allowing them to agglomerate and create larger hydrate chunks that plug the system upon restart.

3.2 500T Mineral Oil

This section will describe the short study that was performed with 500T mineral oil. As mentioned previously, this oil was selected to be studied as it has a similar density and viscosity to the crude oil being studied than the 200T mineral oil. Crude oil viscosity was 100 ±1.5 cP at 20 °C and 100 s^{-1}, density was 0.908 ±0.003 g/cm^3.

500T viscosity was 88 cP at 37.8 °C, density was 0.864 g/cm^3. The objective behind this short study was to investigate whether physical properties would make a difference in the results observed or if the chemical properties would be a more telling factor. This objective is realized by comparing the results between the 200T and the 500T mineral oil. Experiments performed with 500T mineral oil were performed using exactly the same parameters and procedures used with the 200T mineral oil.

3.2.1 Untreated 500T Mineral Oil

As with the 200T mineral oil, a baseline had to be established with the 500T, i.e. what would happen to the system at 75 vol.% WC when no extra chemicals were present. Two experiments were performed to establish this baseline, 75 vol.% WC and 75 vol.% WC + 3.5 wt.% salt. The results from these experiments can be observed in Figure 3.13. These results can be compared to the 200T mineral oil by examining Figure 3.13 and Figure 3.3. Examining the 200T and 500T cases with no salt there are a couple of minor differences but nothing significant. Following the motor traces, it is clear from the spikes that both systems formed hydrate chunks during operating conditions, although the 500T experiment formed a significantly higher volume of hydrates than the 200T experiment. The 500T experiment also plugged during operating conditions as indicated by the spike in the motor current. Although this spike subsides a little, the motor current remains high indicating that once the experiment plugged it did not unplug.

Both experiments with salt show very consistent behavior between the two systems as well as a comparable hydrate volume. Additionally bottle tests show that these systems form an oil-in-water emulsion which is consistent with the 200T results and with the hydrate morphology observed at the end of the experiment (Figure 3.14.

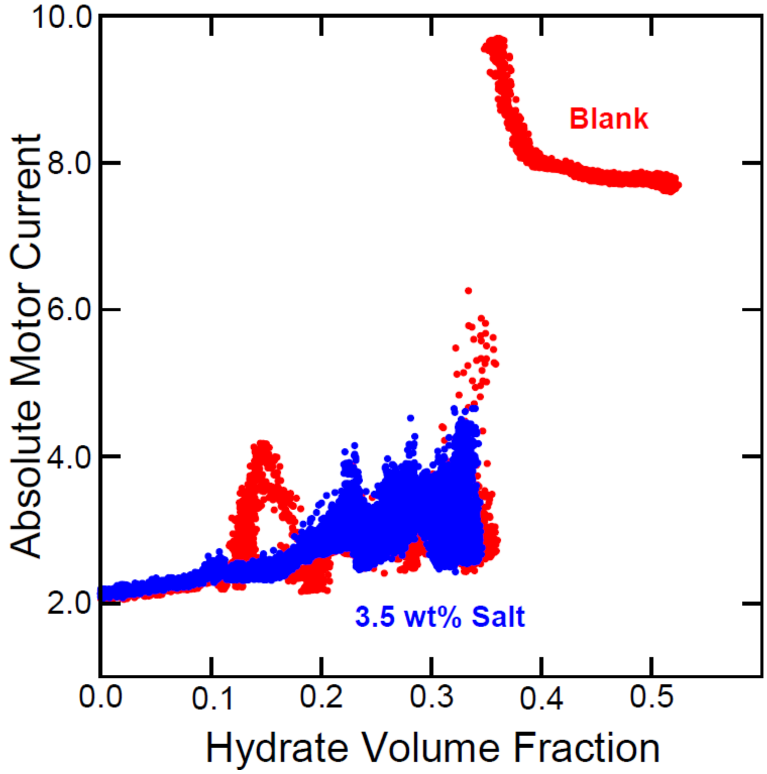

Figure 3.13: Motor current trace for the two base line experiments performed with 500T mineral oil. Red trace: 75 vol.% WC. Experiment did plug during operating conditions. Blue trace: 75 vol.% WC + 3.5 wt.% salt. Experiment did plug after shut-in conditions.

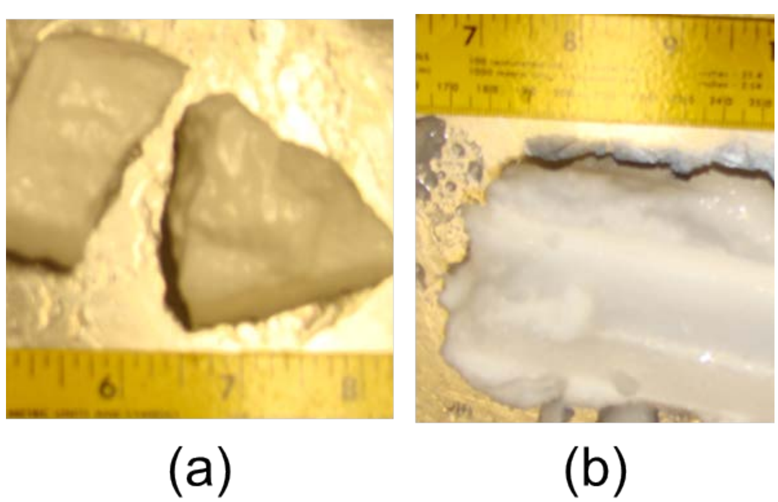

Figure 3.14: Hydrate morphology for the two base line experiments performed with 500T mineral oil. (a) 75 vol.% WC, hydrate chunks. (b) 75 vol.% WC+ 3.5 wt.% salt, hydrate chunks.

3.2.2 500T Mineral Oil with AA

Once the base cases were established, studies moved on to investigate the effects of adding AA to the 500T mineral oil system. Two different systems were studied here, 2 wt.% AA and 2 wt.% AA + 3.5 wt.% salt, to investigate whether there were any differences in the behavior between 200T and 500T. The results of these experiments can be observed in Figure 3.15. Comparing Figure 3.15 and Figure 3.5 behavior between the two systems is similar. The red traces, the 2 wt.% AA experiments, plugged during running conditions; although, the 500T system plugged much quicker than the 200T system. The blue traces, the 2 wt.% AA + 3.5 wt.% salt experiment, show much the same behavior between the 200T and 500T, where hydrate chunks were experienced around 23 vol.% hydrates. Additionally both systems did not plug during operating conditions but plugged after shut-in. Hard chunks of hydrate were observed at the end of the experiment, as can be observed in Figure 3.16. Bottle tests indicated that all systems formed the same type of emulsion, oil-in-water.

3.3 Chapter Conclusions

From the work performed with mineral oil, a number of baseline cases have been measured to compare to crude oil. From these experiments it can be seen that adding AA to mineral oil will not help the system to remain non-plugging, even when the system is overloaded with 5 wt.% AA. This is likely due to the fact that the system forms an oil-in-water emulsion and so the AA is not able to effectively keep the hydrate particles form agglomerating together. Experiments also showed that when the system is under-inhibited with 5 wt.% MeOH it produces a low viscosity fluid that does not plug, indicating that a system can be successfully under-inhibted with only 40% of the full inhibition amount. When combining MeOH and AA together in the same system, no real benefit appears to be achieved. The 2.5 wt.% MeOH + 2wt.% AA system still plugged after shut-in conditions, again likely due to the fact that this

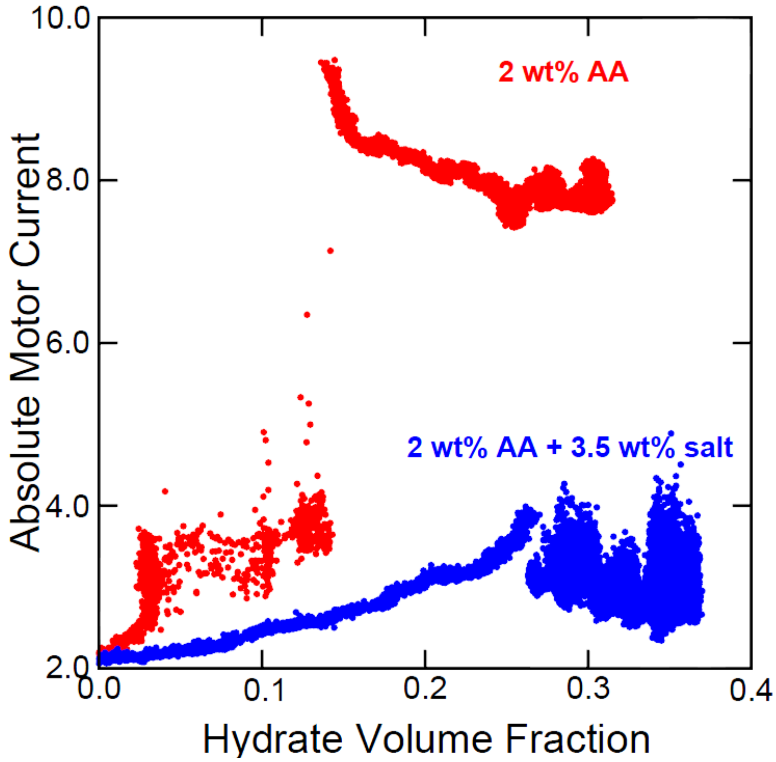

Figure 3.15: Motor current trace experiments performed with AA and 500T mineral oil. Red trace: 75 vol.% WC + 2 wt.% AA. Experiment did plug during operating conditions. Blue trace: 75 vol.% WC + 2 wt.% AA + 3.5 wt.% salt. Experiment did plug after shut-in conditions.

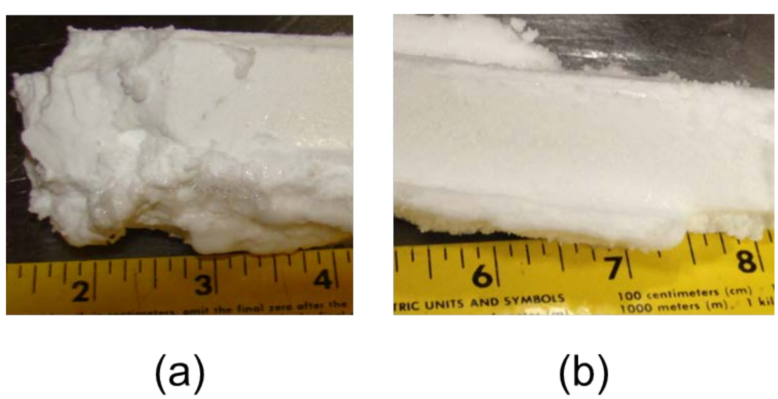

Figure 3.16: Hydrate morphology from experiments performed with AA and 500T mineral oil.(a) 75 vol.% WC + 2 wt.% AA, hydrate chunks. (b) 75 vol.% WC + 2 wt.% AA + 3.5 wt.% salt, hydrate chunks

system formed an oil-in-water emulsion. Before plugging the motor current appeared to be very smooth indicating a flowable system, however after shut-in conditions, the hard plug that had appeared made it clear that the system was, overall, a plugging system. When 5 wt.% MeOH was added to 2 wt.% AA the system was non-plugging, however, no clear advantage appeared to be gained by combing the two systems, since 5 wt.% MeOH on its own produced a non-plugging, low viscosity fluid. The overall conclusion from this portion of work is that under-inhibition can work but no clear benefit is gained by combing AAs and MeOH together into the same system.

CHAPTER 4

CRUDE OIL

This section will detail the work performed with the crude oil. It is highly recommended that the reader have read at least, chapter two and three before this chapter, as many of the procedures and mechanisms that are discussed throughout this chapter have been explained in these previous chapters. This work is similar to the mineral oil work, in that it investigates the crude oil system without the addition of chemicals and with the addition of chemicals in order to understand the different effects of adding each chemical. In addition, these results will be frequently compared to the mineral oil experiments, as these experiments were intended to be run as a base case to the crude oil, to investigate the differences between using an oil with no natural chemistry present and an oil with natural chemistry present. Additionally, this chapter is split into two sections, work done at 75 vol.% WC and work done at 50 vol.% WC.

4.1 75% WC

The study with crude oil was expanded to include two different water cuts in order to investigate the effect of water cut on hydrate slurry formation. Part of the motivation for this expansion was because AAs are known to behave differently at high water cuts. It was hoped that by varying the water cut, this anomalous behavior could be observed.

4.1.1 Untreated Crude Oil

As with the mineral oil investigation, the first step was to investigate the behavior of crude oil at 75 vol.% WC with no other chemicals present other than salt. Two experiments were run to establish this baseline, 75 vol.% WC and 75 vol.% WC +

3.5 wt.% salt. The results from these two experiments can be observed in Figure 4.1. The results from these runs are very similar to the results observed with the baseline scenarios run with the mineral oil systems. Following the red trace in Figure 4.1 it can be observed that this experiment plugged during operating conditions after forming 40 vol% of hydrates. In the blue trace, however, the stochastic behavior of plugging in the autoclave cell during operating conditions can be well observed. Even though the experiment with salt also formed around 40 vol% of hydrates, which according to the motor current were large chunks of hydrate, this experiment did not plug during operating conditions. After shut in conditions, however, the autoclave cell had plugged. After depressurizing the cell hard chunks of hydrates were observed as can be seen in Figure 4.2.

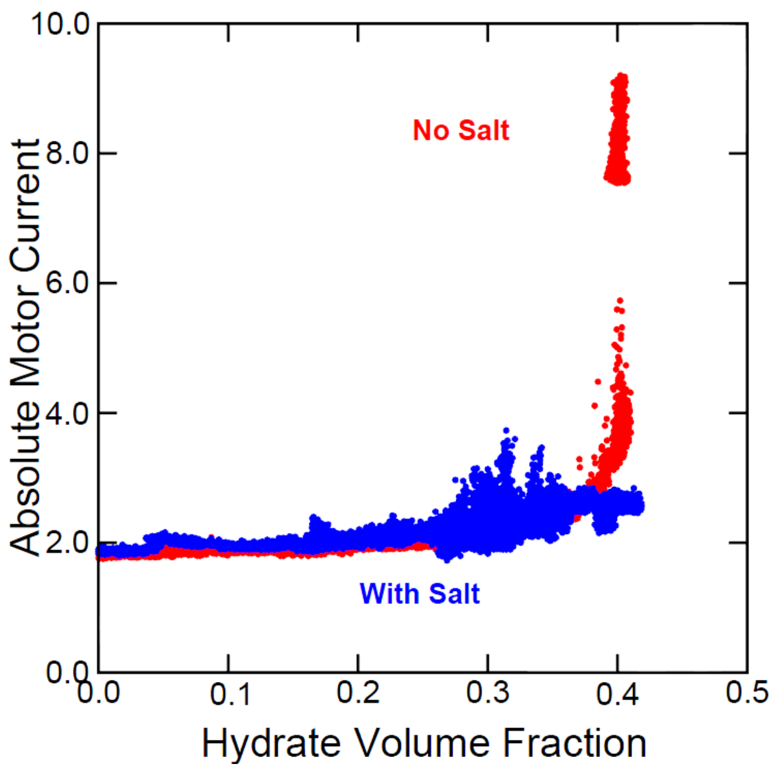

Figure 4.1: Motor current traces showing the baseline experiments performed for crude oil. Red trace: 75 vol.% WC. Experiment plugged during operating conditions as indicated by extreme spike in motor current. Blue trace: 75 vol.% WC + 3.5 wt.% salt. Experiment plugged after shut in conditions. Spikes in motor current indicate presence of hydrate chunks.

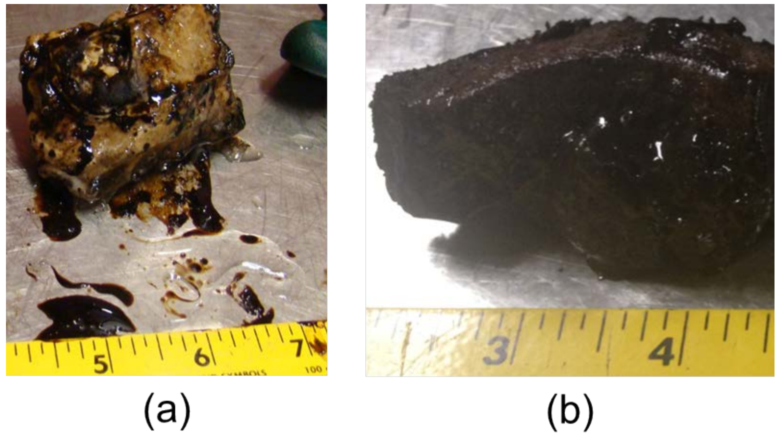

Figure 4.2: Hydrates obtained from crude oil baseline experiments after depressurization: (a) Hydrate chunks from 75 vol.% WC; (b) Hydrate chunks from 75 vol.% WC + 3.5 wt.% salt.

When the bottle tests were performed on the two systems it was found that they both formed a water-in-oil emulsion, which is the opposite from that formed by the baseline mineral oil systems. The implication of these results is twofold. The first implication is that the plugging mechanism that crude oil system followed would be different than the mechanism followed by the mineral oil baseline experiments. The details of this mechanism can be found in chapter two. The second implication is that the natural chemistry present in the crude oil is having a significant effect on the type of emulsion it forms, likely due to the presence of natural surfactants. Since, the type of emulsion formed can have significant effects on factors such as plugabillity, etc. it can be expected that the behavior observed in crude oil will have several key differences to the behavior that has been observed in mineral oil.

4.1.2 Crude Oil with AA

Once it was established that the 75 vol.% WC and salt crude oil system with no added chemicals would plug, the effects of adding anti-agglomerants to this system was investigated. The chosen baseline AA concentration was 2 wt.%. Two different systems were tested using this concentration. One system had 3.5 wt.% salt present while the other did not. The motor current traces for both runs can be observed in Figure 4.3.

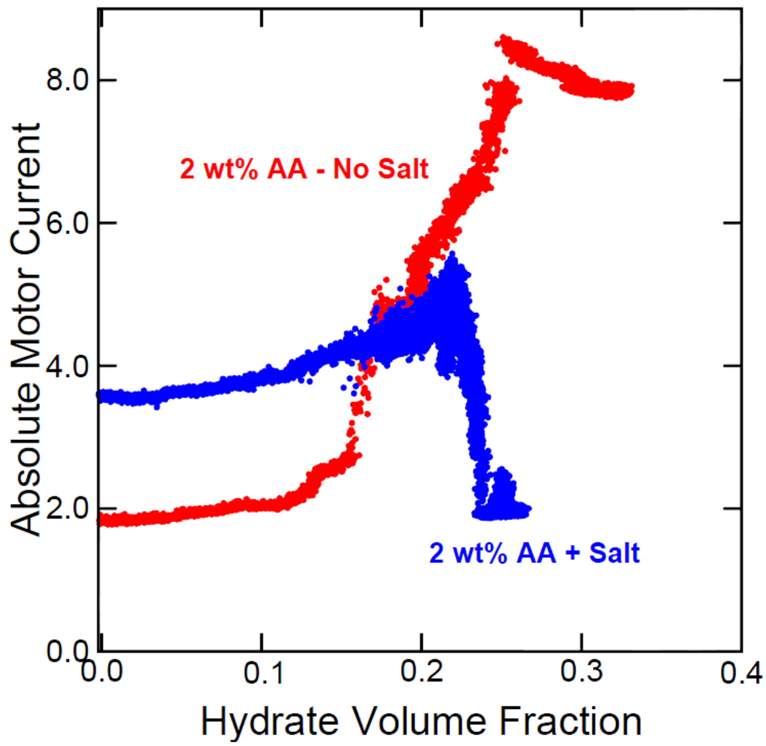

Figure 4.3: Motor current traces showing the AA with salt and with no salt experiments performed for crude oil. Red trace: 75 vol.% WC + 2 wt.% AA. Experiment plugged during operating conditions as indicated by spike in motor current. Blue trace: 75 vol.% WC + 2 wt.% AA + 3.5 wt.% salt. Soft, flowable hydrate slurry formed. Experiment didnt plug after shut in conditions.

Examining the two motor current traces in Figure 4.3 it is clear that there was significant difference in behavior indicating that the combination of AA and salt and crude oil is having a considerable effect on the system behavior. This is indicated by the experiment with no salt plugging during operating conditions, indicating that solid chunks of hydrate had formed impeding the impellers ability to rotate within the cell. This is in contrast to the non-plugging behavior of the blue trace, i.e. the experiment that did have salt present. The blue motor current trace starts off fairly high and continues to increase as more and more hydrates form. However, once hydrate formation is about 90% complete, the motor current drops off substantially, indicating that the fluid viscosity has decreased significantly. In addition, the hydrate morphology observed at the end of this experiment (Figure 4.4) is very different from the experiment with no salt. The hydrate morphology from the experiment with no salt is similar to the baseline experiments with no chemicals present, hard chunks of hydrate that are not easily broken. However, the hydrate morphology from the experiment with salt looks more like a hydrate slurry which easily falls apart to the touch.

(a) (b)

Figure 4.4: Hydrates obtained from crude oil AA experiments after depressurization: (a) Hydrate chunks from 75 vol.% WC + 2 wt.% AA; (b) Hydrate slurry from 75 vol.% WC + 2 wt.% AA + 3.5 wt.% salt.

The investigation was extended to cover a range of AA concentrations in order to discover the limit of the AA and salt in combination. The AA limit in this case would be defined as the lowest AA concentration that stops the system from plugging. The concentrations investigated were, 2 wt.% AA, 0.5 wt.%, 0.3 wt.% AA and 0.1 wt.% AA, all with 3.5 wt.% salt. The results of these experiments can be observed in Figure 4.5.

As can be observed from Figure 4.5 it is apparent that the non-plugging behavior that was observed when AA and salt were combined can be seen in concentrations down to 0.5 wt.% AA. The morphology from 2 and 0.5 wt.% AA experiments can be observed in Figure 4.6. These two non-plugging experiments formed a flowable hydrate slurry. The 0.3 wt.% AA experiment also did not plug after shut in conditions

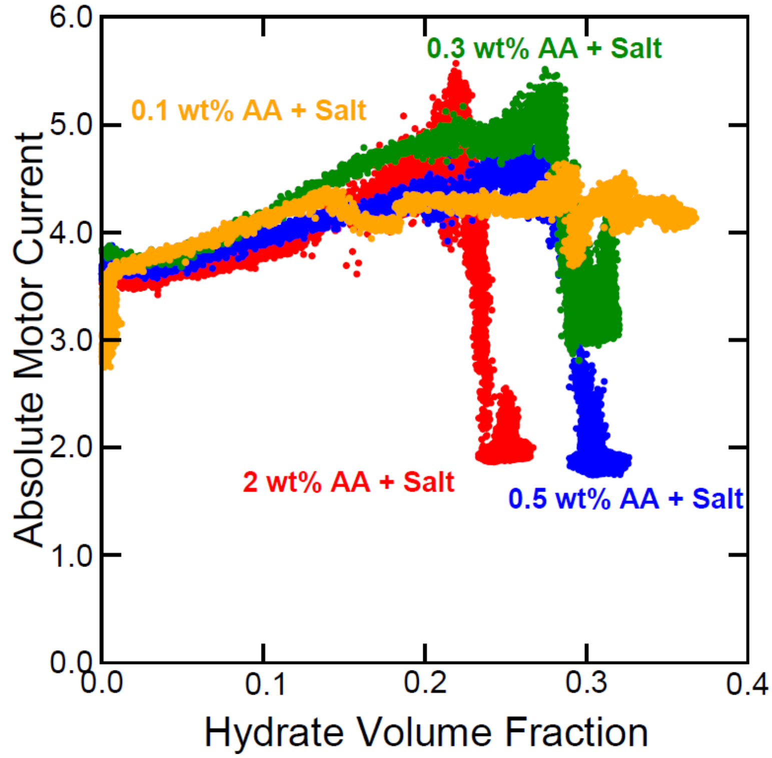

Figure 4.5: Motor current traces showing the AA with salt expeirments. Red trace: 75 vol.% WC + 2 wt.% AA + 3.5 wt.% salt. Experiment did not plug after shut-in conditions. Blue trace: 75 vol.% WC + 0.5 wt.% AA + 3.5 wt.% salt. Experiment did not plug after shut-in conditions. Green trace: 75 vol.% WC + 0.3 wt.% AA + 3.5 wt.% salt. Experiment did not plug after shut-in conditions. Orange trace: 75 vol.% WC + 0.1 wt.% AA + 3.5 wt.% salt. Experiment did plug after shut-in conditions.

although it is apparent from the motor current and the hydrate morphology (Figure 4.7) that, at this concentration, the limit of this type of system is being reached. Indeed when 0.1 wt.% AA was used, the experiment plugged after shut in conditions. The consequence of this lower AA concentration appears to be small hydrate chunks appearing in the hydrate morphology, which makes sense, as there is not enough AA present to keep the hydrate particles from agglomerating together. These hydrate chunks are most likely what cause the system to plug after shut in conditions. As mentioned the 0.3 wt.% experiment appears to be the borderline case as the motor current trace does not go down to the same level as the 0.5 and 2 wt.% AA cases, which are clearly non-plugging systems. In addition to this, the hydrate morphology shows that there were some very small chunks of hydrate in this system suggesting that the effectiveness of the AA starts to decrease once the concentration is lowered to 0.3 wt.% AA and below. An important aspect to note about these experiments is that the volume of hydrates formed throughout these experiments remains fairly high and is on par with other experiments that did plug. This indicates that the reason the hydrate slurry is flowable is not because of a decrease in the hydrate volume fraction, but is rather because of a increase in the ability of the hydrates to remain dispersed throughout the system.

(a) (b)

Figure 4.6: Hydrate morphology from the AA with salt expeirments. (a) 75 vol.% WC + 2 wt.% AA + 3.5 wt.% salt Hydrate slurry. (b) 75 vol.% WC + 0.5 wt.% AA + 3.5 wt.% salt Hydrate slurry.

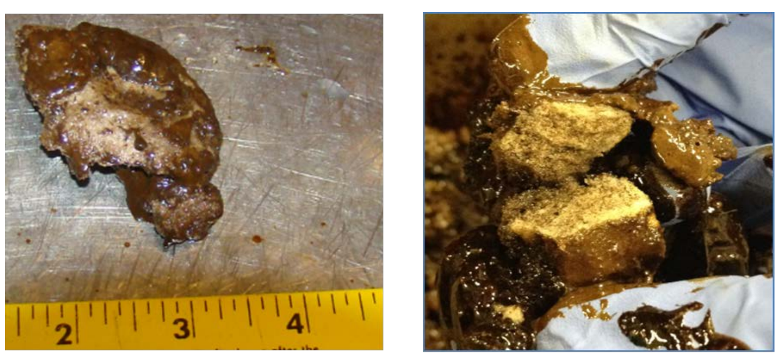

(a) (b)

Figure 4.7: Hydrate morphology from the AA with salt expeirments. (a) 75 vol.% WC + 0.3 wt.% AA + 3.5 wt.% salt Hydrate slurry with small chunks. (b) 75 vol.% WC + 0.1 wt.% AA + 3.5 wt.% salt Small hydrate chunks.

4.1.3 AA Emulsion Test Investigation

As with the previous systems, bottle tests were performed on the AA systems in order to investigate what type of emulsions were formed. The results from the bottle tests revealed that the 2 wt.% AA system with no salt would form an oil-in-water emulsion, while the 2 wt.% AA + 3.5 wt.% salt system formed a water-in-oil system. Therefore the addition of salt to the AA system is inverting the emulsion type. This is not an uncommon occurrence, as it is a well-documented fact that changing the salinity of a system has a direct impact on the emulsion type (Salager *et al.*, 1983). This inversion in emulsion type helps to explain why the addition of salt can convert the system from plugging to non-plugging. In the oil-in-water emulsion, since the surfactant is oil soluble, it is not able to keep the hydrate particles from agglomerating together. Therefore, the hydrate particles will agglomerate together to form large chunks that will plug the system. When the water is dispersed in the oil phase however, the surfactant located at the oil/water interface will be able to keep the water droplets and since the AA should also be able to adhere to the hydrate surface, the hydrate particles will also be kept from agglomerating together (Lo *et al.*, 2010). A conceptual diagram of the oil-in-water mechanism can be observed in Figure 3.7, the water-in-oil mechanism is shown in Figure 4.17. It is suspected that the inability of the mineral oil system to form a water-in-oil system is one of the major reasons the addition of AA and salt is unable to prevent this system from plugging. This highlights the importance of the natural chemistry in the crude oil, that it is crucial for the non-plugging behavior observed in the crude oil, AA and salt system. Identifying which component in the crude oil is key to the non-plugging behavior is a difficult task due to the complex nature of crude oil chemistry.

In addition to the bottle tests, autoclave emulsion tests were performed. Autoclave emulsion tests were carried primarily to test whether the emulsions produced with the bottle tests were consistent with the emulsions produced by the autoclave. To investigate this the autoclave cell is loaded with the fluids as has been described previously, however for the initial tests the cell was not pressurized with methane gas, since the bottle tests were not performed using methane. Additionally the tests were run at 20 °C so hydrates are not formed during these autoclave emulsion tests. Therefore, any changes to the motor current will solely be due to a change in the fluid viscosity and not due to the appearance of solids. The initial set of results for 2 wt.% AA and 2 wt.% AA + 3.5 wt.% salt can be observed in Figure 4.8.

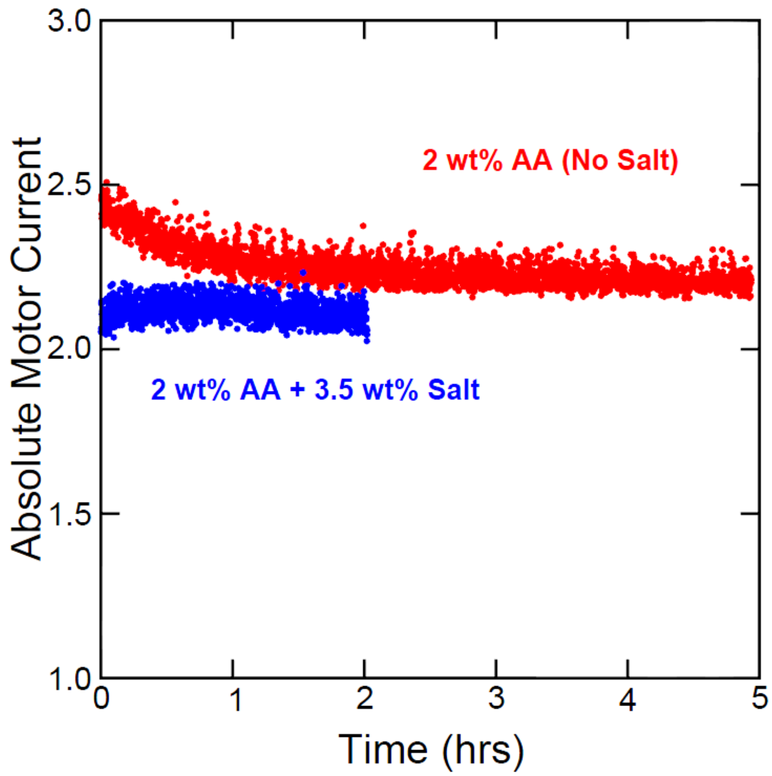

Figure 4.8: Motor current traces showing the emulsions test performed with AA + salt and AA with no salt. Red trace: 75 vol.% WC + 2 wt.% AA. Blue trace: 75 vol.% WC + 2 wt.% AA + 3.5 wt.% salt.

Figure 4.8 shows that both systems formed the same type of emulsion that was formed in the bottle tests. What is interesting to note from this figure however, is that the motor current for the 2 wt.% AA + 3.5 wt.% salt system is much lower in the autoclave cell emulsion test than it was at the start of the hydrate formation experiment, which can be confirmed by comparing this figure and Figure 4.3. As can be seen, there is a difference of around 1.8 mA between the motor currents. This discrepancy between the hydrate and emulsion experiment cannot be due to the presence of solids as solids have not had a chance to form in either experiment. In addition, previous tests have indicated it would take a large volume of solids in the cell to cause such a large increase in the motor current, therefore, another factor must be involved. The only other two differences between the emulsion experiment and the trace shown for the hydrate experiment is that the emulsion experiment is run at 20 °C and has no methane present, while the hydrate experiment does have methane present and the temperature is around 2 °C at the point of hydrate nucleation. In order to rule out the operating temperature being the cause of this discrepancy, the motor current trace for the saturation period of the experiment can be examined. As described in chapter two, the saturation period involves saturating the phases with gas at 20 °C, at the same temperature that the emulsion experiment was run at. The motor current trace for the saturation period can be observed in Figure 4.9 alongside a repeat on the 2 wt.% AA + 3.5 wt.% salt emulsion test. Both runs were performed at 20 °C. The only difference between the two runs is that the red trace has methane present and the blue trace does not. In addition to this, the motor current trace between the 2 wt.% AA and the 2 wt.% AA + 3.5 wt.% salt is quite different. It would be expected that the 2 wt.% AA + 3.5 wt.% salt would form an emulsion which would have a larger fluid viscosity than the 2 wt.% AA experiment, however from the motor current it appears that the 2 wt.% AA experiment has a higher viscosity. This could be due to the fact that the 2 wt.% AA + 3.5 wt.% salt at the point in the expeirment has not been fully emulsified and so doesn't reflect the high fluid viscosity that would be expected. Another explantion could be that the motor allignment between the two experiments was off leading to a different motor current for both experiments.

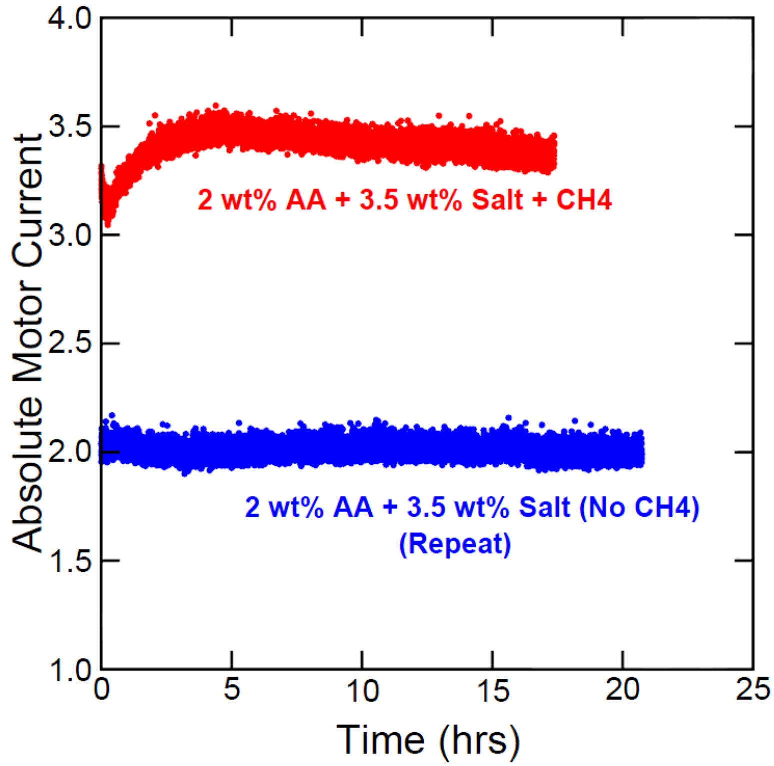

Figure 4.9: Motor current traces showing the saturation motor current trace for the saturation period before hydrate formation for 75 vol.% WC, 2 wt.% AA + 3.5 wt.% salt (red trace) beside the emulsion test for 75 vol.% WC, 2 wt.% AA + 3.5 wt.% salt (blue trace) Both traces taken at 20 °C.

The evidence points to the conclusion, that when methane gas is added to AA, salt and crude oil, the viscosity of the fluid increases significantly. In order to determine what change the fluid is undergoing when methane is added to the AA and salt system, another emulsion test was performed. For this experiment, methane gas was added to the 2 wt.% AA + 3.5 wt.% salt system and the temperature was kept constant at 20 °C so that the experiment would not enter hydrate formation conditions. The result from this experiment can be observed in Figure 4.10. There are two traces shown in this figure. The red trace shows the 2 wt.% AA + 3.5 wt.% salt run with no methane injected and the blue trace shows the same system but with methane injected. As can be seen from Figure 4.10, the experiment that had methane injection saw an immediate increase in the motor current confirming that methane injection causes the fluid viscosity to increase substantially.

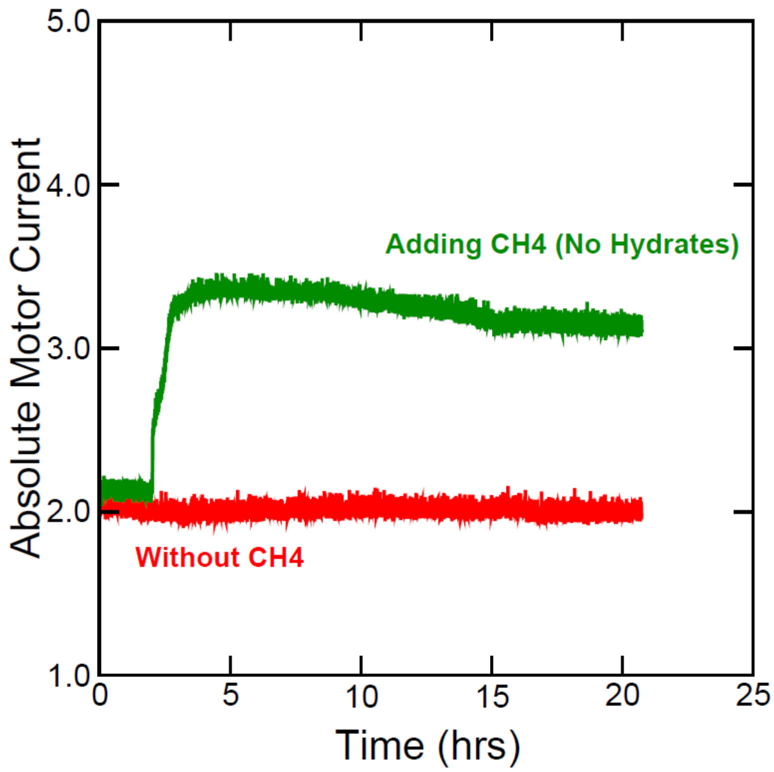

Figure 4.10: Motor current traces for the emulsion test with and without methane. Red trace: 75 vol.% WC, 2 wt.% AA + 3.5 wt.% salt. Green Trace: 75 vol.% WC, 2 wt.% AA + 3.5 wt.% salt + CH_4. Both runs performed at 20 °C.

By opening the cell after the emulsion experiments, it was observed (Figure 4.11) that when methane is added to the AA + salt, the system undergoes a physical change. The presence of gas causes the system to form a highly viscous foam. The viscosity of this foam is at least an order of magnitude greater than the viscosity of the same system with no gas present, although it appears to break down at high shear rates, as can be observed in Figure 4.12. The foam viscosity was measured using a Discovery Hybrid Rheometer-3 (DHR-3) from TA Instruments using a gap width of 0.5 mm. The full details of the procedure used can be found in (Webb *et al.*, 2012). Despite the fact that the foam is extremely viscous, which is generally an undesirable trait for a fluid to have in a pipeline, the foam formation leads to a flowable hydrate slurry which does not plug, even after prolonged shut in conditions (24 hrs).

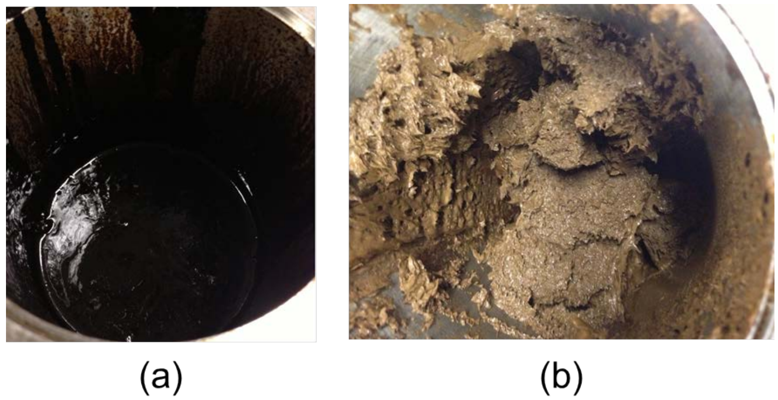

Figure 4.11: Morphology from AA + salt emulsion test. (a) 75% WC + 2 wt% AA + 3.5 wt% salt With no methane injection fluid remains in liquid phase with no solids present. (b) 75% WC + 2 wt% AA + 3.5 wt% salt + CH_4 When methane is injected foam appears.

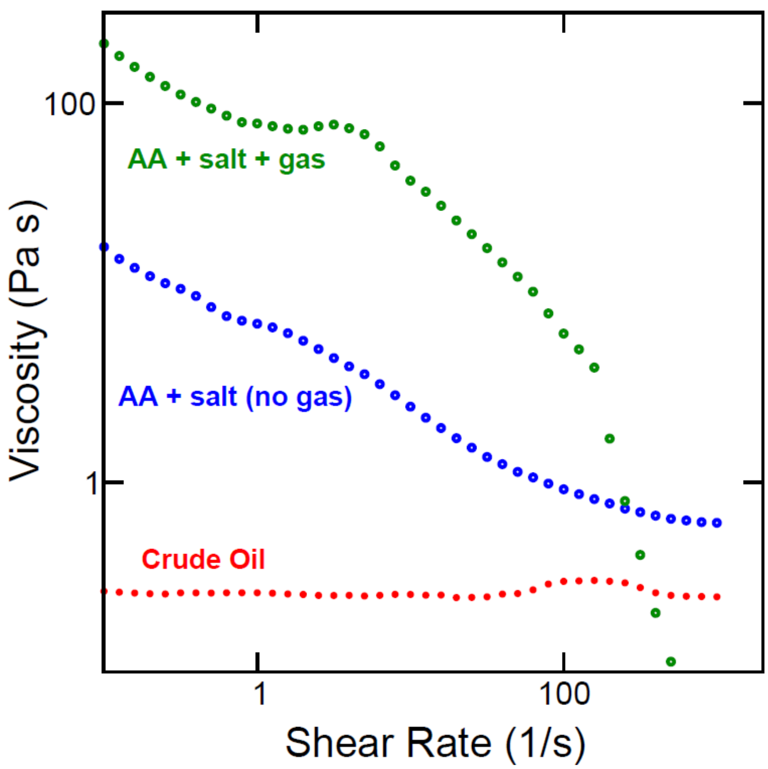

Figure 4.12: Viscosity trace showing the differences in viscosity between the 75 vol.% WC + 2 wt.% AA + 3.5 wt.% salt system with and without methane. The measured crude oil viscosity trace is also shown.

A series of emulsion experiments were performed in order to confirm that the AA + salt system was the only system that would form this foam. Autoclave emulsion experiments were run for 75 vol.% WC, 75 vol.% WC + 3.5 wt.% salt and 75 vol.% WC + 2 wt.% AA systems. The experiments were run for around 18 22 hours at 20 °C with no gas at which point methane gas would be injected up to 950 psig. The results from these runs can be observed in Figure 4.13.

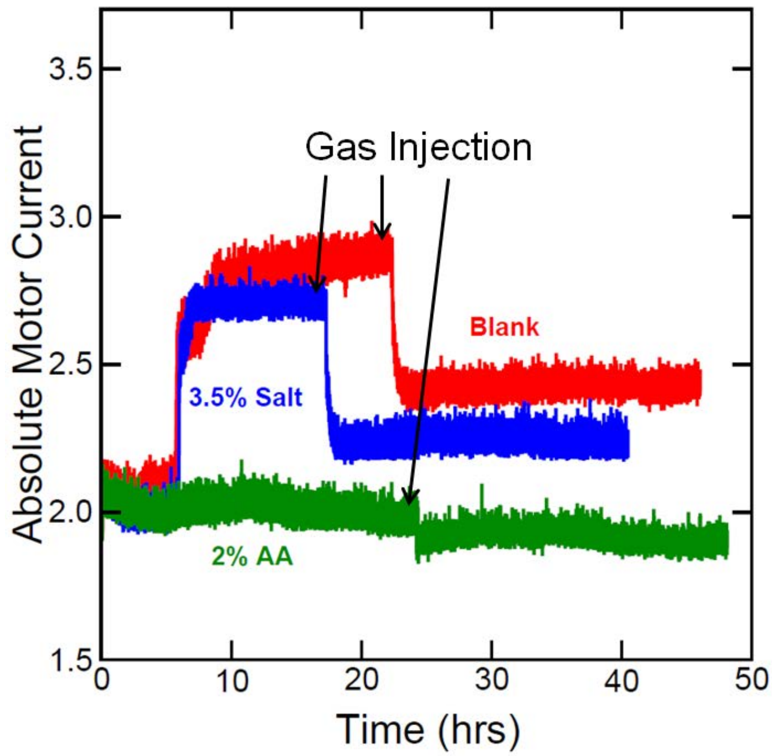

Figure 4.13: Motor current trace for autoclave cell emulsion experiment. Red trace: 75 vol.% WC. Blue trace 75 vol.% WC + 3.5 wt.% salt. Green trace 75 vol.% WC + 2 wt.% AA.

Referring to Figure 4.13, at time 0, each run starts off at the baseline motor current of 2 Amps. After around 5 hours for the salt and blank experiment, the motor current increases substantially, however, at this point no gas has been injected so the increase in motor current is not due to foam formation. Looking at PVM images for these experiments (**??** it is probable that the motor current increase is taking place due to a decrease in droplet size from 60 to 30 μm and a corresponding increase in the droplet frequency, as the system becomes fully emulsified. When gas is injected into these systems the motor current drops immediately, as would be expected when a lighter component is introduced into the system. For the 2 wt.% AA system, the motor current does not increase at all and only a small decrease in the motor current is observed when gas is injected. This system does not see an increase in motor current due to the fact that this system forms an inverse emulsion to the other two, it forms an oil-in-water emulsion rather than a water-in-oil. Therefore, because there is not a lot of oil in the system, the droplet frequency remains relatively low keeping the system viscosity low as well.

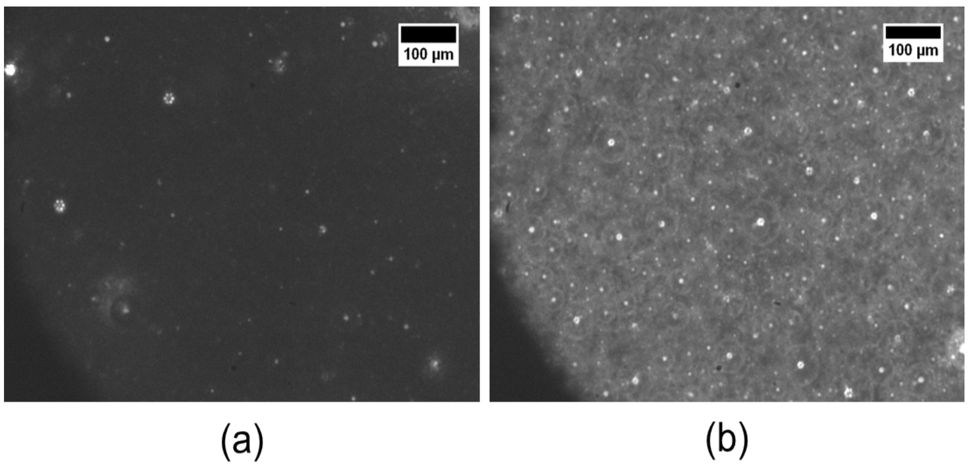

Figure 4.14: (a) 75 vol.% WC after 1 hour. Droplet size is around 40-60 μm and very infrequent. (b) 75 vol.% WC after 9 hours. Droplet size is around 30 μm and very frequent.

In addition to this evidence, the morphology from the emulsion tests confirmed that none of the other systems formed a foam when gas was injected. The emulsion morphology can be observed in Figure 4.15.

4.1.4 AA IFT Investigation

It is well know that the addition of a surfactant to a component can have a significant impact on the surface tension of that component. This is an important aspect of surfactants since the surface tension between fluids can have a significant effect on the resulting droplet size of the emulsion. Having small water droplets in the emulsion is important as small water droplets will convert to small hydrate particles which are

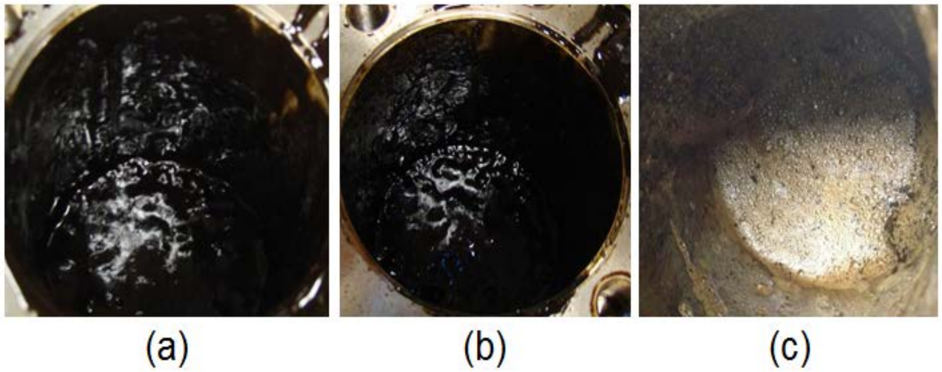

Figure 4.15: Oil morphology from emulsion tests. (a) 75 vol.% WC, Liquid, no foam formed. (b) 75 vol.% WC + 3.5 wt.% salt, Liquid, no foam formed. (c) 75 vol.% WC + 2 wt.% AA, mostly liquid with a little foam.

easier to transport in a pipeline than large hydrate chunks. Once a small droplet size has been achieved then the surfactant will also have to keep the droplets/particles from agglomerating together via a combination of steric and electrostatic repulsion. Since experiments were clearly indicating that the combination of AA + salt in the same system was having a positive effect on the hydrate slurry, IFT experiments were performed in order to determine if this combination was having a significant effect on the surface tension. The results of this investigation can be observed in Figure 4.16.

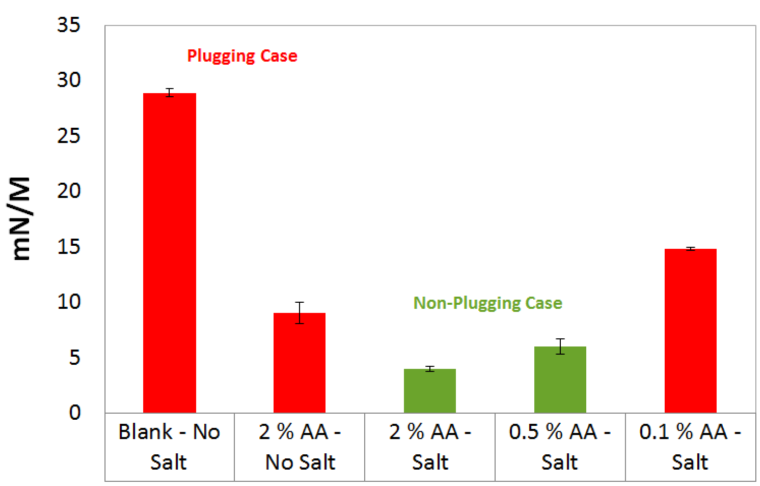

Figure 4.16: IFT results performed on Dalia crude oil at 75 vol.% WC investigating the effects of AA + salt on surface tension.

As can be seen from Figure 4.16, the effects of adding AA + salt to the crude oil system have a significant effect on the surface tension between the crude oil and water. The initial surface tension value between crude oil and water, with no added surfactants, is around 28 mN/m. When 2 wt.% of AA is added, this value drops an order of magnitude to around 8 mN/m. This value is effectively halved when salt is added along with the AA, to around 4 mN/m. This demonstrates that the AA + salt is able to decrease the surface tension significantly, which helps to explain why this combination leads to a flowable hydrate slurry. This is in contrast to a previous study which showed a negative impact on hydrate agglomeration when salt was used along with a quaternary AA (York & Firoozabadi, 2009).It is also interesting to note that for the AA and salt system, as the AA concentration is decreased, the surface tension value increases, which is to be expected as there is less AA available to pack at the oil-water interface. The significant jump in the surface tension between 0.5 and 0.1 wt.% AA suggests that the critical micelle concentration of this AA is probably somewhere between 0.5 and 2 wt.% AA. The critical micelle concentration, or CMC, is the concentration at which the system is saturated with surfactant. At this point the oil-water interface is fully packed the surfactant molecules will tend to interact with other surfactant molecules and form micelles. The CMC value is typically at low concentrations of surfactant which helps to explain why AAs can usually be utilized effectively at low concentrations.

One of the key questions that this IFT study brings up, is why does the addition of salt lead to a more effective AA system. It has already been discussed that the addition of salt will actually invert the system from an oil-in-water emulsion to a water-in-oil emulsion, and the benefits of having a water-in-oil emulsion have already been discussed. In chapter 3 the addition of salt to the AA mineral oil system caused the system to become highly unstable, however for the crude oil study, since the opposite type of emulsion is being formed, the chemistry that causes the mineral oil,

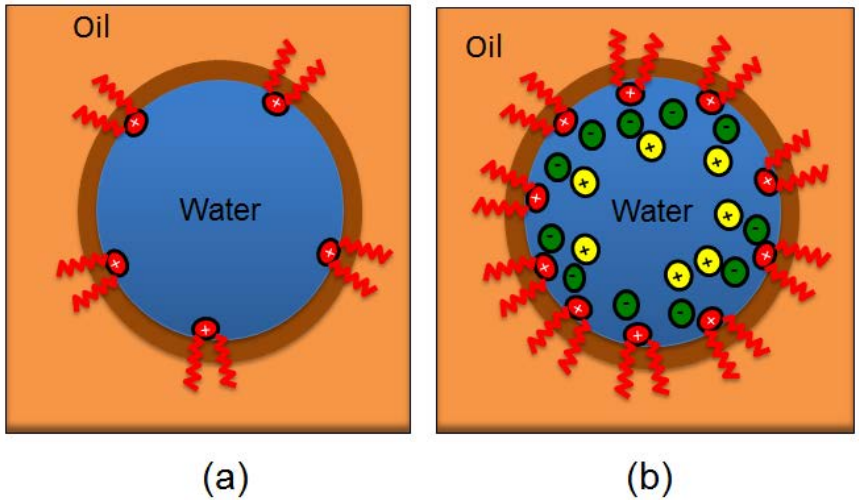

Figure 4.17: (a) Conceptual picture showing how salt can shield repulsion charges between AA molecules, improving ability of the AA to pack at the oil/water interface. (a) With no salt present. (b) With salt present.

AA + salt system to be unstable is what causes the crude oil AA + salt system to become much more stable. The current theory on why this happens is that the AA molecules, due to their cationic nature, have a large repulsion effect on other AA molecules. This prevents the AA molecules from packing together tightly at the water/oil interface, which reduces the effectiveness of the AA (Figure 4.17 (a)). However, when salt is introduced into the system, the ions in the salt are free to interact with the AA ions Figure 4.17 (b)). This electrostatic interaction reduces the repulsion effect between the AA molecules, as the salt ions have a shielding effect. Since the AA molecules have a weaker repulsion effect, they are able to pack into the water/oil interface more tightly and so be more effective. Another possibility that could be affecting the emulsion type behavior is that as the salt concentration is increased, the debye length of the surfactant will be decreased which would also lead to an increase in the packing factor of the AA at the water/oil interface (Israelachvili, 2011). Overall the addition of salt and the effect of lowering the surface tension between the two components, allowing for smaller droplet sizes in the system. The surfactant is also able to prevent the water droplets from agglomerating together due a combined steric and electrostatic repulsion effect, which leads to the flowable hydrate slurry found in this crude oil study. It should be noted that for emphasis of the salt effect, the conceptual picture shows a water-in-oil emulsion for both systems, even though the system with no salt forms an oil-in-water emulsion.

4.1.5 Foam Mechanism

This section will propose a mechanism for why a foam is forming within the AA + salt system. As has been described in the previous section, the combination of AA and salt in Dalia crude oil, at 75 vol.% WC, will form a highly stabilized water-in-oil emulsion (Figure 4.17). A conceptual picture of the suggested foam mechanism can be seen in Figure 4.18, please note that this is a modified picture from Marcanos paper. Since it has been shown that gas is a key component of the foam (the foam will not form until gas has been injected into the system) then it can also be inferred that the gas must be playing a key role in this mechanism. Since, water droplets are already being stabilized by the AA and salt, it is possible that when gas is injected, gas is migrating to the center of the water droplet and being stabilized there. This type of mechanism is well known as being the cause of foaming behavior in some oils (Marcano *et al.*, n.d.).

It can be difficult to prove that this is the actual mechanism that is causing the foam formation, to help back up this theory a number of points will be made here that will help to support this proposed mechanism.

First of all, it has been shown that the foam will only form when gas is injected into the system, so gas uptake must be a key part of this mechanism. When gas is normally injected into any crude oil and water system, it can dissolve into the crude oil phase, the water phase or remain as part of a free gas phase. This will happen regardless of any added chemicals. Since this will always happen and a foam does not always form, then these mechanisms alone cannot be responsible for the foam formation. Emulsions tests show that the AA and salt combination will form

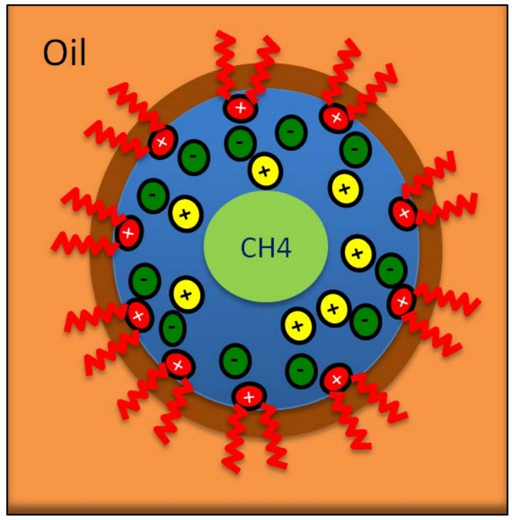

Figure 4.18: Conceptual picture showing gas uptake into a stabilized water droplet leading to a stabilized foam.

a highly stabilized in oil formation and that according to PVM pictures (Figure 4.19 the droplet size is small, on the order of 5-10 μm. Therefore, there already exists a stable emulsion and water droplet for the gas to enter. Finally, when a small sample of the foam was put into a beaker of toluene, there was a rapid dissolution of gas bubbles indicating that gas was being trapped within this stable foam.

4.1.6 Crude Oil with MeOH

Crude oil experiments with MeOH were performed to investigate whether high water cut systems could be under-inhibited with MeOH and not plug, as well as to establish a baseline for comparison purposes between MeOH only experiments and experiments that use a combination of MeOH and AA. In order to have a fully inhibited system a MeOH concentration of 14 wt.% is required, when using salt water. Two concentrations of MeOH were chosen to be investigated, 2.5 and 5 wt.%. The results from this investigation can be observed in Figure 4.20.

As can be observed from Figure 4.20, the experiment with 5 wt.% MeOH formed around 5 vol.% less hydrates than the 2.5 wt.% MeOH experiment, which is to be expected since the more MeOH present, then the more hydrate inhibition that would

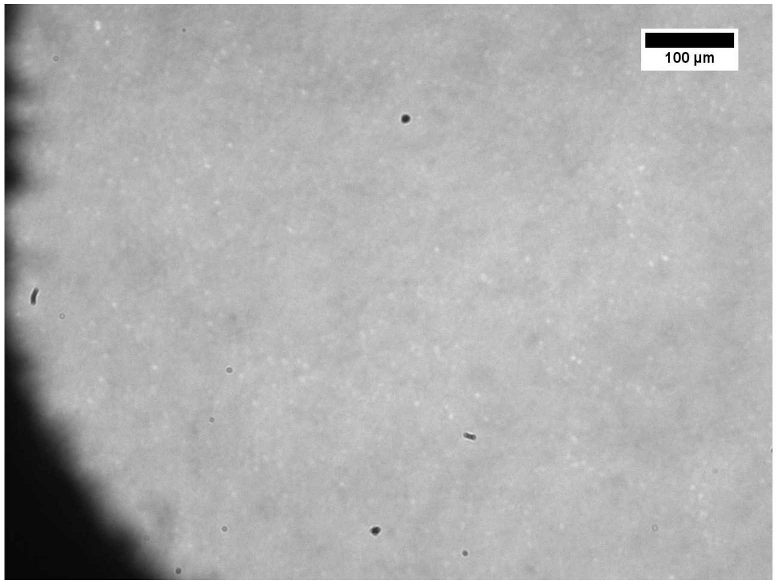

Figure 4.19: PVM image of the 2 wt.% AA + 3.5 wt.% salt emulsion system. Droplet size is on the order of 5-10 μm.

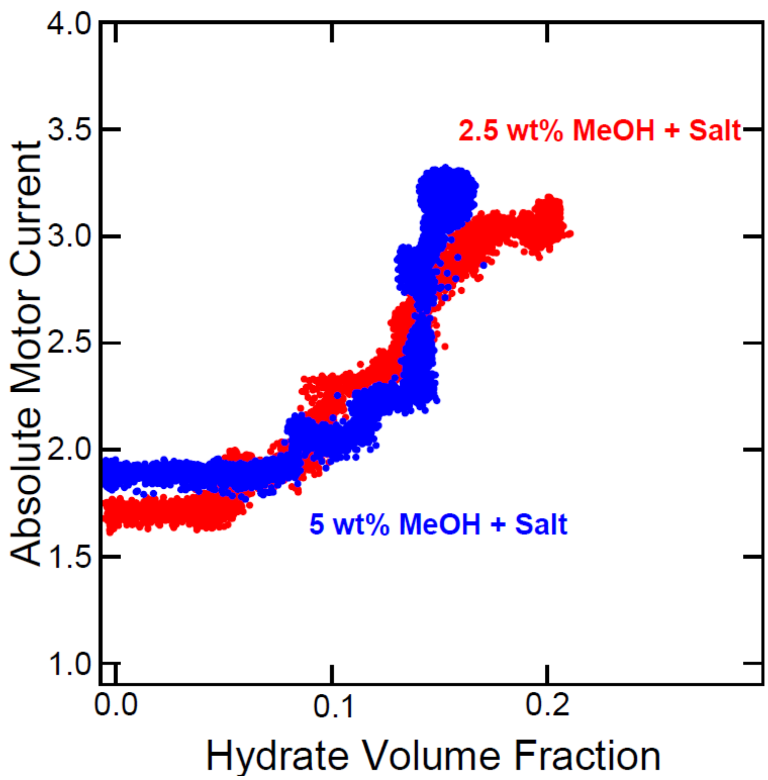

Figure 4.20: Motor current traces for MeOH base cases. Red trace: 75 vol.% WC, 2.5 wt.% MeOH + 3.5 wt.% salt. Experiment did plug after shut-in conditions. Blue trace: 75 vol.% WC, 5 wt.% AA + 3.5 wt.% salt. Experiment did not plug after shut-in conditions.

take place. It is interesting to note here that the fluid viscosity, according to the motor current, is around the same for both sets of experiments and the lack of spikes in the motor current data suggests only small chunks of hydrates formed, if any at all. It is also important to note here that the 2.5 wt.% MeOH experiment plugged after shut in conditions while the 5 wt.% MeOH experiment did not. The hydrate morphology can be observed in Figure 4.21. This figure shows that small chunks of hydrates formed during the 2.5 wt.% MeOH experiment. It is probable that these chunks agglomerated together during shut in conditions leading to the hydrate plug. Figure 4.21 indicates that the 5 wt.% MeOH experiment formed a hydrate slurry with very small hydrate chunks. This experiment didnt plug because the hydrates that were present werent able to form large enough chunks to cause a plug, however they did contribute to the high viscosity that was observed in this experiment.

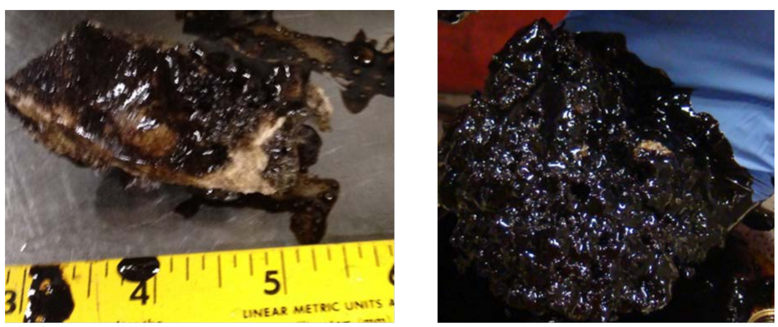

(a) (b)

Figure 4.21: Hydrates obtained from crude oil MeOH experiments after depressurization: (a) Small hydrate chunks from 75 vol.% WC + 2.5 wt.% MeOH + 3.5 wt.% salt; (b) Viscous hydrate slurry from 75 vol.% WC + 5 wt.% MeOH + 3.5 wt.% salt.

Bottle tests with the MeOH systems indicated that a water-in-oil emulsion would be formed for both experiments. Tests also indicated that the emulsion would separate out after around 4 hours which suggests that during normal shut in conditions, it would be expected that there would be some phase separating. This phase separating would likely encourage a hydrate plug as it would be easier for hydrate particles to encounter each other and agglomerate.

The implication from these MeOH experiments is that a system can be under-inhibited by 60% and not plug. This is similar to the mineral oil case, as the system also did not plug when under-inhibited with 5 wt.% MeOH. However, there is a key difference between the mineral oil experiment and the crude oil experiment and that is even though the 5 wt.% MeOH crude oil experiment did not plug, the fluid viscosity increased dramatically. In the mineral oil system, the fluid viscosity remained quite low. This should give cause for some concern, as a high viscosity system such as this one could still represent a dangerous, high risk system when flowed in a pipeline.

4.1.7 Crude Oil with MeOH and AA

MeOH and AA experiments were run to investigate the effect of adding the two chemicals to the same system. The main aim here was to find a system that plugged when just one of the two chemicals was present but would convert to a non-plugging system when the second component was added. The ideal situation here would be to take two systems that were plugging when only one of the chemicals was present but would convert to non-plugging when the two chemicals were combined, as this would show that a true synergistic effect was taking place between the two components, rather than just the added chemical merely helping out the already non-plugging system. For example, it has been shown that the 2.5 wt.% MeOH system plugs. Additionally the 0.1 wt.% AA system also plugged. The ideal situation would be to add the 0.1 wt.% AA to the 2.5 wt.% MeOH and see the system convert to a non-plugging system. The results from this investigation can be observed in Figure 4.22.

Figure 4.22 has a lot of information and is arguably one of the most important figures in this thesis. 2.5 wt.% MeOH was chosen as the common MeOH concentration due to the fact that when the 2.5 wt.% MeOH baseline experiment was run, this experiment plugged after shut in conditions. Therefore, it was desirable to investigate whether this plugging experiment could be converted to a non-plugging experiment by adding AA. Previous experiments have shown that down to 0.3 wt.% AA, the system

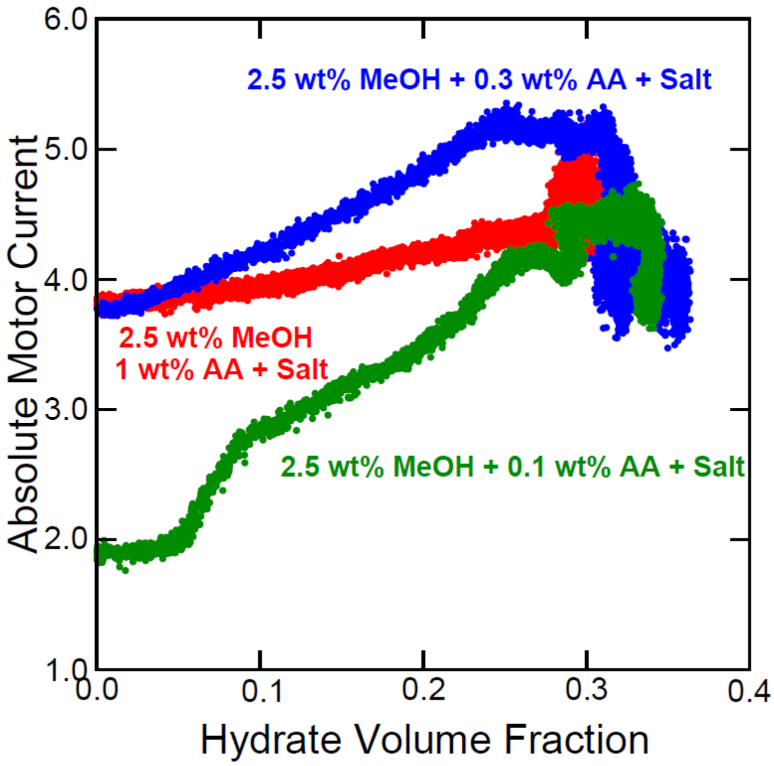

Figure 4.22: Motor current traces for MeOH + AA systems: Red: 75 vol.% WC + 2.5 wt.% MeOH + 1 wt.% AA + 3.5 wt.% salt. Experiment did not plug after shut-in conditions. Blue: 75 vol.% WC + 2.5 wt.% MeOH + 0.3 wt.% AA + 3.5 wt.% salt. Experiment did not plug after shut-in conditions. Green: 75 vol.% WC + 2.5 wt.% MeoH + 0.1 wt.% AA + 3.5 wt.% salt. Experiment did plug after shut-in conditions.

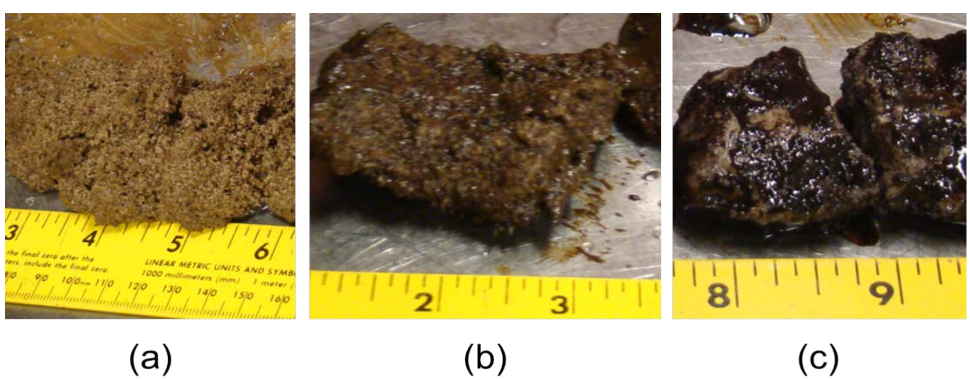

Figure 4.23: Hydrates obtained from crude oil MeOH + AA experiments after depressurization: (a) 75 vol.% WC + 2.5 wt.% MeOH + 1 wt.% AA + 3.5 w.t% salt, sticky hydrate slurry; (b) 75 vol.% WC + 2.5 wt.% MeOH + 0.3 wt.% AA + 3.5 wt.% salt, small hydrate chunks interspersed throughout slurry. (c) 75 vol.% WC + 2.5 wt.% MeOH + 0.1 wt.% AA + 3.5 wt.% salt, hard hydrate chunks.

remains non-plugging after shut in conditions and at 0.1 wt.% AA the system plugs (Figure 4.5). The results from the combined MeOH and AA experiments show similar results to the AA only experiments in terms of plugability. The 2.5 wt.% MeOH + 1 wt.% AA and the 2.5 wt.% MeOH + 0.3 wt.% AA experiment both did not plug after shut in conditions. However, the 2.5 wt.% MeOH + 0.1 wt.% AA experiment did plug. From these results it can be said that taking a non-plugging AA system and adding MeOH will cause that system to continue not to plug. However, taking a plugging AA system and adding up to 2.5 wt.% MeOH will not help that system to convert to a non-plugging system.

It can be inferred from Figure 4.5 and Figure 4.22 that the systems with 0.1 wt.% AA did not form a foam before hydrate formation unlike the other experiments that had AA present as the motor current starts off low compared to the other systems. This low motor current suggests that the fluid viscosity is fairly. For the 0.1 wt.% AA experiment, the motor current does increase up to around the same level as the other experiments, however, this is more likely due to the presence of hydrates rather than the appearance of a viscous foam.

Continuing to compare Figure 4.5 and Figure 4.22, it is apparent that there is a key difference between AA only experiments and AA + MeOH experiments. As has been discussed, the non-plugging AA only experiments tend to see an increase in motor current as hydrates are formed, followed by a sharp decrease in the motor current once hydrate formation has finished. However, the AA + MeOH experiments show a different trend. The motor current instead of dropping once hydrate formation ends, continues to stay high suggesting that the addition of MeOH to the AA system creates a more viscous hydrate slurry. This would imply that MeOH addition has a negative effect on the hydrate slurry rather than the expected positive effect. However, despite the large viscosity of the system, most of the AA + MeOH experiments are able to remain non-plugging. Bottle tests indicate that these systems form a stable water-in-oil emulsions, similar to the emulsion type formed by the AA + salt system.

Looking at Figure 4.23 it can be seen that the hydrate morphology is highly dictated by the amount of AA used in the system, when keeping the MeOH concentration constant. At 1 wt.% AA, the hydrates form a sticky slurry. However, as the AA concentration is decreased down to 0.3 wt.% AA, hydrate chunks start to appear in between the slurry. When 0.1 wt.% AA is used, larger,hard hydrate chunks become more freqeunt. This hydrate morphology trend is very similar to the trend observed in Figure 4.6 and Figure 4.7 indicating that the hydrate morphology at 2.5 wt.% MeOH, is dictated by the AA concentration.

4.2 50% WC

A series of experiments were performed using a water cut of 50 vol.% to investigate the effects of under-inhibition and combined under-inhibition at a lower water cut. It has been suggested AAs have an upper water cut limit and a series of experiments at a lower water cut could help to investigate this statement.

4.2.1 Untreated Crude Oil

The first step was to establish the baseline experiments, i.e. experiments at 50 vol.% WC with no additional chemicals, in order to find out how the system behaves when no chemicals are present. The results from this work can be observed in Figure 4.24.

Looking at Figure 4.24, the motor current traces are different between the experiments. The experiment with no salt actually underwent a plugging event at around 18 vol% hydrates indicated by the spike in the motor current. At this point, the hydrate growth essentially stops due to a lack of mixing within the cell. After some time, however, the hydrate plug was broken and hydrate growth was resumed, now that mixing was once again taking place within the cell. During shut in conditions the hydrates agglomerated together, so that when the system was restarted the sys-

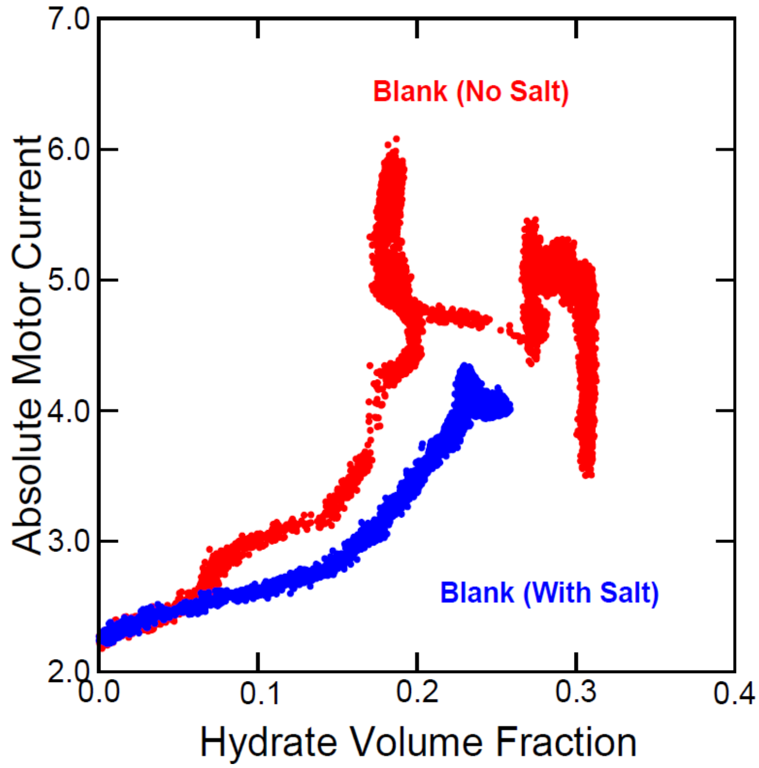

Figure 4.24: Motor current trace from untreated crude oil at 50 vol.% WC. Red: 50 vol.% WC. Experiment did plug after shut-in conditions. Blue: 50 vol.% WC + 3.5 wt.% salt. Experiment did plug after shut-in conditions.

tem plugged. The experiment with salt exhibited slightly different behavior but also plugged after shut in conditions. Hydrate chunks were observed in both systems when the cell was opened as can be observed in Figure 4.25. These experiments show that without chemical addition, this system will plug at 50 vol.% WC.

4.2.2 Crude Oil with AA

Once the untreated crude oil baseline experiments had been established work was continued to investigate the effects of AA treatment on the 50% WC. Initial emulsion experiments were run to find out whether the 50% WC + 2 wt% AA + 3.5 wt% salt system would form a viscous foam like the one formed at 75% WC. To investigate this an emulsion experiment was run with the AA + salt system at 50% WC using the same procedure as the one used for the 75% WC system. The results from this

(a) (b)

Figure 4.25: Hydrate morphology of 50 vol.% WC experiments with no added chemicals. (a) 50 vol.% WC, full hydrate plug formed with hydrate chunks. (b) 50 vol.% WC + 3.5 wt.% salt, plug with hydrate chunks.

emulsion test are compared to the emulsion test at 75% WC for comparison and can be seen in Figure 4.26.

In Figure 4.26 it can be seen that when methane was injected into the 75 vol.% WC system, the motor current shot up substantially indicating that the fluid viscosity increased substantially. When methane was injected into the 50 vol.% WC system the motor current actually decreased back down to the baseline. This figure, as well as Figure 4.27, indicates that the foam does not form at 50 vol.% WC.

Once it was established that the 50 vol.% WC system did not form a foam work was performed to investigate what happens in these systems when hydrates were formed. To investigate this 3 AA experiments were run. The first experiment was run with 2 wt.% AA with no salt, in order to investigate the effect of salt on the system. The other two experiments were run with salt and two concentrations of AA were chosen, 2 and 5 wt.% AA. The 5 wt.% AA system was chosen in order to investigate whether the foam formation could be forced by overloading the system with AA. The results from these experiments can be observed in Figure 4.28.

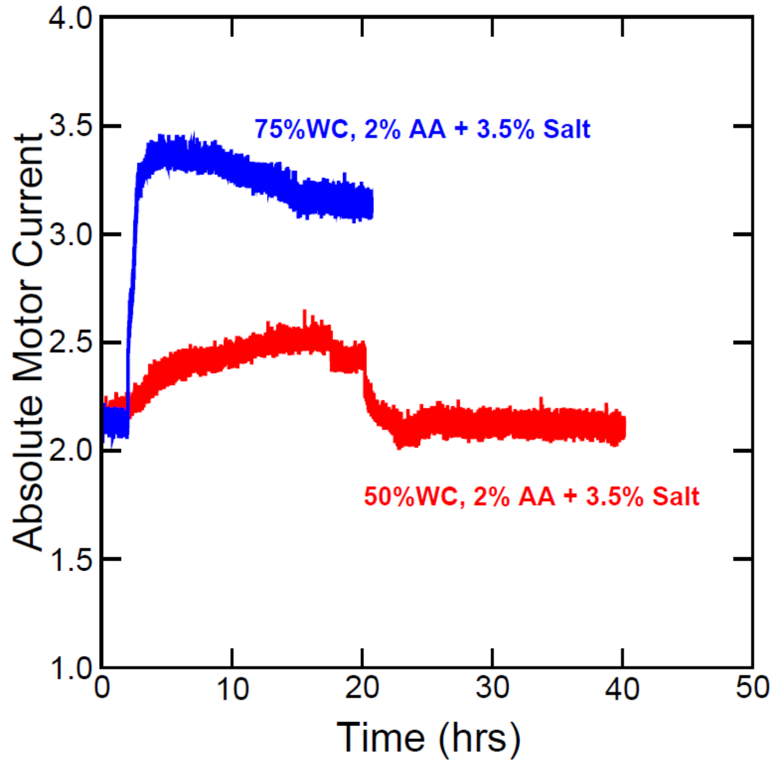

Figure 4.26: Motor current trace from emulsion test with methane. Red: 50 vol.% WC + 2 wt.% AA + 3.5 wt.% salt methane was injected around 20 hours into the experiment. Blue: 75 vol.% WC + 2 wt.% AA + 3.5 wt.% salt methane was injectecd around 2 hours into the experiment

Figure 4.27: Emulsion morphology of AA + salt systems investigating the effect of WC on foam formation. (a) 75 vol.% WC + 2 wt.% AA + 3.5 wt.% salt. (b) 50 vol.% WC + 2 wt.% AA + 3.5 wt.% salt.

As can be seen from Figure 4.28 the behavior between the experiments with and without salt is exhibits different behavior. The experiment with no salt appears to decrease in motor current indicating that a flowable system is present here. The other

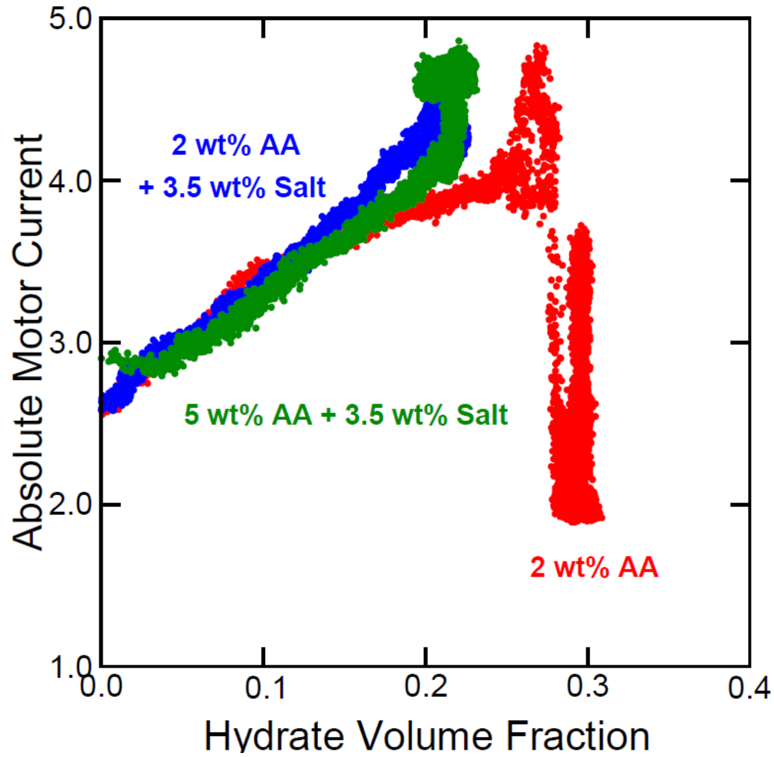

Figure 4.28: Motor current traces from 50 vol.% WC + AA investigation. Red trace: 50 vol.% WC + 2 wt.% AA. Experiment did plug after shut-in conditions. Blue Trace: 50 vol.% WC + 2 wt.% AA + 3.5 wt.% salt. Experiment did plug after shut-in conditions. Green trace: 50 vol.% WC + 5 wt.% AA + 3.5 wt.% salt. Experiment did not plug after shut-in conditions.

two AA experiments with salt also appear to be flowable systems, albeit with a high viscosity. For the 2 wt.% AA, no salt experiment, this system did not plug after shut in conditions. However, when the cell was opened, the impeller was found to be surrounded by large hydrate chunks. The impeller was not impeded from turning, however, because the hydrates had formed around the baffles and had not formed between the impeller and the baffles, effectively creating a hydrate free zone within the impellers turning space. Any hydrates that had formed in the impellers turning radius were not strong enough to prevent the impeller from rotating when it was restarted. So, even though the experiment hadnt technically plugged, the observed hydrate morphology would suggest that this experiment would have plugged under other circumstances. The resulting hydrate chunks from this experiment can be observed in Figure 4.29. Emulsion tests showed that this system formed an oil-in-water emulsion, similar to the one formed at 75 vol.% WC under the same conditions. This helps to explain why this system formed hydrate chunks as the AA is not able to keep the hydrate particles from agglomerating.

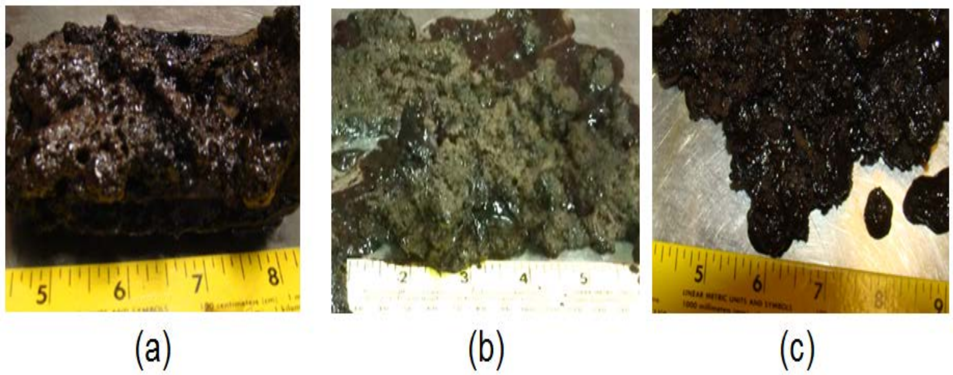

Figure 4.29: Hydrate morphology from the 50 vol.% WC +AA investigation. (a) 50 vol.% WC + 2 wt.% AA, large hydrate chunks.(b) 50 vol.% WC + 2 wt.% AA + 3.5 wt.% salt, small hydrate chunks dispersed in slurry. (c) 50 vol.% WC + 5 wt.% AA + 3.5 wt.% salt, small hydrate chunks dispersed in slurry.

The AA experiments with salt did plug after shut in conditions despite the fact that the hydrate morphology would suggest that they formed a hydrate slurry. The formation of this slurry was enabled by the water-in-oil emulsion that this system formed as the anti-agglomerants are able to keep water droplets dispersed throughout the oil and so the resulting hydrate particles are kept dispersed. The motor current suggests that the resulting hydrate slurry was extremely viscous and the slurry was not able to keep the hydrates dispersed during shut in conditions. This lack of dispersion allowed the hydrates to agglomerate together creating enough of a hydrate plug that the impeller couldnt restart after shut in. This series of experiments helps to highlight the importance of the foam that was formed at 75 vol.% WC under similar conditions. At 75 vol.% WC, the salt and AA experiments did not plug due to the foams ability to keep the hydrates dispersed in the system.

4.2.3 Crude Oil with MeOH

A set of experiments were run with MeOH at 50 vol.% WC similar to those run at 75 vol.% WC. Again, two concentrations of MeOH were chosen, 2.5 wt.% and 5 wt.% MeOH. Similar to the 75 vol.% WC systems, both of these systems would form an unstable water-in-oil emulsion. The results from these two runs can be observed in Figure 4.30.

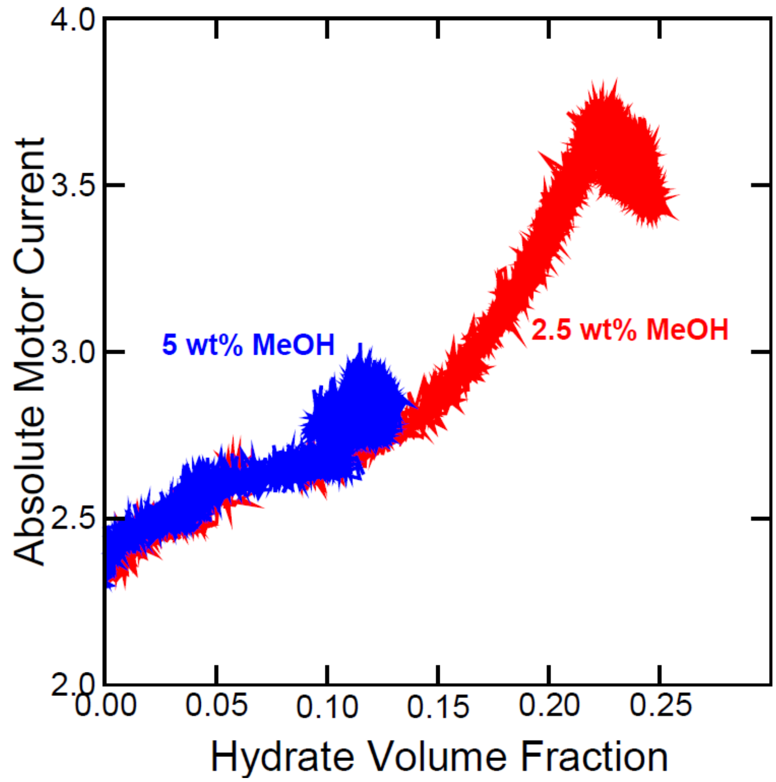

Figure 4.30: Motor current trace from MeOH baseline experiments. Red: 50 vol.% WC + 2.5 wt.% MeOH+ 3.5 wt.% salt. Experiment did plug after shut-in conditions. Blue: 50 vol.% WC + 5 wt.% MeOH + 3.5 wt.% salt. Experiment did not plug after shut-in conditions.

As can be observed from Figure 4.30 there is a clear difference between the two concentrations of MeOH. The 2.5 wt.% MeOH formed significantly more hydrates than the 5 wt.% MeOH experiment which is consistent with our understanding of the more MeOH that is added, the more water that is tied up and unable to form hydrates. Both systems show relatively smooth motor current traces which are not uncommon for the MeOH cases, even when under-inhibited. As has been shown before, this type of behavior can be attributed to a hydrate slurry or small chunks of hydrate in the system and as has been demonstrated previously, both types of systems can cause a system to plug. In these experiments, the 2.5 wt.% MeOH experiment plugged after shut in conditions, while the 5 wt.% MeOH experiment did not. The hydrate morphology from both experiments can be observed in Figure 4.31.

(a) (b)

Figure 4.31: Hydrate morphology from MeOH baseline experiments. (a): 50 vol.% WC + 2.5 wt.% MeOH+ 3.5 wt.% salt Hydrate chunks. Blue: 50 vol.% WC + 5 wt.% MeOH + 3.5 wt.% salt Hydrate slurry.

As can be observed from Figure 4.31 and Figure 4.21the hydrate morphology between the two different water cuts for the same MeoH concentration are very similar. For example, the 2.5 wt.% MeOH system for both water cuts produced small hydrate chunks that plugged the system. For the 5 wt.% MeOH system, both water cuts produced a hydrate slurry that did not plug the system after shut in conditions.

4.2.4 Crude Oil with MeOH and AA

Once the experiments with single chemical injection had been run, the mixed under-inhibited experiments were run. For these experiments, 2 wt.% AA + 2.5 wt.% MeOH system was chosen in order to investigate whether two plugging systems could be combined to create a non-plugging system. In addition to this, 2 wt.% AA + 5 wt.% MeOH was also chosen to be run, to investigate whether adding AA to a non-plugging MeOH experiment would help the system or make it worse. Salt water was used in both experiments. The results from these experiments can be observed in Figure 4.32.

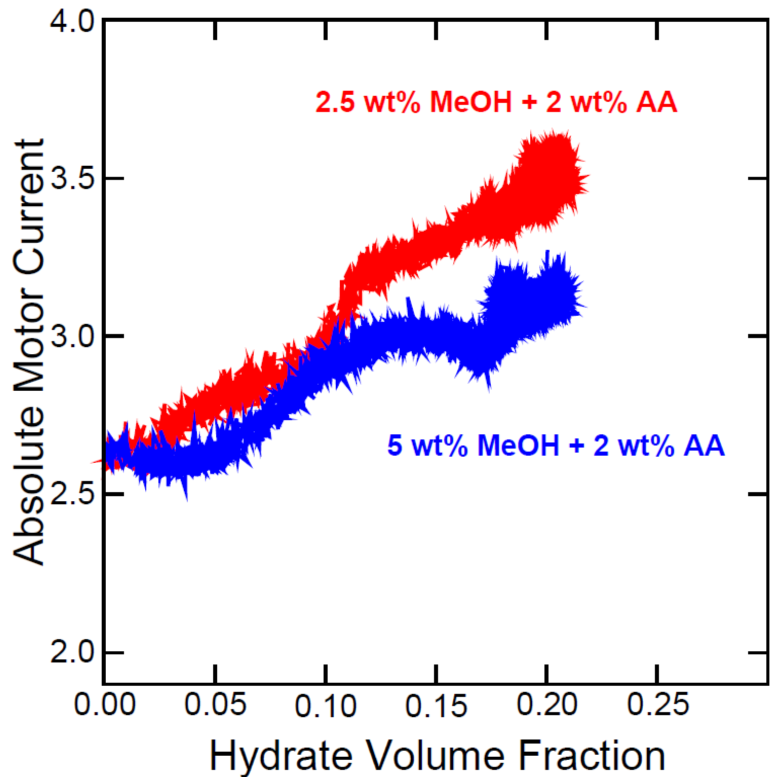

Figure 4.32: Motor current trace from MeOH + AA experiments. Red Trace: 50 vol.% WC+ 2.5 wt.% MeOH + 2 wt.% AA + salt. Experiment did plug after shut-in conditions. Blue Trace: 50 vol.% WC + 5 wt.% MeOH + 2 wt.% AA + 3.5 wt.% salt. Experiment did not plug after shut-in conditions.

The 2.5 wt.% MeOH + 2 wt.% AA experiment plugged while the 5 wt.% MeOH + 2 wt.% AA experiment did not plug. Additionally, bottle tests showed that the emulsions formed with these systems were stable water-in-oil emulsions. As can be observed from Figure 4.32 the 2.5 wt.% MeOH + 2wt.% AA experiment had a much higher system viscosity than the 5 wt.% MeOH + 2 wt.% experiment. Both experiments, however, despite the difference in MeOH concentration, appeared to form a similar volume of hydrates, so the increase in viscosity cannot be due to an increase in the hydrate volume but possibly due to larger hydrate chunks appearing. The hydrate morphology from the 2.5 wt.% MeOH + 2 wt.% AA experiment appeared to have a higher number of hydrate chunks than the 5 wt.% MeOH + 2 wt.% AA experiment (Figure 4.33). It should be noted that these chunks were extremely soft in both cases, which is why the motor current trace does not show spikes in the data, which would be indicative of hard hydrate chunks present in the system.

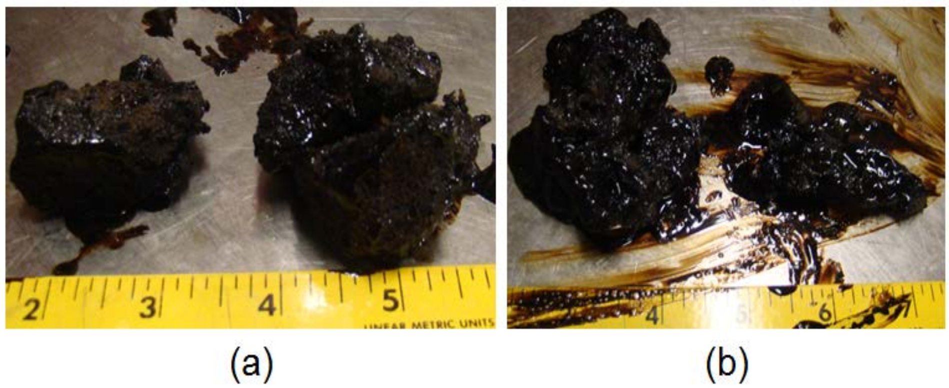

Figure 4.33: Hydrate morphology from MeOH + AA experiments. (a) 50 vol.% WC+ 2.5 wt.% MeOH + 2 wt.% AA + salt. (b) 50 vol.% WC + 5 wt.% MeOH + 2 wt.% AA + salt.

One of the conclusions from these experiments is that it appears that a plugging system, such as 2 wt.% AA, cannot be combined with another plugging system, such as 2.5 wt.% MeOH, and create a non-plugging system. It would appear that if one of the base systems is non-plugging then it can be reasonably expected that when combined with another base experiment, the resulting system will also be non-plugging. In addition to this point it would appear that even taking a non-plugging system such as 5 wt.% MeOH and adding in some AA, an improvement in the resulting systems performance cannot always be expected. Indeed in the last experiment, when AA was added to the non-plugging MeOH experiment the system viscosity increased substantially as well as the total volume of hydrates formed. The actual increase in viscosity was unmeasured but can be inferred from the motor current traces. An increase in hydrate formation may have been observed due to a decrease in the droplet size with the introduction of the AA, which could have led to an increase in the droplet to hydrate conversion rate.

4.3 Chapter Conclusions

There are a number of conclusions that can be extracted from this crude oil work. First of all, it has been shown that at both, 50 vol.% and 75 vol.% WC, a system can be under-inhibited with only 40 vol.% of the total inhibition amount and remain non-plugging. This work has also shown that when AA + salt is combined with gas at a water cut of 75 vol.%, a highly viscous foam is formed that leads to a flowable hydrate slurry. This foam is not formed at 50 vol.% WC and the resulting hydrate slurry plugs the system after shut in conditions. A combination of MeOH and AA at both water cuts do not lead to a more flowable system. At 75 vol.% WC the addition of MeOH to the AA system actually led to a more viscous slurry than the one formed with just AA. Results also showed that a plugging system could not be combined with another plugging system to create a non-plugging system. When combining two systems together at least one of the base systems must have been non-plugging for the combined system to also be non-plugging.

CHAPTER 5
SUMMARY OF THESIS CONCLUSIONS

This chapter will summarize all of the conclusions that have been obtained during the course of this work. One of the main conclusions here is that the natural chemistry in crude oil has a substantial impact on the hydrate results as the natural chemistry can affect AA + salt interaction and also plays a part in the emulsion type that will be formed which is a significant factor in determining plugging or non-plugging behavior.

When under-inhibiting with MeOH, all experiments showed that a system could be successfully under-inhibited with 40 vol.% of the full inhibition amount and not plug. However, this led to a highly viscous slurry that may be dangerous to run in a pipeline.

Results showed that when AA + salt + gas were combined in crude oil at a water cut of 75 vol.%, a highly viscous foam appeared. This foam did not appear at 50 vol.% WC indicating that water was a critical component to the appearance of this foam. Additionally, and more importantly, the appearance of the foam led to a flowable hydrate slurry that did not plug after shut in conditions. Experiments showed that when this foam did not appear, the hydrate slurry would plug the system. When adding MeOH to this the AA + salt experiment at 75 vol.% WC, the foam would still appear, however the resulting hydrate slurry would be much more viscous than if the MeOH was not added.

There was no evidence that combing MeOH and AA together would lead to a better, non-plugging system. Whenever the two chemicals were combined and compared to their base cases, at least one of the base cases would have performed better than the case where the chemicals were combined. This leads to the conclusion that a mixed under-inhibited system of AA and MeOH does not lead to a more controllable hydrate slurry for the selected crude oil and AA. Additionally there is evidence that a plugging case cannot be combined with another plugging case to create a non-plugging case. When the two chemicals are combined, at least one of the base cases has to have been non-plugging for the combined system to be non-plugging.

CHAPTER 6

RECOMMENDATIONS FOR FUTURE WORK

The work of this thesis has continued to indicate the importance of natural chemistry in crude oil and the large effect it can have on the ability of the oil to keep hydrates dispersed and prevent a plug from taking place. It is suggested that this line of work is continued using a range of different crude oils, as different crude oils will have different natural chemistry associated with them (Sjoblom *et al.*, 2003). Such a study would be able to investigate whether the foam phenomena discovered during this work also appears in other crude oils and investigate whether it would be just as beneficial to hydrate slurry flow as it appears to be for this crude oil. It is hoped that by studying a range of different crude oils a trend in the type of natural chemistry that is favorable for foam formation could be identified.

Experiments could also be continued to be run with mineral oil by extracting some of the natural chemistry in crude oil and placing it into the blank system that is mineral oil. For example extracting the asphaltene component from crude oil and placing it into the mineral oil system, would be useful for indicating the importance of asphaltenes in the system results. In addition to this, the oil that has had the asphaltenes extracted could also be studied to investigate what effect removing the asphaltenes would have on that oil.

In addition to this a study could be carried out to investigate the effects of using monoethylene glycol in place of methanol, and investigate whether this thermodynamic inhibitor will behave in the same manner as methanol or whether it will exhibit different behavior. It could also be beneficial to investigate the effect of using a divalent salt such as calcium chloride as it has been demonstrated in this work that electrostatic interactions between anti-agglomerants and salt can influence the results. This line of work could investigate the effect of using a salt with stronger electrostatic interactions.

APPENDIX A - LIST OF AUTOCLAVE EXPERIMENTS

Table A.1: Crude Oil Autoclave Experimental Results

Experiment	WC (vol.%)	MeOH (wt.%)	AA (wt.%)	Salt (wt.%)	Comments
1	75	0	0	0	Plugged during operating conditions
2	75	0	0	3.5	Plugged after shut-in
3	75	0	2	0	Plugged during operating conditions
4	75	0	2	3.5	Did not plug after shut-in
5	75	0	0.5	3.5	Did not plug after shut-in
6	75	0	0.3	3.5	Did not plug after shut-in
7	75	0	0.1	3.5	Plugged after shut-in
8	75	2.5	0	3.5	Plugged after shut-in
9	75	5	0	3.5	Did not plug after shut-in
10	75	2.5	1	3.5	Did not plug after shut-in
11	75	2.5	0.3	3.5	Did not plug after shut-in
12	75	2.5	0.1	3.5	Plugged after shut-in
13	50	0	0	0	Plugged after shut-in
14	50	0	0	3.5	Plugged after shut-in
15	50	0	2	0	Did not plug after shut-in
16	50	0	2	3.5	Plugged after shut-in
17	50	0	5	3.5	Plugged after shut-in
18	50	2.5	0	3.5	Plugged after shut-in
19	50	5	0	3.5	Did not plug after shut-in
20	50	2.5	2	3.5	Plugged after shut-in
21	50	5	2	3.5	Did not plug after shut-in
22	75	0	0	3.5	Repeat, plugged after shut-in
23	75	0	2	3.5	Repeat, did not plug after shut-in
24	75	0	0.5	3.5	Repeat, did not plug after shut-in
25	75	2.5	0	3.5	Repeat, plugged after shut-in
26	50	0	2	3.5	Repeat, plugged after shut-in

Table A.2: 200T Mineral Oill Autoclave Experimental Results

Experiment	WC (vol.%)	MeOH (wt.%)	AA (wt.%)	Salt (wt.%)	Comments
1	75	0	0	0	Plugged after shut in
2	75	0	0	3.5	Plugged after shut-in
3	75	0	2	0	Plugged during operating conditions
4	75	0	2	3.5	Plugged after shut-in
5	75	0	5	3.5	Plugged after shut-in
6	75	2.5	0	3.5	Plugged after shut-in
7	75	5	0	3.5	Did not plug after shut-in
8	75	2.5	0	3.5	Plugged after shut-in
9	75	5	0	3.5	Did not plug after shut-in
10	75	2.5	2	3.5	Plugged after shut-in
11	75	5	2	3.5	Did not plug after shut-in
12	75	0	2	3.5	Repeat, plugged after shut-in
13	75	2.5	0	3.5	Repeat, plugged after shut-in
14	75	2.5	2	3.5	Repeat, plugged after shut-in

Table A.3: 500T Mineral Oill Autoclave Experimental Results

Experiment	WC (vol.%)	MeOH (wt.%)	AA (wt.%)	Salt (wt.%)	Comments
1	75	0	0	0	Plugged during operating conditions
2	75	0	0	3.5	Plugged after shut-in
3	75	0	2	0	Plugged during operating conditions
4	75	0	2	3.5	Plugged after shut-in

APPENDIX B - LIST OF EMULSION EXPERIMENTS

Table B.1: Crude Oil Emulsion Experiments

System	Type	Stability	Comments
75% WC	W/O	$<$ 1 hour	Plug
75% WC + 2 wt.% AA	O/W	$>$ 24 hours	Plug
75% WC + 3.5 wt.% Salt	W/O	$<$ 1 hour	Plug
75% WC + 3.5 wt.% Salt + 2 wt.% AA	W/O	$>$ 24 hours	No Plug
75% WC + 3.5 wt.% Salt + 2.5 wt.% MeOH	W/O	$<$ 1 hour	Plug
75% WC + 3.5 wt.% Salt + 5 wt.% MeOH	W/O	$<$ 1 hour	No Plug
75% WC + 3.5 wt.% Salt + 2 wt.% AA + 2.5 wt.% MeOH	W/O	$>$ 24 hours	No Plug
75% WC + 3.5 wt.% Salt + 2 wt.% AA + 5 wt.% MeOH	W/O	$>$ 24 hours	No Plug
50% WC	W/O	$<$ 1 hour	Plug
50% WC + 2 wt.% AA	O/W	$>$ 24 hours	Plug
50% WC + 3.5 wt.% Salt	W/O	$<$ 1 hour	Plug
50% WC + 3.5 wt.% Salt + 2 wt.% AA	W/O	$>$ 24 hours	Plug
50% WC + 3.5 wt.% Salt + 2.5 wt.% MeOH	W/O	$<$ 1 hour	Plug
50% WC + 3.5 wt.% Salt + 5 wt.% MeOH	W/O	$<$ 1 hour	No Plug
50% WC + 3.5 wt.% Salt + 2 wt.% AA + 2.5 wt.% MeOH	W/O	$>$ 24 hours	Plug

From the emulsion and autoclave experiment it was possible to come up with a general summary of the crude oil experiments that were run at 75 vol.% WC. The summary can be found in Figure B.1 and it shows that for a non-plugging system to occur it is helpful to have an oil continuous phase and a stable emulsion as systems that formed these types of emulsions were consitently non-plugging.

Table B.2: 200T Mineral Oil Emulsion Experiments

System	Type	Stability	Comments
75% WC	O/W	< 1 hour	Plug
75% WC + 2 wt.% AA	O/W	> 24 hours	Plug
75% WC + 3.5 wt.% Salt	O/W	< 1 hour	Plug
75% WC + 3.5 wt.% Salt + 2 wt.% AA	O/W	< 1 hour	Plug
75% WC + 3.5 wt.% Salt + 2.5 wt.% MeOH	O/W	< 1 hour	Plug
75% WC + 3.5 wt.% Salt + 5 wt.% MeOH	O/W	< 1 hour	No Plug
75% WC + 3.5 wt.% Salt + 2 wt.% AA + 2.5 wt.% MeOH	O/W	< 1 hour	Plug
75% WC + 3.5 wt.% Salt + 2 wt.% AA + 5 wt.% MeOH	O/W	< 1 hour	No Plug

Table B.3: 500T Mineral Oil Emulsion Experiments

System	Type	Stability	Comments
75% WC	O/W	< 1 hour	Plug
75% WC + 2 wt.% AA	O/W	> 24 hours	Plug
75% WC + 3.5 wt.% Salt	O/W	< 1 hour	Plug
75% WC + 3.5 wt.% Salt + 2 wt.% AA	O/W	< 1 hour	Plug

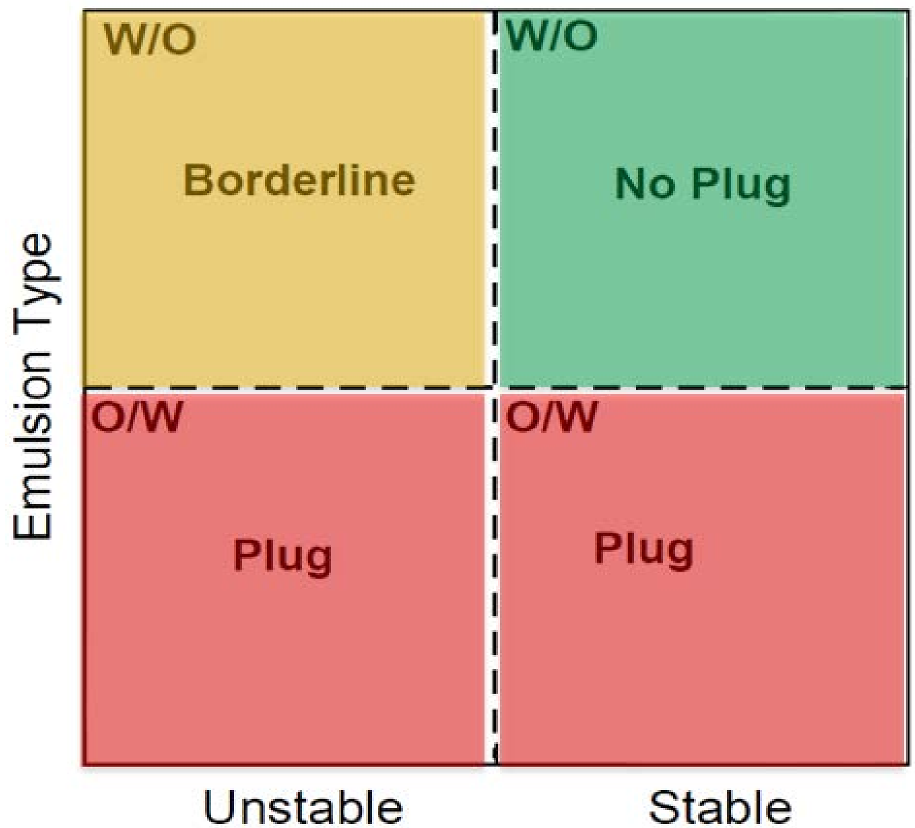

Figure B.1: Summary of emulsion experiments done with crude oil at 75 vol.% WC and linking results to autoclave plugging potential

APPENDIX C - FLUID PROPERTIES

Table C.1: Fluid Properties

Oil	API	Viscosity (cP)	Density (g/cm^3)
Crude	25.9	100	0.908
200T	33.8	40	0.856
500T	32.2	88	0.864

APPENDIX D - EXPERIMENTAL PROCEDURE

This section will detail the different procedures used throughout this work.

D.1 Autoclave Cell Loading Procedure

The following is the procedure used to set up an autoclave cell experiment for forming hydrates.

- Insert false bottom into autoclave cell.
- Insert FBRM and PVM probe into the autoclave cell.
- Secure probes in place using tri-clamps.
- Measure gravimetrically the amount of oil required.
- Measure gravimetrically the amount of anti-agglomerant required and add to oil.
- Mix the oil and anti-agglomerant using a magnetic stirrer until anti-agglomerant is dissolved.
- Pour oil mixture into autoclave cell.
- Measure gravimetrically the amount of water required.
- Measure gravimetrically the amount of salt required and add to water.
- Mix the water and salt (can be mixed by swirling beaker with hand) until salt is fully dissolved.
- Measure gravimetrically the amount of methanol required and add to water.
- Pour water mixture into autoclave cell.

- Seal autoclave cell by fixing the lid into place and tightening bolts using a criss-cross pattern.
- Ensure valves L and M are closed.
- Place cell into cooling bath and connect the top and bottom thermocouples, inlet and outlet gas lines as well as the safety release valve.
- Position motor into place above autoclave cell, secure with clamps.
- Ensure hose lines are in position in the bath and turn on chiller. Set to 20 °C.
- Set motor speed to 300 RPM.
- Open gas tank and and header valve.
- Open “Methane Gas Line” valve and set valve “A1” to “Fill Reservoir”.
- Pressurize air line to 60 psig and turn valve B to “Res Charge”
- Open valve D to “Charge Cell”.
- Open valve M and allow cell to be pressurized up to 300 psig then close valve D.
- Stop motor and open valve L so that cell is depressurized, then close valve L. This step is used to purge any atmospheric air from the cell.
- Open valve D again and switch on motor.
- Pressurize cell up to 950 psig.
- Open valve G fully to boost reservoir pressure up to 1800 psig.
- Once reservoir is at 1800 psig and cell is at 950 psig, close valve G and valve B (Note, do not let pressure exceed stated values).

- Pressurize the pressure control valve air line to 32 psig.
- Turn valve D to “Constant P”.
- Start labview program and set constant pressure to 950 psig.
- After saturating cell with methane for 12 hours, set chiller to 1 °C.

D.2 Autoclave Cell Depressurization Procedure

The following is the procedure used to safely depressurize and open the autclave cell when it is being used to form hydrates.

- Stop Labview program and motor.
- Depressurize air line controlling Pressure Control Valve
- Close valve M and valve D.
- Slowly open valve H to “Vent” to vent methane from the inlet gas line.
- Slowly open valve L to start depressurizing cell. Decouple motor from cell.
- Turn off chiller and remove hoses from bath.
- Close valve L and decouple gas lines and thermocouples.
- Take cell out of bath.
- Open valve L and M and allow cell to fully depressurize.
- Slowly open cell by loosening bolts in criss-cross pattern.
- Remove lid and observe hydrate morphology.

APPENDIX E - HYDRATE VOLUME CALCULATION

Below is an example calculation to show how the hydrate volume fraction has been calculated throughout this work. Starting with the Peng-Robinsion EOS (E.1):

$$P = \frac{RT}{V_m - b} - \frac{a\alpha}{V_m^2 + 2bV_m - b^2} \tag{E.1}$$

Where P is the recorded cell or reservoir pressure in Pa, R is the universal gas constant, T is the cell or reservoir temperature in K. V_m is the molar volume, a is a constant which is based on the critical temperature (T_c) and pressure (P_c) of methane as is b. α is calculated using (E.8). In (E.8), T_r is the reduced temperature and is calculated using (E.2), κ is calculated using E.5. From (E.1) the molar volume can be calculated at every time step which can then be used to track the number of moles of gas in the system. Any depletion in this number is assumed to be because of gas consumption due to hydrate formation. For this example $a = 0.2496$, $b = 2.68 \times 10^{-5}$ and $R = 8.314$ J/mol.K.

$$T_r = \frac{T}{T_c} \tag{E.2}$$

$$T_r = \frac{293.3}{190.56} \tag{E.3}$$

$$T_r = 1.54 \tag{E.4}$$

$$\kappa = 0.37464 + 1.54226\omega 0.26992\omega^2 \tag{E.5}$$

$$\kappa = 0.37464 + 1.54226 \times 0.011 - 0.26992 \times 0.011^2 \tag{E.6}$$

$$\kappa = 0.3916 \tag{E.7}$$

$$\alpha = (1 + \kappa(1 - T_r^{0.5}))^2 \tag{E.8}$$

$$\alpha = (1 + 0.3916(1 - 1.53^{0.5}))^2 \tag{E.9}$$

$$\alpha = 0.8204 \tag{E.10}$$

Putting everything into the Peng Robinson EOS:

$$10284448 = \frac{8.314 \times 292.1}{V_m - 2.68 \times 10^{-5}} - \frac{0.2496 \times 0.822}{V_m^2 + 2 \times 2.68 \times 10^{-5} \times V_m - (2.68 \times 10^{-5})^2} \tag{E.11}$$

The left hand side of the Peng Robinson equation (E.1) is known from recorded data, and from the right hand side the only variable missing is V_m. Therefore we use solver to find the Vm. Once the molar volume is known the number of moles of gas (n_g) can be calculated since the volume of the vessels are known. This is calculated using equation (E.12):

$$n_g = \frac{V}{V_m} \tag{E.12}$$

$$n_g = \frac{0.0029}{2.559 \times 10^{-4}} \tag{E.13}$$

$$n_g = 8.93\, mols \tag{E.14}$$

This indicates that 8.93 moles of gas are in the reservoir. At the start of the experiment 10.4 moles of gas were present. Therefore 1.5 moles of gas are assumed to have been consumed by hydrate formation. CSMGem calculations indicate that the methane small and large cage occupancy of sI at the thermodynamic conditions of 1°C and 950 psig would be 0.911 and 0.973, respectively. The gas occupancy of the small cage is labeled s_o and the gas occupancy of the large cage is labeled l_o. Since it is known that there are 2 small cages and 6 large cages in the unit cell of sI, the number of mols of gas per unit cell (n_{guc}) can be calculated using (E.15) and (E.18). Since the total number of gas moles is known, the total number of unit cells ($N_{UnitCell}$) that this gas would occupy can be calculated using (E.21). Since the volume of a unit cell ($V_{UnitCell}$) is known (McMullan & Jeffrey, 1965) the total hydrate volume ($V_{Hydrate}$)

can be calculated using (E.24).

$$n_{gc} = s_o \times 2 + l_o \times 6 \tag{E.15}$$

$$n_{gc} = 0.911 \times 2 + 0.973 \times 6 \tag{E.16}$$

$$n_{gc} = 7.66\, molecules/unitcell \tag{E.17}$$

$$n_{guc} = \frac{n_{gc}}{6.02 \times 10^{-4}} \tag{E.18}$$

$$n_{guc} = \frac{7.66}{6.02 \times 10^{-4}} \tag{E.19}$$

$$n_{guc} = 1.272 \times 10^{-23}\, mols/unitcell \tag{E.20}$$

$$N_{UnitCell} = \frac{n_{gcon}}{n_{guc}} \tag{E.21}$$

$$N_{UnitCell} = \frac{1.5}{1.272 \times 10^{-23}} \tag{E.22}$$

$$N_{UnitCell} = 1.18 \times 10^{23} \tag{E.23}$$

$$V_{Hydrate} = V_{UnitCell} \times N_{UnitCell} \tag{E.24}$$

$$V_{Hydrate} = 1.2 \times 10^{-9} \times 1.1.8 \times 10^{23} \tag{E.25}$$

$$V_{Hydrate} = 2.09 \times 10^{-4}\, m^3 \tag{E.26}$$

The volume fraction of hydrates (ϕ_H) can now be calculated:

$$\phi_H = \frac{V_{Hydrate}}{V_{Hydrate} + V_{remainingwater} + V_{oil}} \tag{E.27}$$

$$\phi_H = \frac{2.09 \times 10^{-4}}{2.09 \times 10^{-4} + 5.83 \times 10^{-4} + 2.5 \times 10^{-4}} \tag{E.28}$$

$$\phi_H = 0.2 \tag{E.29}$$

REFERENCES CITED

Alapati, R., Lee, J., Beard, D., & Technologies, Champion. Two Field Studies Demonstrate That New AA LDHI Chemistry is Effective at High Water Cuts Without Impacting Oil/Water Quality. *In: Offshore Technology Conference Proceedings, Houston, 2008, Paper 19505.*

Aman, Z. M. 2012. *Interfacial Phenomena of Cyclopentane Hydrate*. Ph.D. thesis, Colorado School of Mines.

Aman, Z. M., Brown, E. P., Sloan, E. D., Sum, A. K., & Koh, C. A. 2011. Interfacial Mechanisms Governing Cyclopentane Clathrate Hydrate Adhesion/Cohesion. *Physical Chemistry Chemical Physics*, **13**(44), 19796 – 19806.

Azarinezhad, R., Chapoy, A., Anderson, R., & Tohidi, B. HYDRAFLOW : A Multiphase Cold Flow Technology for Offshore Flow Assurance Challenges. *In: Offshore Technology Conference Proceedings, Houston, 2008, Paper 19485.*

Borgund, A. E. 2007. *Crude Oil Components with Affinity for Gas Hydrates in Petroleum Production*. Ph.D. thesis, The University of Bergen.

Boxall, J. 2009. *Hydrate Plug Formation From < 50 % Water Content Water-in-Oil Emulsions*. Ph.D. thesis, Colorado School of Mines.

Clark, L. W., Frostman, L. M., Anderson, J., & Petrolite, Baker. Low-Dosage Hydrate Inhibitors (LDHI): Advances in Flow Assurance Technology for Offshore Gas Production Systems. *In: International Petroleum Technology Conference, Doha, 2005, Paper 11538.*

Colombel, E., Gateau, P., Barré, L., Gruy, F., & Palermo, T. 2009. Discussion of Agglomeration Mechanisms between Hydrate Particles in Water in Oil Emulsions. *Oil & Gas Science and Technology - Revue de l'IFP*, **64**(5), 629–636.

Creek, J. L., Subramanian, S., & Estanga, D. New Method for Managing Hydrates in Deepwater Tiebacks. *In: Offshore Technology Conference Proceedings, Houston, 2011, Paper 22017.*

Davy, H. 1811. On a Combination of Oxymuriatic Gas and Oxygene Gas. *Philosophical Transactions of the Royal Society of London*, **101**(1), 155–162.

Erstad, K., Hø iland, S., Fotland, P., & Barth, T. 2009. Influence of Petroleum Acids on Gas Hydrate Wettability. *Energy & Fuels*, **12**, 2213–2219.

Ese, M. E., & Kilpatrick, P. K. 2004. Stabilization of Water-in-Oil Emulsions by Naphthenic Acids and Their Salts: Model Compounds, Role of pH, and Soap:Acid Ratio. *Journal of Dispersion Science and Technology*, **25**(3), 253–261.

Esteban, A., Hernandez, V., & Lunsford, K. 2000. Exploit the Benefits of Methanol. *In: 79th Gas Processors Association Conference Proceedings, Atlanta, 2000.*

Faraday, M., & Davy, H. 1823. On Fluid Chlorine. *Philosophical Transactions of the Royal Society of London*, **113**, 160–165.

Frostman, L. M., Przybylinski, J. L., & Petrolite, Baker. Successful Applications of Anti-agglomerant Hydrate Inhibitors. *In: Society of Petroleum Engineers Conference Proceedings, 2001, Houston, Paper 65007.*

Gao, S. 2008. Investigation of Interactions between Gas Hydrates and Several Other Flow Assurance Elements. *Energy & Fuels*, **22**(5), 3150–3153.

Gao, S. 2009. Hydrate Risk Management at High Watercuts with Anti-agglomerant Hydrate Inhibitors. *Energy & Fuels*, **23**(4), 2118–2121.

Gluyas, J. G., & Hichens, H. M. 2003. *United Kingdom Oil and Gas Fields Commemorative Millennium Volume.*

Greaves, D. P. 2007. *The Effects of Hydrate Formation and Dissociation on High Water Content Emulsions*. Ph.D. thesis, Coloardo School of Mines.

Hammerschmidt, E. G. 1934. Gas Hydrates in Natural Gas Transmission Lines. *Industrial & Engineering Chemistry*, **26**(8), 851–855.

Hemmingsen, P. V., Li, X., & Kinnari, K. Hydrate Plugging Potential in Underinhibited Systems. *In: Proceedings of the 6th International Conference on Gas Hydrates, 2008, Vancouver,.*

Huo, Z., Freer, E., Lamar, M., Sannigrahi, B., Knauss, D. M., & Sloan, E. D. 2001. Hydrate Plug Prevention by Anti-Agglomeration. *Chemical Engineering Science*, **56**(17), 4979–4991.

Ilahi, M. 2005. *Cold Flow Concepts Compared*. Ph.D. thesis, Norwegian University of Science and Technology.

Israelachvili, J. N. 2011. *Intermolecular and Surface Forces*. 3rd edn. Elsevier Inc.

Joshi, S. V. 2012. *Experimental Investigation and Modeling of Gas Hydrate Formation in High Water Cut Producing Oil Pipelines*. Ph.D. thesis, Colorado School of Mines.

Kelland, M. A. 2006. History of the Development of Low Dosage Hydrate Inhibitors. *Energy & Fuels*, **20**(3), 825–847.

Kelland, M. A., Svartaas, T. M., & Dybvik, L. A New Generation of Gas Hydrate Inhibitors. *In: Society of Petroleum Engineers Conference Proceedings, 1995, Dallas, Paper 30695*.

Lederhos, J. P., Long, J. P., Sum, A. K., Christiansen, R. L., & Sloan, E. D. 1996. Effective Kinetic Inhibitors for Natural Gas Hydrates. *Chemical Engineering Science*, **51**(8), 1221–1229.

Lo, C., Zhang, J. S., Couzis, A., Somasundaran, P., & Lee, J. W. 2010. Adsorption of Cationic and Anionic Surfactants on Cyclopentane Hydrates. *The Journal of Physical Chemistry C*, **114**(31), 13385–13389.

Makogen, Y. F. 1965. Hydrate Formation in Gas-Bearing Strata in Permafrost Regions. *Gazov. Promst.*, **14**(5).

Marcano, L., Gutierrez, X., Intevep, P., Perez, B., & Martínez, E. Effect of Some Physicalchemical Variables on the Formation and Stability of Foam in an Oil-Air System and Their Correlation With the Formation of Foamy Crude Oil. *In: Society of Petroleum Engineers Conference Proceedings, 2009, Cartagena de Indias, Paper 123060*.

Mcculfor, J., Himes, P., & Anklam, M. R. 2011. The Effects of Capillary Forces on the Flow Properties of Glass Particle Suspensions in Mineral Oil. *AIChE Journal*, **57**(9), 2334–2340.

McMullan, R. K., & Jeffrey, G. A. 1965. Polyhedral Clathrate Hydrates. IX. Structure of Ethylene Oxide Hydrate. *The Journal of Chemical Physics*, **42**(8), 2725 – 2732.

Neumann, A. W., David, R., & Zuo, Y. 2010. *Applied Surface Thermodynamics*. Second edn. Taylor & Francis Group.

Salager, J. L., Minana-Perez, M., Perez-Sanchez, M., Ramirez-Gouveia, M., & Rojas, C. I. 1983. Surfactant-Oil-Water Systems Near the Affinity Inversion Part III: The Two Kinds of Emulsion Inversion. *Journal of Dispersion Science and Technology*, **4**(3), 313–329.

Sjoblom, J., Aske, N., Auflem, I. H., Brandal, O., Havre, T. E., Saether, O., Westvik, A., Johnsen, E. E., & Kallevik, H. 2003. Our Current Understanding of Water-in-Crude Oil Emulsions. Recent Characyerization Techniques and High Pressure Performance. *Advances in Colloid and Interface Science*, **100-102**, 399–473.

Sjöblom, J., Ø vrevoll, B., Jentoft, G., Lesaint, C., Palermo, T., Sinquin, A., Gateau, P., Barré, L., Subramanian, S., Boxall, J., Davies, S., Dieker, L., Greaves, D., Lachance, J., Rensing, P., Miller, K., Sloan, E. D., & Koh, C. A. 2010. Investigation of the Hydrate Plugging and Non-Plugging Properties of Oils. *Journal of Dispersion Science and Technology*, **31**(8), 1100–1119.

Sloan, E. D. 1991. Natural Gas Hydrates. *Society of Petroleum Engineers*, **43**(12), 1414–1417.

Sloan, E. D. 2003. Fundamental Principles and Applications of Natural Gas Hydrates. *Nature*, **426**(11), 353–359.

Sloan, E. D., & Koh, C. A. 2008. *Clathrate Hydrates of Natural Gases*. 3rd edn. Boca Raton, FL: Taylor & Francis Group - CRC Press,.

Sloan, E. D., Koh, C. A., & Sum, A. K. 2010. *Natural Gas Hydrates in Flow Assurance*. 1st edn. Gulf Professional Publishing.

Thompson, D. G., Taylor, A. S., & Graham, D. E. 1985. Emulsification and Demulsification Related to Crude Oil Production. *Colloids and Surfaces*, **15**, 175–189.

Turner, D. J. 2006. *Clathrate Hydrate Formation in Water-in-Oil Dispersions*. Ph.D. thesis, Colorado School of Mines.

Webb, E. B., Rensing, P. J., Koh, C. A., Sloan, E. D., Sum, A. K., & Liberatore, M. W. 2012. High-Pressure Rheology of Hydrate Slurries Formed from Water-in-Oil Emulsions. *Energy & Fuels*, **26**(6), 3504–3509.

Wroblewski, S. 1882. On the Combination of Carbonic Acid and Water. *Philisophical Magazine Series 5*, **13**(80).

York, J. D., & Firoozabadi, A. 2008. Alcohol Cosurfactants in Hydrate Antiagglomeration. *The Journal of Physical Chemistry. B*, **112**(34), 10455–65.

York, J. D., & Firoozabadi, A. 2009. Effect of Brine on Hydrate Antiagglomeration. *Energy & Fuels*, **23**(6), 2937–2946.

Yousif, M. H. 1998. Effect of Underinhibition With Methanol and Ethylene Glycol on the Hydrate-Control Process. *Society of Petroleum Engineers*, **13**(3), 184–189.

Zanota, M. L., Dicharry, C., Graciaa, A., & Complexes, Fluides. 2005. Hydrate Plug Prevention by Quaternary Ammonium Salts. *Energy & Fuels*, **19**(11), 584–590.

Zerpa, L. E., Salager, J-L., Koh, C. A., Sloan, E. D., & Sum, A. K. 2011. Surface Chemistry and Gas Hydrates in Flow Assurance. *Industrial & Engineering Chemistry Research*, **50**(1), 188–197.